

University of Manitoba  
Faculty of Engineering

Mechanical and Manufacturing Department



UNIVERSITY  
OF MANITOBA

MECH 4860: Engineering Design

Manitoba Hydro

**Redesign of Shaft Seal Running Ring and Fastener Testing**

Team 9

Prepared by: **Eric Morrish**  
**Mihskakwan James Harper**  
**Andrew Skorpad**  
**Yang Qin**  
**Shenghui Yao**

Prepared for: **Paul Labossiere, P. Eng**  
**Hannah Guenther, MIT**

Date Submitted: **December 7, 2016**



Generation Solutions  
EITC E2-229  
University of Manitoba  
Winnipeg, MB R3T 5V6

December 7, 2016

Dr. Paul Labossiere, P. Eng.  
Mechanical Engineering Design Instructor  
Department of Mechanical Engineering  
University of Manitoba  
Winnipeg, MB R3T 5V6

Dear Dr. Labossiere,

Please find the attached final design report, "Redesign of Shaft Seal Running Ring and Fastener Testing", sponsored on behalf of Manitoba Hydro, and submitted on the 7<sup>th</sup> of December, 2016 by Generation Solutions.

This report details the design of an improved version of the running ring, a major component of a turbine shaft seal at Jenpeg Generating Station. This new running ring is designed to decrease the installation time by having a smaller deflection value when suspended by its own weight. The running ring also will be made of stainless steel to address the corrosion concerns that the existing running ring has. Finally, Generation Solutions designed, fabricated, and tested a bolt testing apparatus and procedure, which is encouraged to be used for a variety of other fasteners to retrieve nut factors to assist designers.

On behalf of Generation Solutions, I would like to thank you for your time and effort on helping deliver this project, and please do not hesitate to contact me if you have any questions regarding the project.

Sincerely,

Eric Morrish  
Team 9 Project Manager  
Generation Solutions

## Executive summary

Manitoba Hydro's Jenpeg generating station was experiencing difficulties with their turbine shaft from corrosive river water conditions. Revisiting Manitoba Hydro's initial shaft seal solution, found that deflection of a running ring, while being installed during the repair, was excessive. They had also determined that the running ring was exhibiting corrosion concerns. Manitoba Hydro has requested that Generation Solutions redesign the running ring of the shaft seal to simultaneously improve alignment, installation times, and corrosion concerns. They have also asked us to create a standard system that can determine the Nut factor  $k$  of fasteners.

Following the completion of a rigorous design process and finite element analysis, Generation Solutions has successfully increased the stiffness of the running ring. The change in vertical diameter of the running ring was reduced from 0.033" to 0.007", corresponding to an improvement of 77.3%. Generation Solutions and Manitoba Hydro were hoping to achieve a deflection value of 0.005" in order to conform to assembly tolerance, however the achieved value will significantly reduce the deflection despite not meeting our goal.

Research conducted by Generation Solutions determined that changing the material of the running ring from ASTM A516 Gr 70 steel to 410 stainless steel will reduce the corrosion of the running ring from greater than 0.050" per year to less than 0.020" per year.

Through extensive detailed design and optimization, we have created an apparatus that both the team and the client are happy with. We have created a procedure for how to use the apparatus to determine the Nut factor, along with its corresponding analysis program. We have received acceptable results from our apparatus, with an average Nut factor value of 0.177 for a 5/8" x 5" stud under 5.2" of tension with Loctite applied undergoing 0.010" elongation length with a standard deviation of 0.0263 and a confidence level of 85%. Given the many different sources of error with regards to determining the Nut factor, we believe that our results are acceptable and well within the scope of the project.

# Table of Contents

<b>Letter of transmittal .....</b>	<b>ii</b>
<b>Executive summary .....</b>	<b>iii</b>
<b>Table of Figures .....</b>	<b>vi</b>
<b>List of Tables .....</b>	<b>ix</b>
<b>1 Introduction.....</b>	<b>1</b>
1.1 Project Background .....	1
1.2 Problem Statement.....	3
1.3 Project Objectives.....	4
1.4 Customer Needs.....	4
1.5 Limitations.....	6
1.6 Target Specifications .....	7
<b>2 Research and Theory .....</b>	<b>10</b>
2.1 Deformation of Running Ring .....	10
2.2 Corrosion of the Running Ring .....	13
2.3 Behaviour and Testing of Bolt Properties .....	15
<b>3 Concept Generation and Search Results .....</b>	<b>19</b>
3.1 Addressing Running Ring Deformation (CN5).....	19
3.1.1 Methods of Increasing Moment of Inertia (A1) .....	19
3.1.2 Methods of Increasing Modulus of Elasticity (A2).....	22
3.2 Addressing Running Ring Corrosion (CN6) .....	23
3.1.3 Coatings (B1) .....	24
3.2.1 Material Change (B2).....	26
3.2.2 Electro-chemical methods (B3).....	26
3.2.3 Environment Changes (B4) .....	28
3.3 Bolt Testing Concepts (CN10) .....	29
3.3.1 Bolt Specifications .....	29
3.3.2 Nut Factor Conceptual Design .....	33
3.4 Concept Generation Summary.....	36
<b>4 Concept Analysis and Selection .....</b>	<b>38</b>
4.1 Addressing Running Ring Deformation (CN5).....	38
4.1.1 Methods of Increasing Moment of Inertia (A1) .....	38
4.1.2 Methods of Increasing the Modulus of Elasticity (A2).....	40
4.2 Addressing Running Ring Corrosion (CN6) .....	42
4.3 Bolt Testing (CN10) .....	47
4.4 Concept Selection Summary .....	49
<b>5 Detailed design .....</b>	<b>51</b>
5.1 Running Ring Optimization .....	51
5.1.1 FEA Analysis and Validation on Running Ring .....	51
5.1.2 Loading on Fasteners .....	64

5.1.3 Total Loading.....	69
5.1.4 Fatigue on Fasteners.....	72
5.1.5 Comparison of Materials and Optimization.....	72
5.2 Running Ring Final Design.....	81
5.2.1 Final Cross-section, material and features.....	82
5.2.2 Updated installation procedure.....	83
5.2.3 New Running Ring Design Comparison to Customer Needs.....	83
5.3 Bolt Testing Finalization.....	84
5.3.1 Bolt Testing Experimental Design.....	84
5.3.1 Bolt Testing Experimental Design.....	84
5.3.2 Optimized Test Apparatus.....	87
5.4 Bolt Test Results.....	92
5.4.1 Manufacturing Details.....	92
5.4.2 Observations.....	93
5.4.3 Final Results.....	97
5.4.4 Discussion and Compare to CN's.....	97
<b>6 Conclusion.....</b>	<b>100</b>
6.1 Recommendations for Running Ring.....	100
6.2 Recommendations for Bolt Testing.....	101
6.3 Design Lessons Learned from Team.....	101
6.4 Design Summary and Recommendations.....	102
<b>7 Bibliography.....</b>	<b>103</b>

## Table of Figures

Figure 1: Exploded view of the redesigned running ring. ....	2
Figure 2: Running ring deformation under its own weight. ....	3
Figure 3: Running ring variables .....	11
Figure 4: Moment of inertia variables .....	12
Figure 5: Corrosion on the running ring .....	14
Figure 6: Lantern ring in contact with running ring .....	15
Figure 7: Illustration of tensile load applied through fastener actual and simplified .....	17
Figure 8: Original running ring cross-section .....	19
Figure 9: Original versus concept A1.1.1: increased thickness.....	20
Figure 10: Original versus resulting A1.1.1 concept turbine flange hole pattern.....	20
Figure 11: Original versus concept A1.1.2: increased flange dimensions .....	21
Figure 12: Running ring flange cap screw .....	21
Figure 13: Original versus concept A1.1.3: added flange .....	22
Figure 14: Original versus concept A1.1.4 ribbed .....	22
Figure 15: Methods of corrosion control.....	24
Figure 16: Unpowered cathodic protection chemistry .....	27
Figure 17: ICCP system diagram .....	28
Figure 18: Description of metric bolt .....	31
Figure 19: Concept C1.1.1a sketch side view .....	34
Figure 20: Concept C1.1.1b side and top view .....	34
Figure 21: Concept C1.1.1c stabilizing design side views.....	35
Figure 22: Concept C1.1.1d side and top view .....	35
Figure 23: Design C1.1.2: Side and top view.....	35
Figure 24: Design C1.1.3: Side and top view.....	36
Figure 25: Final preliminary design side view .....	49
Figure 26: SolidWorks model of running ring. ....	52
Figure 27: Running ring base fixture.....	52
Figure 28: Deformation of current running ring design. ....	53
Figure 29: Convergence plot of FEA analysis of current running ring. ....	54
Figure 30: Fine mesh in region of base fixture.....	54
Figure 31: Bolt hole fixture .....	55
Figure 32: Deflection of current running ring under actual loading conditions. ....	55

Figure 33: Convergence plot for actual loading scenario of current design.....	56
Figure 34: Fine mesh in fixed bolt hole region. ....	56
Figure 35: General shape of optimized cross section. ....	57
Figure 36: Flange chamfer functionality. ....	58
Figure 37: Theoretical added flange and space constraints.....	60
Figure 38: Optimized running ring geometry.....	62
Figure 39: Optimized geometry vertical deflection.....	62
Figure 40: Optimized geometry convergence plot. ....	63
Figure 41: Geometry mesh at the end of fourth loop of optimization. ....	63
Figure 42: Optimized running ring geometry in shaft assembly. ....	64
Figure 43: Packing compression. ....	65
Figure 44: Water supply inlet. ....	67
Figure 45: Running ring water pressure spikes. ....	68
Figure 46: Lantern ring cross section ....	69
Figure 47: Loading conditions at top dead center. ....	70
Figure 48: Loading conditions at bottom dead center. ....	70
Figure 49: Free body diagram of running ring at top dead center. ....	71
Figure 50: Shear forces on bolt. ....	72
Figure 51: Goodman fatigue analysis.....	75
Figure 52: Goodman analysis for shear stress. ....	77
Figure 53: Simplified galvanic series.....	79
Figure 54: Risk of corrosion from bimetallic contact in neutral electrolytes.....	80
Figure 55: Cross section of the new running ring. ....	82
Figure 56: Measuring the elongation length of the bolt after torqueing.....	86
Figure 57: Sample data results in Summary Report from Minitab.....	87
Figure 58: 7 Gage plate apparatus side view.....	88
Figure 59: 7-Gage plate.....	89
Figure 60: 3/8" Plate apparatus isometric view.....	89
Figure 61: 3/8" Plate.....	90
Figure 62: 3/8" Plate apparatus 2 side view ....	90
Figure 63: 3/8" Plate 2.....	91
Figure 64: 1" Spacer plates with two and six holes.....	91
Figure 65: Final apparatus isometric view ....	92
Figure 66: 4x4 Block testing apparatus.....	93

Figure 67: Bolt cleaning.....	94
Figure 68: Nut clearance during test .....	94
Figure 69: Test run through torque application.....	95
Figure 70: Test run through measurement.....	96
Figure 71: <i>Minitab</i> graphical results of Nut Factor K testing.....	97



## List of Tables

TABLE I: CUSTOMER NEEDS FOR RUNNING RING REDESIGN .....	5
TABLE II: CUSTOMER NEEDS FOR BOLT TESTING DESIGN .....	5
TABLE III: CONSTRAINTS AND LIMITATIONS ON RUNNING RING REDESIGN.....	6
TABLE IV: CONSTRAINTS AND LIMITATIONS ON BOLT TESTING DESIGN.....	7
TABLE V: DESIGN METRICS FOR RUNNING RING REDESIGN.....	7
TABLE VI: DESIGN METRICS FOR BOLT TESTING DESIGN .....	8
TABLE VII: RUNNING RING DESIGN VALUES .....	11
TABLE VIII: PROPERTIES OF CONSIDERED MATERIALS .....	23
TABLE IX: RESISTANCE OF COMMON COATINGS TO VARIOUS ENVIRONMENT.....	25
TABLE X: SCREENING MATRIX OF THE TESTING METHODS FOR DESIGN IDEA BASIS ...	30
TABLE XI: MANITOBA HYDRO M16X2X70MM BOLT PROPERTIES .....	32
TABLE XII: CALCULATED M16X2X70MM BOLT PROPERTIES.....	33
TABLE XIII: DM A1: INCREASING MOMENT OF INERTIA CRITERIA WT MATRIX.....	39
TABLE XIV: DM A1: INCREASING MOMENT OF INERTIA SELECTION MATRIX .....	40
TABLE XV: DM A2.1: MATERIAL FEASIBILITY SCREENING.....	41
TABLE XVI: DM A2.2: WEIGHING MATRIX FOR MATERIAL .....	41
TABLE XVII: DM A2.2: MATERIAL SELECTION MATRIX .....	42
TABLE XVIII: DM B.0: FEASIBILITY SCREEN ON CORROSION METHODS.....	42
TABLE XIX: DM B4.2.1 CORROSION CONCEPT SELECTION CRITERIA.....	43
TABLE XX: DM B4.2.1: CORROSION PRELIMINARY CONCEPT SCREENING .....	43
TABLE XXI: DM B4.2.2: CORROSION CRITERIA WEIGHING MATRIX .....	44
TABLE XXII: DM B4.2.2 WEIGHT CONCEPT SCORING FOR MATERIAL.....	44
TABLE XXIII: DM B4.1.1 FEASIBILITY MATRIX FOR MET. AND NON-MET. COATINGS .....	45
TABLE XXIV: ADDITIONAL COATING SELECTING CRITERIA .....	45
TABLE XXV:DM B4.1.2 CRITERIA WEIGHING MATRIX.....	45
TABLE XXVI: DM B4.1.2 WEIGHTED CONCEPT SCORING RESULTS FOR COATING .....	46
TABLE XXVII: B4.4.1 FEASIBILITY MATRIX FOR OPERATING VARIABLES .....	46
TABLE XXVIII: DM C1.1 NUT FACTOR METRIC WEIGHTING.....	47
TABLE XXIX: DM C1.1 NUT FACTOR DESIGN SCORING MATRIX .....	48
TABLE XXX: CURRENT RUNNING RING DIMENSIONS AND DESIGN CONSTRAINTS .....	58
TABLE XXXI: MASS VS DEFLECTION DECREASE.....	59
TABLE XXXII: ORIGINAL VS. OPTIMIZED RUNNING RING PROPERTIES .....	60

TABLE XXXIII: INLET WATER PRESSURE.....	67
TABLE XXXIV: RUNNING RING FASTENER LOADING .....	69
TABLE XXXV: NET FORCES ON FASTENERS .....	70
TABLE XXXVI: REACTION FORCES.....	71
TABLE XXXVII: BOLT AND JOINT STIFFNESS .....	73
TABLE XXXVIII: AXIAL STRESS ON FASTENERS .....	74
TABLE XXXIX: SHEAR STRESS ON FASTENERS .....	77
TABLE XL: MECHANICAL PROPERTIES OF VARIOUS MATERIALS.....	78
TABLE XLI: CORROSION PERFORMANCE OF VARIOUS MATERIALS.....	78
TABLE XLII: MATERIAL COST BREAKDOWN .....	81
TABLE XLIII: RUNNING RING CUSTOMER NEEDS COMPARISON .....	83
TABLE XLIV: NUT FACTOR K CUSTOMER NEEDS COMPARISON.....	99

# 1 Introduction

This final design report (FDR) was written as a part of the Engineering Design course at the University of Manitoba and was in collaboration with Manitoba Hydro. The FDR is intended to guide the reader through the team's design process from initial problem statement to final design details. Appended to the FDR are final design documents that we recommend Manitoba Hydro implement.

## 1.1 Project Background

Manitoba Hydro is the public utility for electric power and natural gas in the province of Manitoba, generating 30 billion kilowatt-hours of clean renewable energy annually through the use of 15 hydroelectric generating stations. One of the 15 generating stations is Jenpeg, which is located on the upper arm of the Nelson River and features 6 bulb-type, horizontally oriented, turbine generators combining for a capacity of 129 megawatts [1].

In early 2010, Manitoba Hydro was informed that a sister-plant in Europe that featured the same bulb-type generators, had experienced catastrophic failure on the turbine shafts. Manitoba Hydro then inspected the turbine shafts, where it was discovered that there were hundreds of circumferential cracks in a filleted region between the turbine shaft body and the runner flange of the shaft. Manitoba Hydro decided to shut down all six turbine generators to prevent a similar catastrophic failure from taking place. After an extensive investigation, Manitoba Hydro concluded that the filleted region of the shaft should have an infinite fatigue life given ideal operating conditions. However, further analysis of the shaft indicated that the surface finish of the shaft had been pitted due to corrosion from the river water, meaning that the shafts could be reworked and salvaged. Although machining out the cracks would increase the stresses in the fillet region, the radius of the filleted area was also increased to decrease the corresponding stress concentration factor, ultimately resulting in allowable stress values [2].

Although the cracks had been machine out and the shaft was ready for service, a new method of protecting the filleted region of the shaft still needed to be determined. Several methods were considered including a grease filled cover over the fillet and a corrosion resistant spray. These ideas were dismissed due to environmental and maintenance intensiveness concerns. Manitoba Hydro decided to redesign the existing shaft seal to protect the filleted area of the shaft by keeping it dry. The result was a packing box style seal that consisted of a steel ring, which was

attached to the running flange of the shaft that would then contain the rest of the packing box. An exploded view of the new shaft seal can be seen in Figure 1. This packing box was designed so that no disassembly is required for inspection and maintenance reasons. The shafts were returned to service in August 2011.

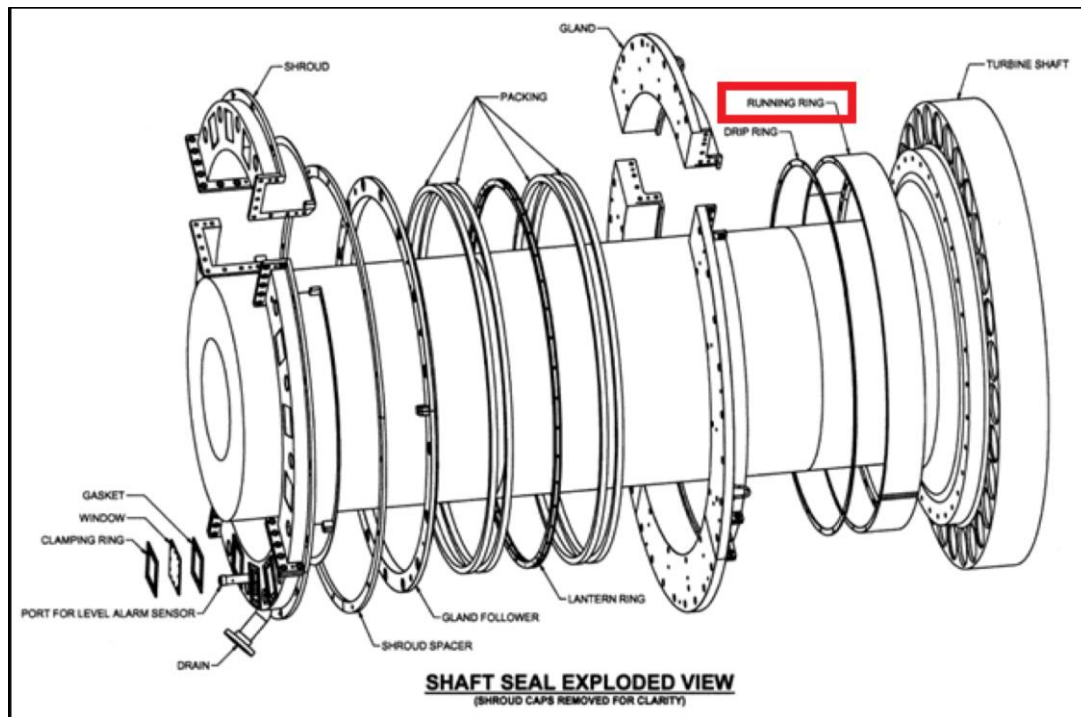


Figure 1: Exploded view of the redesigned running ring.

The new packing box design has been operational with minimal issues since its implementation. Although the shaft seal is considered an overall success among Manitoba Hydro employees, lengthy installation times for the new seal remains to be troublesome due to the lost generation opportunities during turbine downtime. This lengthy installation time can be greatly attributed to the installation of the running ring portion of the shaft seal. The alignment of the running ring during installation is time consuming as the ring is not rigid enough to maintain the specified assembly tolerances, which is illustrated in Figure 2.

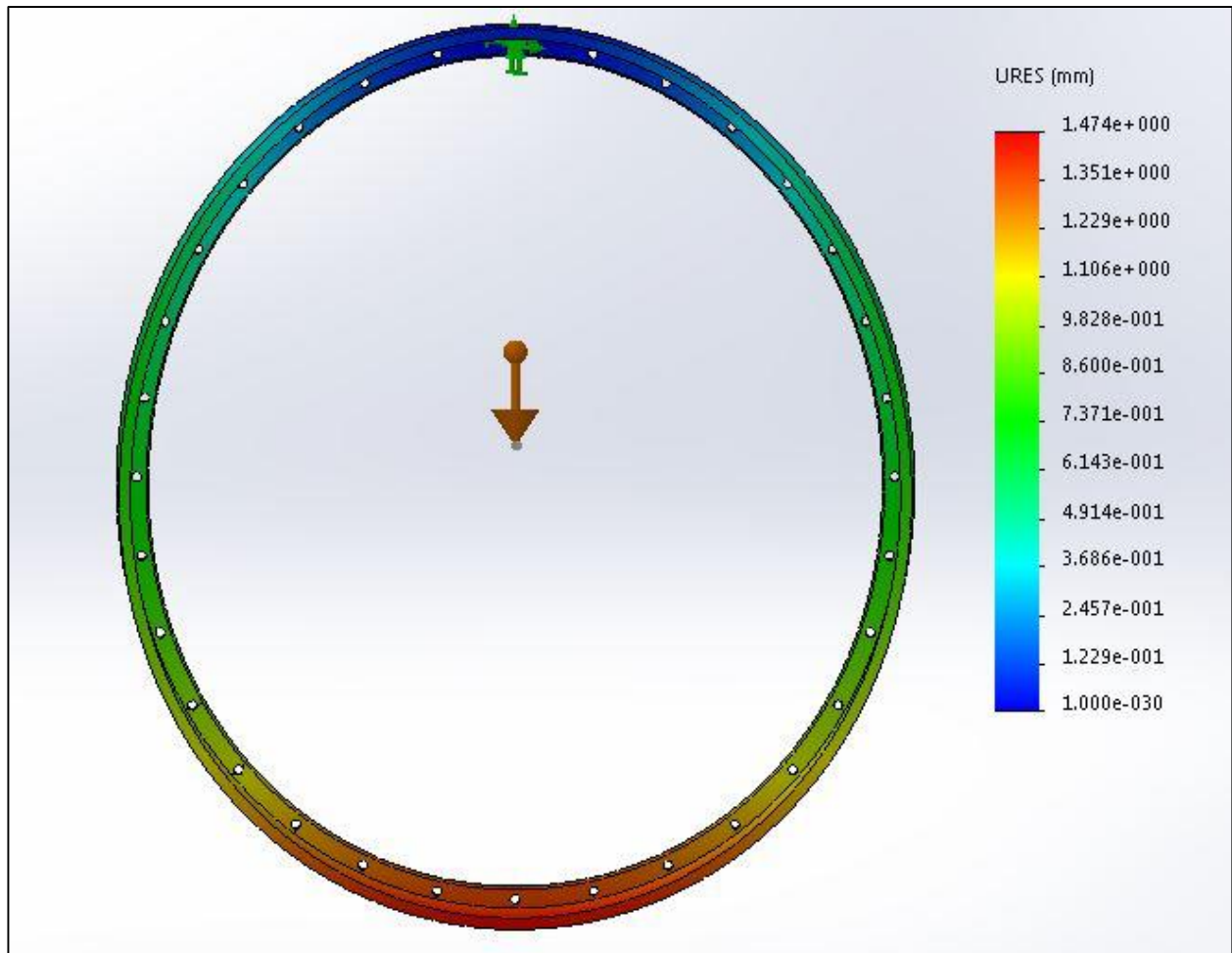


Figure 2: Running ring deformation under its own weight.

Additionally, corrosion concerns relating to the running ring arise when the turbine is inoperative. Stagnant river water causes corrosion of the running ring when the turbine is down for maintenance. When corrosion is excessive, the running ring must be disassembled for cleaning and repairs, ultimately adding turbine downtime causing Manitoba Hydro to lose potential profits from power generation.

## 1.2 Problem Statement

Manitoba Hydro is requesting that Generation Solutions redesign the running ring of the shaft seal to simultaneously improve alignment and installation times, and eliminate corrosion concerns. Once the design is changed, the associated fasteners connecting the running ring to the turbine shaft must be analyzed to ensure an infinite fatigue life. Manitoba Hydro is also requesting that a test be designed to ensure the repeatability of preload generated when torque is applied to the running ring fasteners previously mentioned.

### 1.3 Project Objectives

The overall project objective is to redesign the running ring while maintaining manufacturability and result of minimal changes to the mating components. Furthermore, a testing apparatus has to be designed to determine the locking mechanism properties in a repeatable and consistent manner. The project objective essentially consists of three main aspects which are outlined below:

1. The new design of the running ring should be able to eliminate the corrosion concerns when the unit sits dewatered for any period of time while still maintaining manufacturability.
2. The new design of the running ring should have the ability to be aligned faster and more precisely within allowable assembly tolerances to ensure the easy installment for maintenance staff. The new design should also be able to fit within the current seal assembly with minimal changes to the other mating components.
3. Design a testing apparatus to ensure the repeatability of preload generated when torque and a thread locking compound is applied to the running fasteners. In addition, fabrication of the testing apparatus as well as conducting an experiment to collect and analyze the results is also part of the objective.

### 1.4 Customer Needs

Customer needs were developed by taking input from Manitoba Hydro employees Hannah Guenther and Kevin Wilson. Key objectives of this project were discussed, such as determining aspects of the design, which TABLE I and TABLE II communicate. Importance was ranked on a scale from 1 to 5, with 5 being crucial, and 1 being least crucial.

Importance scores were determined by weighing the possible impacts of them not occurring or lack thereof occurring in the design. For example, one of the needs is that the running ring will not fail; this is of high importance because if the running ring were to fail, there is a high chance that further damages could incur to the company, public and environment.

TABLE I: CUSTOMER NEEDS FOR RUNNING RING REDESIGN

ID	Needs	Importance
CN1	The running ring will be economical.	5
CN2	The running ring will not fail.	5
CN3	The running ring time between maintenance will be low.	4
CN4	The running ring maintenance time will be reduced.	4
CN5	The running ring will eliminate corrosion concerns.	4
CN6	The running ring will align within tolerance.	4
CN7	The running ring will not be time consuming throughout installation.	3
CN8	The running ring mating components remain unchanged.	3
CN9	The running ring can be crane lifted and easily maneuvered.	3
CN10	Running ring and components will be manufactured locally.	2

TABLE II: CUSTOMER NEEDS FOR BOLT TESTING DESIGN

ID	Needs	Importance
CN11	A test will be designed to replicate running ring fasteners on the running ring design.	5
CN12	The test will replicate conditions of the running rings hardware.	5
CN13	The test will be able to determine bolt properties precisely.	5
CN14	The test rig will be able to repeat tests.	4
CN15	The test will have a set procedure.	4
CN16	The test will be easy to perform.	2

Approval of customer's needs and priorities were sought before to moving forward in the project, which was obtained from Hannah Guenther.

## 1.5 Limitations

In addition to the needs identified from the customer, certain constraints and limitations were made, summarized in TABLE III and TABLE IV.

**TABLE III: CONSTRAINTS AND LIMITATIONS ON RUNNING RING REDESIGN**

ID	Limitation Type	Description
<b>L1</b>	Space and geometry of running ring	The running ring has to fit in the seal assembly, between the turbine flange and drip ring; the seal assembly has limited clearance and therefore the running ring will as well.
<b>L2</b>	Interface with other components	Redesign of the running ring should change no components of the seal. Furthermore, any component that may be effected by the change in geometry of the running ring may also need to be adjusted. Changing other components will increase the complexity of the project. Given the limited resources, a design that achieves our objectives without changing other aspects of the seal assembly is ideal.
<b>L3</b>	Time and scheduling	There may not be sufficient time to finish the redesign due to the short project timeline and the overall size of the project assigned by Manitoba Hydro.
<b>L4</b>	Site and remoteness	Due to the remote location of the Jenpeg Generating station, our team will not likely have the opportunity to visit the site. Therefore, the majority of our knowledge on the shaft seal and running ring will be gained through engineering drawings and other information provided by Manitoba Hydro.
<b>L5</b>	Manufacturability	Manitoba Hydro prefers the fabrication and testing be done by a machine shop with which they have a service agreement, making the design efforts and testing limited to their capabilities; active communication with this shop will facilitate the design process to refine what specific limitations to geometry, materials, and processes the machine shop has.



TABLE IV: CONSTRAINTS AND LIMITATIONS ON BOLT TESTING DESIGN

ID	Limitation Type	Description
<b>L6</b>	Repeatability	The testing apparatus will ensure repeatability and performance by anyone with a mechanical background. The test should simulate the function and environment of the running ring. The test shall also determine results non-destructively.
<b>L7</b>	Time and scheduling	There may not be sufficient time to finish the design and fabricate the testing apparatus due to the short project timeline and the overall size of the project assigned by Manitoba Hydro. As the project Gantt chart illustrates in Appendix B, the longest duration for each working activity is only 7 days, which may prove to be difficult due to manufacturing lead times.
<b>L8</b>	Manufacturability	Manitoba Hydro would like to see fabrication done locally; active communication with a machine shop will facilitate the design process to refine what specific limitations to geometry, materials, and processes the shop has.

## 1.6 Target Specifications

The constraints and limitations combined with the customer needs allows Generation Solutions to accurately determine measurable engineering metrics. These metrics will help guide the team to ultimately choosing concepts to proceed into detailed design with TABLE V and TABLE VI.

TABLE V: DESIGN METRICS FOR RUNNING RING REDESIGN

Metric ID	Customer Need ID	Metric	Importance	Units	Marginal Value	Ideal Value
<b>M1</b>	CN1	Labour, material and machining costs	5	CAD\$	\$37000	< \$37000
<b>M2</b>	CN2	Stress on running ring	5	MPa	factor of safety of 3	factor of safety > 3
<b>M3</b>	CN3	Time between maintenance cycles	4	years	1 year	> 1 year
<b>M4</b>	CN4	Maintenance time	4	days	4 days	< 4 days

Metric ID	Customer Need ID	Metric	Importance	Units	Marginal Value	Ideal Value
<b>M5</b>	CN5	Rate of corrosion	4	inches /month	0.005 in/month	0.000 in/month
<b>M6</b>	CN6	Installation runout from hole centers	4	inches	< 0.005 in	0.000 in
<b>M7</b>	CN7	Labour hours of installation	3	hours	192	< 192
<b>M8</b>	CN8	Assembly changed?	3	Yes/no	No	No
<b>M9</b>	CN9	Running ring weight	3	lbs	800 lbs	650 lbs
<b>M10</b>	CN10	Components were manufactured locally	2	Pass / Fail	Pass	Pass

**TABLE VI: DESIGN METRICS FOR BOLT TESTING DESIGN**

Metric ID	Customer Need ID	Metric	Importance	Units	Marginal Value	Ideal Value
<b>M11</b>	CN11	Distance of elongation length represents 60% yield of bolt while in tension	5	inch	0.0063 + 10% in	0.00063 in
<b>M12</b>	CN12	Does the test apparatus replicate running ring conditions	5	Pass / fail	None	Pass
<b>M13</b>	CN13	Torque and preload relationship is found with little standard deviation	5	Factor margin of error from nominal K value	+/- 10%	+/- 5%
<b>M14</b>	CN14	Number of tests for design life	4	number	5000 tests	last forever
<b>M15</b>	CN15	Procedure steps allow for accurate performance	4	Pass/fail	Pass	Pass
<b>M16</b>	CN16	Is the test easy to perform	2	Pass/fail	Pass	Pass

Design metrics M1 through M16 will be used as a guide to achieving goals by measuring concepts importance and the quantitative values that Generation Solutions will achieve.

Each concept developed throughout this report, as well as the decision matrices that they are scored on have unique identifiers, which can be referenced in Appendix A for a detailed 'Design Map.' This is to be used as reference to visually assist with the design process.

## 2 Research and Theory

To understand the behaviours related to the running ring under existing conditions related to corrosion and deformation, as well as bolt properties, sufficient background theory and existing practises must be considered to guide the design process towards understanding what the variables are and how they interact with each other to change the overall design. Understanding these relationships will be useful in optimizing a final design that meets all of the design metrics.

### 2.1 Deformation of Running Ring

Maintenance staff have difficulty meeting the strict assembly tolerances associated with the installation process, specifically aligning the running ring to be concentric to the turbine shaft within tolerance. Complying with the runout tolerance of 0.005” is a time consuming process due to excessive deformation of the running ring. The objective is to reduce the deformation the running ring undergoes when subjected to its own weight.

In order to improve the stiffness of the running ring, Generation Solutions plans to improve the bending stiffness of the existing design. Considering the running ring as a thin ring, the change in vertical diameter  $\Delta D_v$  by its own weight  $w$  is shown in equation (2.1.1) [3].

$$\Delta D_v = \frac{-wR^3}{EAe} \left( \frac{k_1\pi^2}{4} - 2k_2^2 \right) \quad (2.1.1)$$

where,

$$k_1 = 1 - \frac{e}{R} - \frac{FEI}{GAR^2}$$

$$k_2 = 1 - \frac{e}{R}$$

$R$  is the radius from the center of the ring to the centroid of the cross-sectional area

$E$  is the modulus of elasticity

$e$  is the positive distance radial to the centroid axis of cross-section to the neutral axis of pure bending

$F$  is the shape factor

$I$  is the cross-sectional second moment of inertia,

$G$  is the shear modulus of the material

$A$  is the cross-sectional area

$w$  is the weight per unit circumference

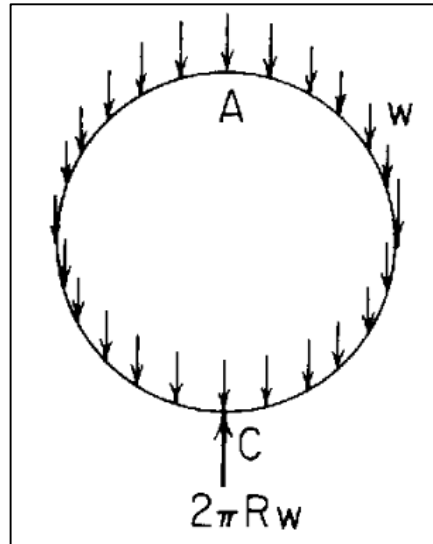


Figure 3: Running ring variables [4].

This equation can be simplified using the following assumptions:

$$e = \frac{I}{RA} \quad (2.1.2)$$

$$F = \frac{12I}{A^2} \quad (2.1.3)$$

Additionally, the existing running ring has approximate values set from its current design, as shown in TABLE VII. These values are estimates and are only used to determine which variables have the greatest impact in the running ring deformation.

TABLE VII: RUNNING RING DESIGN VALUES

Measure	Value	Notes
Weight, w	2158.2 N	
Radius, R	1.823 m	
Modulus of Elasticity, E	200 GPa	Typical carbon steel [5]
Cross-section area, A	0.00556 m <sup>2</sup>	
Moment of inertia, I	1.18E-06 m <sup>4</sup>	
Shear modulus, G	77 GPa	Typical carbon steel [6]

Calculating  $k_1$  and  $k_2$  yields values of near 1.00 for both, indicating that the second term in equation (2.1.1) is generally constant, and most of the deformation is dominated by the first term. Therefore, equation (2.1.1) can be simplified to assume  $k_1$  and  $k_2$  to be near one and constant, thereby making the second term of this equation constant. Additionally, substituting equations (2.1.2) and (2.1.3) into (2.1.1), produces a simplified expression for deformation:

$$\Delta D_v = \frac{-0.4674wR^4}{EI} \quad (2.1.4)$$

As can be seen in the equation above, in order to reduce the change in vertical diameter of the running ring, either the modulus of elasticity,  $E$ , or the second moment of inertia,  $I$ , will have to be increased.

In order to increase the second moment of inertia of the running ring, the geometry will have to be changed. The first step to determining the moment of inertia of the running ring is to determine the location of the neutral axis,  $\bar{y}$ . The neutral axis can be calculated by breaking up the cross section into smaller areas and then using equation (2.1.5):

$$\bar{y} = \frac{\sum y_i A_i}{\sum A_i} \quad (2.1.5)$$

where,

$y_i$  is distance from the centroid of a given area to the bottom of a cross section

$A_i$  is the cross sectional area of a given section

These variables are better illustrated below in Figure 4.

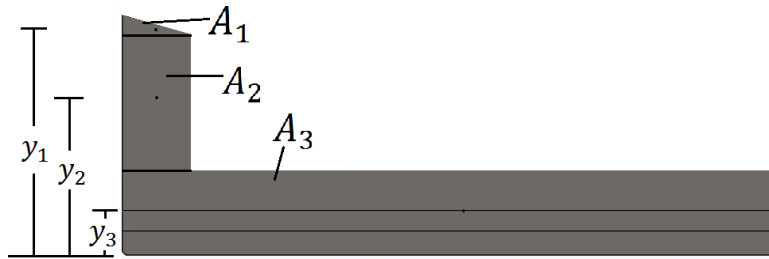


Figure 4: Moment of inertia variables

Once the neutral axis of the cross section is known the moment of inertia can be calculated through equation (2.1.6), which is known as the parallel axis theorem:

$$I = \sum (I_i + A_i d_i) \quad (2.1.6)$$

where,

$I_i$  is the moment of inertia of the given section

$A_i$  is the cross sectional area of the given section

$d_i$  is the distance from the centroid of the given section to the neutral axis

By analysing this calculation process, it can be determined that adding additional areas to the cross section will increase the moment of inertia. More specifically, adding areas whose centroids are distant from the neutral axis will be more effective on increasing the total moment of inertia.

The second method of increasing the bending stiffness is through increasing the modulus of elasticity, which is characterized by equation (2.1.7):

$$\sigma = E\varepsilon \quad (2.1.7)$$

where

$\sigma$  is the normal stress experienced by an object

$E$  is the modulus of elasticity

$\varepsilon$  is the strain experienced by the object

Analysing equation (2.1.7), it becomes clear that the modulus of elasticity is a measurement of how much strain a given material will experience for a given value of stress. Since the modulus of elasticity is a material property, it can only be increased with a change of material. The advantage of a material change is that it can simultaneously improve the stiffness as well as eliminate the existing corrosion concerns. Additionally, a material with a reduced density will experience less deformation given that the previously mentioned properties remain constant or are increased. This is related to equation (2.1.4), where reducing the weight of the ring will also decrease the deformation the ring experiences.

## 2.2 Corrosion of the Running Ring

After visual inspection of the running ring, group analysis concluded that general attack corrosion and galvanic corrosion are the major corrosion concerns on the running ring. General attack corrosion is the most common type of corrosion and is caused by a chemical or

electrochemical reaction that results in the deterioration of the entire exposed surface of a metal [7]. However, general attack corrosion is also the most manageable corrosion. Galvanic corrosion occurs when two different metals are located together in a corrosive electrolyte. A galvanic couple forms between the two metals, where one metal becomes the anode and the other the cathode. The anode, or sacrificial metal, corrodes and deteriorates faster than it would alone, while the cathode deteriorates more slowly than it would otherwise, which is due to the electron transfer between anode and cathode. Two conditions must exist for galvanic corrosion to occur: electrochemically dissimilar metals must be present and the metals must be in electrical contact [8].

As Figure 5 shows, the general attack corrosion happens uniformly on the outer surface of the running ring due to the environment of the water.



**Figure 5: Corrosion on the running ring [9].**

Galvanic corrosion is apparent from the contact between the lantern ring and the running ring which can be seen in Figure 6. The material for the lantern ring is yellow brass while the material for the running ring is carbon steel. This difference in material creates an electrical potential difference between the two metals, thereby increasing the corrosion rate.



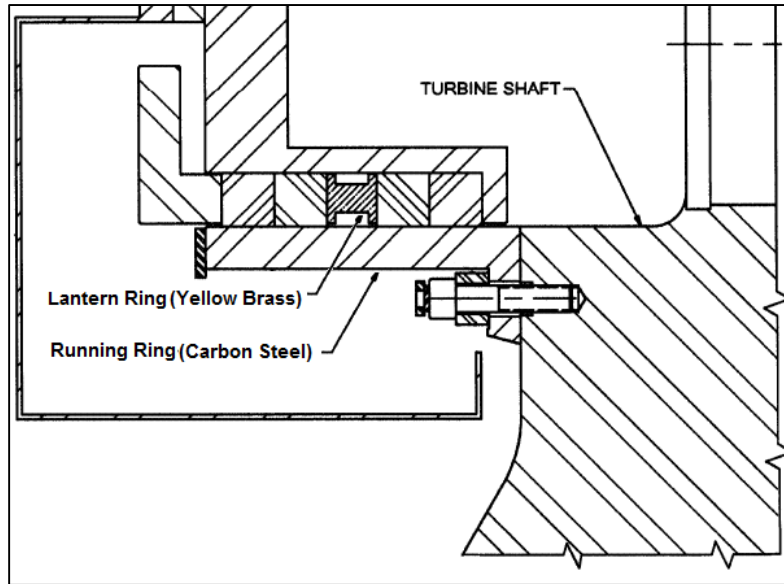


Figure 6: Lantern ring in contact with running ring [9].

## 2.3 Behaviour and Testing of Bolt Properties

It is important to understand that a bolt and nut act like a spring when the bolt is in tension, which is shown in equation (2.3.1):

$$F = kx \quad (2.3.1)$$

where

- $F$  is the load the spring is carrying
- $k$  is the stiffness of the spring
- $x$  is the displacement from equilibrium

Similarly, a ductile material will experience the same behaviour in the elastic zone, which is characterized by (2.3.2):

$$\delta = \frac{FL}{EA} \quad (2.3.2)$$

where

- $\delta$  is the deformation the material undergoes
- $F$  is the axial load applied to the material
- $L$  is the axial length of the material prior to deformation
- $A$  is the cross-sectional area of the material perpendicular to the axial loading axis
- $E$  is the elastic modulus of the material

Using equation (2.3.2), the bolt elongation length can be defined in relation to the preload applied:

$$\Delta L = F_p \left( \frac{L}{EA} \right) \quad (2.3.3)$$

where

$\Delta L$  is the elongation length

$F_p$  is the preload

$\left( \frac{L}{EA} \right)$  is the stiffness factor

However, the cross-sectional area of the bolt is not constant since one section is threaded while the other is not. Since a bolt is treated like a spring, there are two sections as two separate springs in series. Both sections of the bolt undergo the same load and add up to the total deformation, equation (2.3.3) becomes:

$$\Delta L = F_p \left( \frac{L_b}{EA_b} + \frac{L_t}{EA_t} \right) \quad (2.3.4)$$

where

$L_b, A_b$  is the bolt body length and cross-sectional area respectively

$L_t, A_t$  is the threaded length and cross-sectional area respectively

The length of the bolt body will also incorporate half of the length of the bolt head. This is due to the bolt head being in tension, where it is assumed that the tension in the bolt head increases linearly until the bolt body. The same goes for the length of the threads in contact with the nut. To simplify this analysis, it will be assumed that the tension in the bolt head and thread increases linearly. This transition between the bolt head and thread becomes analytically complex because of localized features and stress concentrations. While this simplification is made, the intent is to gather more information about the bolt body undergoing the elongation, where details at this transition zone are minimized. By using half of the length of the bolt head and nut, the situation can be simplified by treating the tension going through the head and nut as area under a triangle. Figure 7 illustrates how tension in the bolt head and nut increases and then plateaus and can be reduced by simplifying the linear increase in stress.

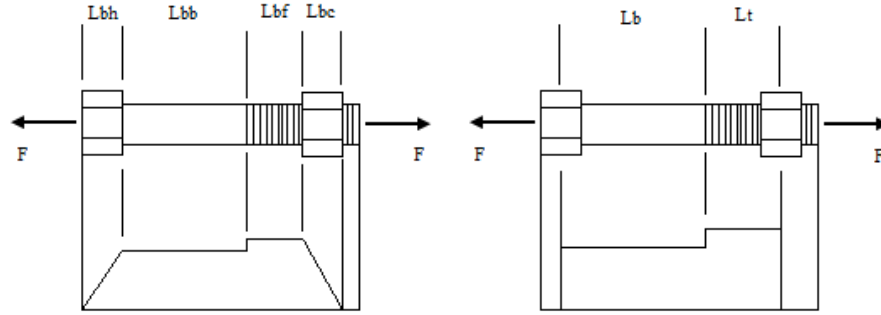


Figure 7: Illustration of tensile load applied through fastener actual and simplified [10].

Given the prior information,  $L_b$  and  $L_t$  can be quantified using equations (2.3.5) and (2.3.6), while threads that are not in tension are not considered:

$$L_b = \frac{L_{bh}}{2} + L_{bb} \quad (2.3.5)$$

$$L_t = \frac{L_{bc}}{2} + L_{bf} \quad (2.3.6)$$

where

$L_{bh}$  is the length of the bolt head

$L_{bb}$  is the length of the bolt body

$L_{bc}$  is the length of the bolt in contact with the nut

$L_{bf}$  is the length of the free threads

Cross sectional area of the bolt body can be found using equation (2.3.7):

$$A_b = \frac{\pi}{4} D^2 \quad (2.3.7)$$

where

$D$  is the diameter of the bolt body

The cross-sectional area of the threads can be found using the equation (2.3.8) [11]:

$$A_b = \frac{\pi}{4} (D - 0.938P)^2 \quad (2.3.8)$$

where

$P$  is the pitch at which the threads lie

Once the cross-sectional areas are determined, the preload needed to achieve 60% of yield of the bolt can be calculated, which is a criterion that is often used by Manitoba Hydro for fasteners in tension. In order to find preload, equation (2.3.9) will be used. The minimum cross-sectional area through the threads is used for the bolt, because higher force occurs in the threads.

$$F_p = 0.6 \sigma_{yld} A_t \quad (2.3.9)$$

where

$\sigma_{yld}$  is the yield stress of the bolt

With all the determined unknowns, the elongation length can be calculated and use it in finding the nut factor. The main equation behind finding the nut factor K and the goal of this project is the short form relation between torque and pre load, is shown by (2.3.10) [11].

$$K = \frac{T}{F D} \quad (2.3.10)$$

where

$K$  is the nut factor

$T$  is the torque applied

$F$  is the pre-load

$D$  is the nominal diameter

By determining the elongation length, the calculated pre-load can be verified and find the associated nut factor. With all the known values, the nut factor K can be determined.

### 3 Concept Generation and Search Results

The next step in the design process is to develop concepts that could be possible solutions to the design problem, using as many creative tools and processes to generate as many ideas as possible. With the variables for each of the problem areas identified, different aspects can be examined more carefully as the team now knows the behavior related to certain design variables and its implications if certain variables are changed. This will be especially helpful in scoring and weighing the concepts to achieve an optimal design to proceed with in detailed design.

#### 3.1 Addressing Running Ring Deformation (CN5)

As mentioned in section 2.1 Deformation of Running Ring, the deformation of the running ring is primarily due to the stiffness of the material, its own weight, and its cross-sectional moment of inertia. Each of the developed concepts are methods of controlling and improving either the cross-sectional moment of inertia, or the modulus of elasticity through a material change.

##### 3.1.1 Methods of Increasing Moment of Inertia (A1)

As previously mentioned, either the second moment of inertia of the running ring or Young's Modulus will have to be increased in order to increase the stiffness of the running ring. The following concepts were generated with the goal of increasing the second moment of inertia of the current running ring design. The current running ring cross section is shown in Figure 8 to compare to the design concepts. The cut slot shown in the running ring is a keyway used during the installation process.

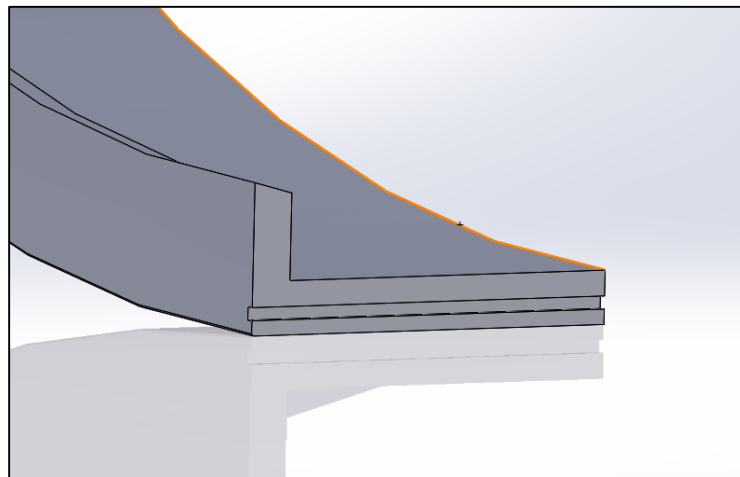


Figure 8: Original running ring cross-section [12].

Concepts below, with concept ID's A1.1.1 through A1.1.4, are ideas on how the cross-section can be modified to increase the moment of inertia.

**A1.1.1 Increased thickness:** This design involves increasing the thickness of the running ring, shown in Figure 9. Because there is limited space within the current shaft seal assembly, there is a maximum amount that this thickness can be increased. Additionally, increasing the thickness will have an impact on other portions of the shaft seal. Increasing this thickness will shift the location of the holes on the running ring flange used to fasten the running ring to the turbine shaft. If this design were to be implemented, the holes in the turbine shaft will also need to be moved. However, the holes would only be required to move a short distance, and therefore the new hole pattern would likely overlap with the existing hole pattern. In order to prevent this overlap, the hole pattern will also have to be shifted radially. The shift in the hole pattern has been approved by Manitoba Hydro, and this concept will be considered despite the changes to mating components. This idea is illustrated in Figure 10.

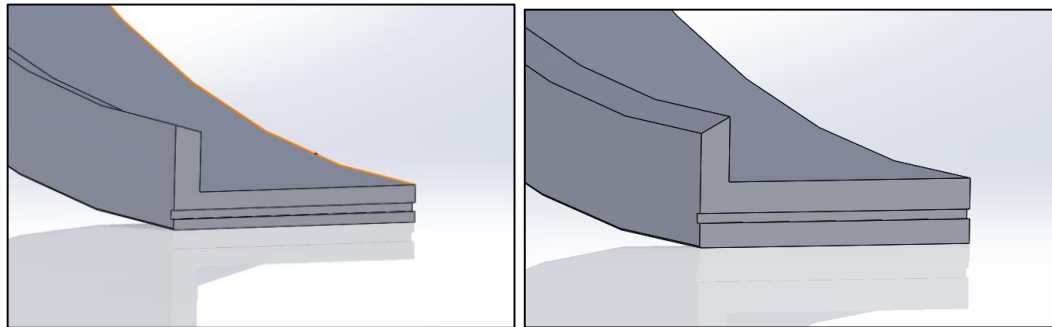


Figure 9: Original versus concept A1.1.1: increased thickness [13].

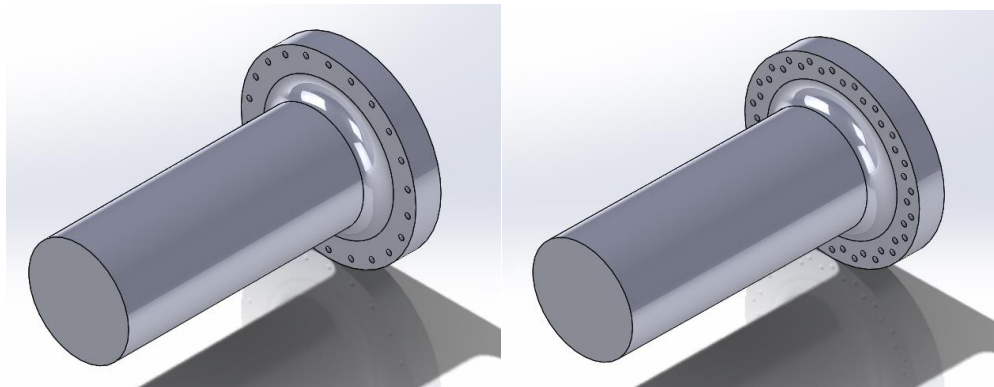


Figure 10: Original versus resulting A1.1.1 concept turbine flange hole pattern [14].

**A1.1.2 Increased flange dimensions:** This design involves increasing the size of the existing flange of the running ring, which is used to fasten the running ring to the turbine shaft. This design can be seen in Figure 11, illustrating the running ring flange with either an increased thickness or length. Just like A1.1.1, changing dimensions of the running ring flange will have implications on other shaft seal components. Increasing the length of the turbine flange will shift the hole pattern in the same way that it would have to be done for concept A1.1.1. Increasing the thickness will require an increased cap screw length used to fasten the running ring to the turbine shaft. This cap screw can be seen in Figure 12.

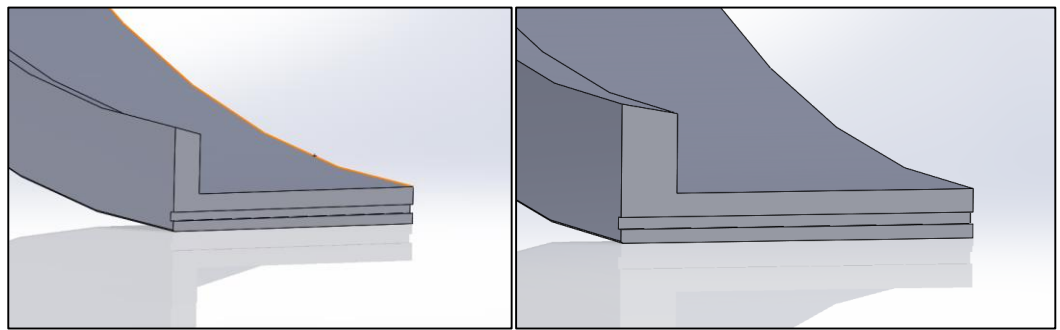


Figure 11: Original versus concept A1.1.2: increased flange dimensions [15].

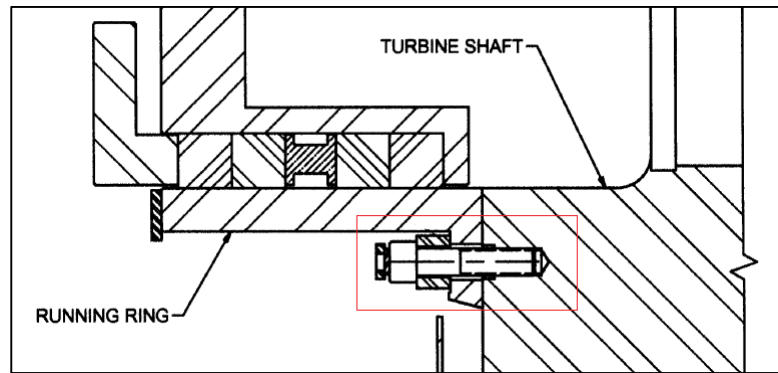


Figure 12: Running ring flange cap screw [16].

**A1.1.3 Added flange:** this concept involves adding an additional flange on the running on the side opposite of the existing flange. This design will not require any changes to other shaft seal components. However, this design may add a level of complexity to the installation process if the added flange causes restricted space for the installation of neighboring components. This concept is demonstrated in Figure 13.

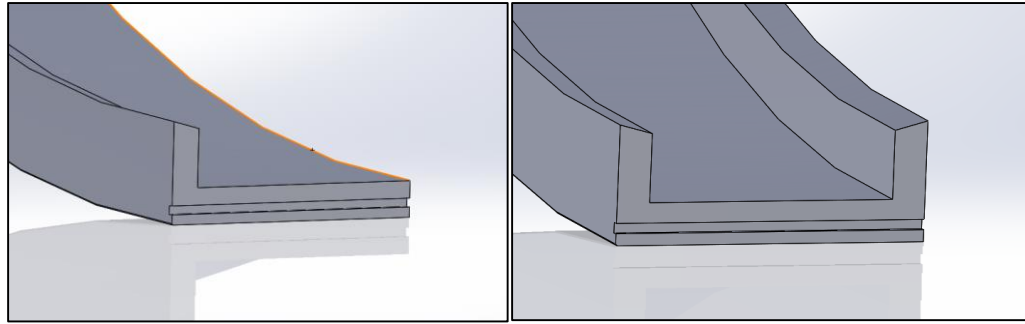


Figure 13: Original versus concept A1.1.3: added flange [17].

**A1.1.4 Ribbed:** This design concept involves adding ribs radially along the running ring. This design will not require any changes to mating seal components. However, this design may not sufficiently increase the moment of inertia as it will only change the moment of inertia value at certain locations of the cross section. This concept is shown below in Figure 14.

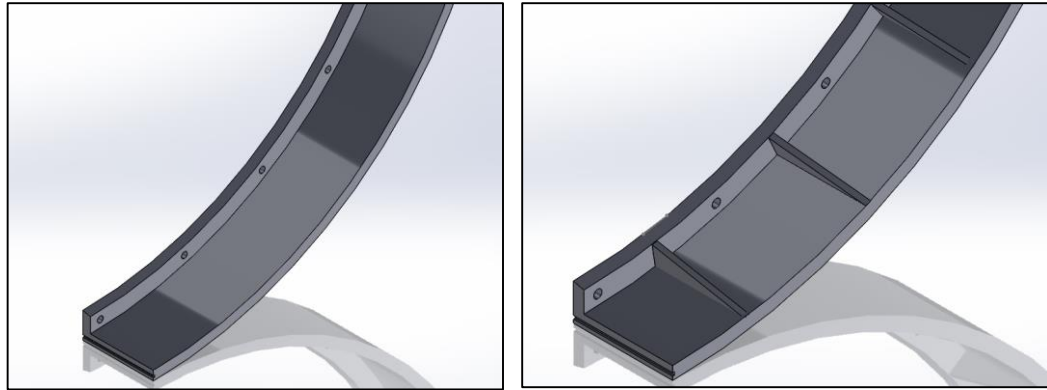


Figure 14: Original versus concept A1.1.4 ribbed [18].

### 3.1.2 Methods of Increasing Modulus of Elasticity (A2)

The second method of increasing the stiffness of the running ring is through a material change, in efforts to increase the modulus of elasticity,  $E$ , and decrease the density,  $\rho$ . Our team researched materials to potentially replace steel to fabricate the running ring. Materials with both high moduli of elasticity and low densities were considered, these materials are shown in TABLE VIII.



TABLE VIII: PROPERTIES OF CONSIDERED MATERIALS

Concept ID	Material	Young's Modulus (GPa) [5]	Density (kg/m <sup>3</sup> ) [19]
A2.1.1	Stainless Steel (302)	180	8000
A2.1.2	Titanium Alloy (Ti-6Al-4V)	105-120	4430
A2.1.3	Nickel Alloy (625)	207.5	8440
A2.1.4	Brass	102-125	8480
A2.1.5	Copper	117	8790
A2.1.6	Gray Cast Iron	130	7200
A2.1.7	Nickel	170	8900
A2.1.8	Steel, Structural ASTM-A36 (Reference)	200	7850
A2.1.9	Beryllium	287	1850
A2.1.10	Diamond	1220	3510
A2.1.11	Graphene	100	2000
A2.1.12	Molybdenum	329	10280
A2.1.13	Sapphire	435	380
A2.1.14	Tungsten	400-410	19250

These materials will be compared with the material recommendations made to address the running ring corrosion to determine a multifunctional material that meets all of the customer requirements.

### 3.2 Addressing Running Ring Corrosion (CN6)

The following chart in Figure 15 illustrates two general methods of increasing corrosion resistance. All the different entries from this chart will be explained, screened and scored in the following section.

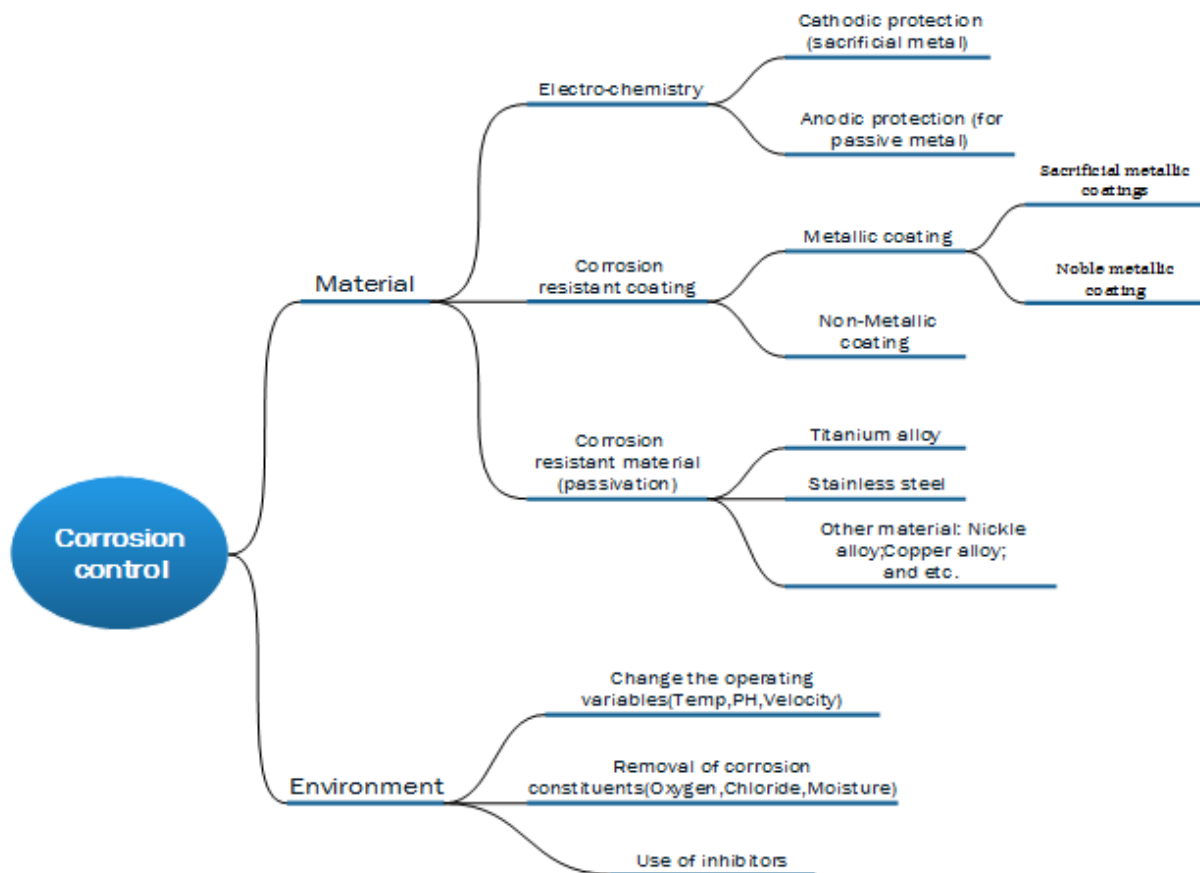


Figure 15: Methods of corrosion control.

### 3.1.3 Coatings (B1)

Each method associated with changing a material to control corrosion resistance will be discussed, addressing how applicable a particular method is for the type of corrosion.

The first method to be considered to make the material more corrosion resistant is by adding a coating. Generally speaking, there are two major types of coatings; metallic and non-metallic.

**B4.1.0 Non-metallic coating:** This method involves adding a non-metallic material to protect the metal from a corrosive environment. Such material includes vinyl, silicone aluminum, and epoxy [7].

**B4.1.1 Metallic Coating:** There are two types of metallic coatings; noble and sacrificial metallic.

Sacrificial metallic coatings achieve galvanic protection, by coating a more active metal layer on top of the protected metal. In this case, the more active metal layer will corrode faster while the protected metal will corrode much slower. Sacrificial metallic coatings include aluminum, zinc, and cadmium.

For noble metallic coatings, there are several corrosion resistant metals, which will passivate with oxygen. The passivated thin film will act as a barrier between environment and substrate. The key factor for noble metallic coatings is having porous free surfaces, as the coatings may accelerate the corrosion if they are both exposed to the surroundings. There are five popular ways to apply the metallic coatings such as electroplating, hot dipping, spray coating, diffusion coating and cladding [8]

TABLE IX shows the corrosion resistance of various non-metallic materials. The coatings were weighed on a scale from 1 to 10, 1 being least corrosion resistant and 10 being most corrosion resistant.

**TABLE IX: RESISTANCE OF COMMON COATINGS TO VARIOUS ENVIRONMENTS [7]**

ID	Name	Acids	Salts	Solvents	Water	Weather	Oxidation	Abrasion
B4.1.2	Oil-base	1	6	2	7	10	1	4
B4.1.3	Alkyd	6	8	4	8	10	3	6
B4.1.4	Chlorinated rubber	10	10	4	10	8	6	6
B4.1.5	Coal-tar epoxy	8	10	7	10	4	5	4
B4.1.6	Catalyzed epoxy	9	10	9	10	8	6	6
B4.1.7	Silicone aluminum	4	6	2	8	9	4	4
B4.1.8	Vinyl	10	10	5	10	10	10	7
B4.1.9	Urethane	9	10	10	9	10	8	10

The current environment that the running ring is exposed to include water, from sitting in stagnant river water, and abrasion, due to the friction between the packing and the running ring.

### 3.2.1 Material Change (B2)

The second method of improving the corrosion resistance is by changing the material of the running ring, which may or may not include a coating. A list of typical materials are presented because they are commonly used in the market. Each material is explained below.

- B4.2.1 Titanium:** The titanium alloy is among the most corrosion resistant materials because it will react with oxygen instantaneously when it is exposed to air and form an oxidized film. This oxidized film is non-polarized and compact [8]. This stable film will protect the alloy beneath and act as a barrier to prevent the titanium alloy from losing electrons to its surroundings. Besides the corrosion resistance, titanium alloy is strong and has a relatively high strength to weight ratio. The material and manufacturing costs associated with titanium alloys are relatively high.
- B4.2.2 Stainless Steel:** Similar to titanium, stainless steel is corrosion resistant due to the passivation of its chromium content. The chromium forms a passivation layer of chromium(III) oxide ( $\text{Cr}_2\text{O}_3$ ) when exposed to oxygen [20]. The layer is too thin to be visible, and the metal remains smooth. The layer is impervious to water and air, protecting the metal beneath, and this layer quickly reforms when the surface is scratched. Stainless steel also has a similar modulus of elasticity to that of carbon steel. The manufacturing cost of stainless steel is relatively low.
- B4.2.3 Nickel alloy:** The high corrosion resistance of nickel alloy is due to the non-corrosive properties of nickel itself. More importantly, the metal can be alloyed with other elements such as copper, chromium, iron, and molybdenum without the formation of unstable, unsuitable or detrimental phase [21]. The cost of nickel alloy can be excessive.
- B4.2.4 Tantalum:** Tantalum has superior resistance to most environments. A few exceptions include alkalis, hydrofluoric acid and hot concentrated sulfuric acid [7]. However, the cost of tantalum is high relative to common metals like steel and aluminum.

### 3.2.2 Electro-chemical methods (B3)

The third method of improving the corrosion resistance is by including an electro-chemical protection, which can be separated into two different types: cathodic and anodic protection.

**B4.3.1 a Cathodic protection:** Generally speaking, there are two types of cathodic protection, which are unpowered cathodic protection and externally powered cathodic protection. Unpowered cathodic protection uses the strong reducibility of one metal to protect the main material. This allows the whole system to become a primary battery. The strong reducibility of metal will have an oxidation-reduction reaction as anode. The protected metal will work as a cathode, which will be protected from corrosion [7]. The methodology is demonstrated in Figure 16.

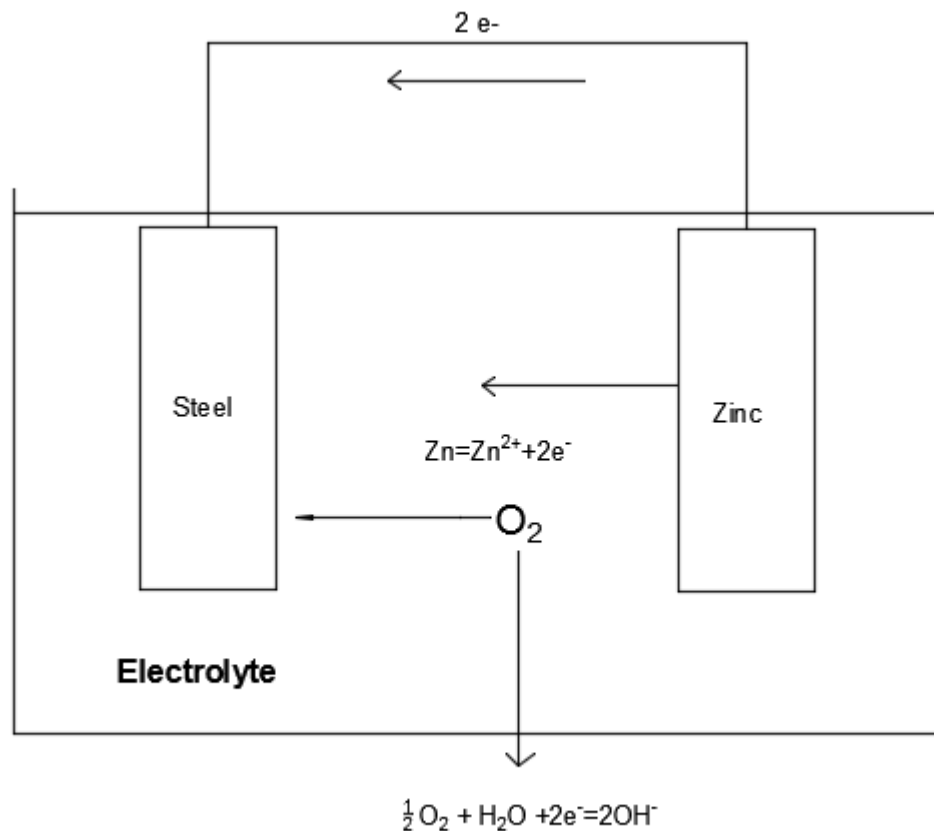


Figure 16: Unpowered cathodic protection chemistry [22].

**B4.3.1b Impressed cathodic protection:** For larger structures, and where electrolyte resistivity is high, galvanic anodes cannot economically deliver enough current to provide protection. In these cases, impressed current cathodic protection (ICCP) systems are used. These consist of anodes connected to a DC power source or often a transformer-rectifier connected to AC power. This methodology is shown in Figure 17.

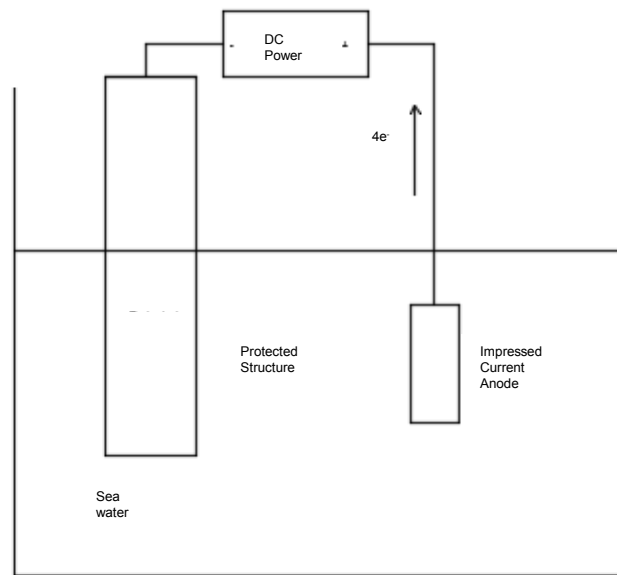


Figure 17: ICCP system diagram [23].

**B4.3.2 Anodic protection (AP):** Is a technique to control the corrosion of a metal surface by adding an external battery to the metal. This generates a passivation coating on the metal, effectively protecting the material from corrosion [24].

### 3.2.3 Environment Changes (B4)

The fourth method of improving the corrosion resistance is by modifying the environment, rather than the running ring itself. There are three common ways to make the environment less corrosive:

- B4.4.1 Changes to the operating variables:** changing the operating variables such as temperature, pH, and velocity can reduce the corrosion rate.
- B4.4.2 Removal of corrosion constituents:** corrosion constituents such as oxygen, chloride, and moisture will create a corrosive environment. Removal of these corrosion constituents will improve the corrosion resistance [8].
- B4.4.3 Inhibitors:** the addition of inhibitors onto the surface of the material to slow the chemical reaction can improve the corrosion resistance.

With the concepts generated to improve the corrosion resistivity and alignment issues proposed, the bolt testing apparatus and procedure are to be considered.

### 3.3 Bolt Testing Concepts (CN10)

The purpose of the bolt testing apparatus and procedure is to determine the nut factor  $K$ . The main variables in calculating the nut factor are, torque and preload, which have been outlined in the Section 2.3.

#### 3.3.1 Bolt Specifications

The initial design process started with brainstorming and intuition. The main areas of focus for design were verification of torque and preload. Basic sketches were created within the generation stage and then screened. Screened sketches were then developed into designs and then weighed and scored again. The scored designs progressed by calculating the variables needed to determine the nut factor. Finally, by taking into consideration variables such as clearances, plate thickness and other factors that affect the environment in which this test is performed, the final design could be developed.

In this design phase, methods of verifying torque and preload were conceptualized. It was found that applying a torque would be more convenient than applying a force, because applying such a force would need to be done with more than just manpower. Torque was ruled as a constant input variable, while preload was ruled as a measurement value.

In the screening matrix below, testing methods are compared against each other. Testing methods included load cells, strain gages and destructive testing. The elongation length measurement methods were then considered as a method of verification of pre-load. These testing methods were compared to areas such as design repeatability, similar conditions to that of the current fasteners on the running ring, and adequate strength against loading conditions. Furthermore, consideration of cost and accuracy of measurements were also assessed in the matrix.

TABLE X communicates the various methods of measurement and how they scored against the design metrics. The benchmarking for the screening matrix followed a +,0,- criteria. Where + states that the idea in consideration is better than average, 0 states that the idea is neutral to average, and – states that the idea is worse than average.

TABLE X: SCREENING MATRIX OF THE TESTING METHODS FOR DESIGN IDEA BASIS

	Accurate	Safety	Ease of use and analysis	Repeatability	Manufacturability	Cost	Similar Conditions	Weight	Total Pluses	Total Same	Total Minuses	Overall Score
Apply torque and measure preload with strain gages	+	0	-	0	-	-	0	0	1	4	3	-2
Apply torque and measure preload through destructive testing	-	0	+	0	0	0	-	0	1	5	2	-1
Apply torque and measure elongation length through the use of a micrometer or caliper.	0	0	+	0	0	0	0	0	1	7	0	1
Apply torque and measure preload with load cells	+	0	-	0	-	-	0	0	1	4	3	-2

Exploring the option of strain gages and load cells uncovered that equipment for testing and supporting devices was complex and expensive. The purpose of this test is to remain simple and inexpensive. Therefore, strain gages and load cells were ruled out for the test design.

Having preload determined by destructive testing was another viable option. When a bolt is torqued until failure the nut factor  $k$  may be determined by relating the rated ultimate stress and max torque achieved on the bolt. Unfortunately, this solution caused problems with obtaining accurate readings due to a variance in destructive loads. It was also limiting in trying to recreate a similar environment with what is currently occurring on the running ring.

Exploring options within preload such as elongation length have found that simple, affordable and accurate devices can be used to determine elongation length. However, this type of analysis



may lack in accuracy when compared to load cells. With enough results, convergence is still possible for the applicable nut factor  $K$  (averaging results). Given that, it was determined to further explore designs related to verifying preload through a measure elongation length.

Generation of concepts was completed, by making sketches and considering things such as ease of use, cost and similar conditions to that of the running ring. Final designs were created and scored to determine which would be best to carry forward with, and apply further conditions on.

Once a final design was approved, determining dimensions that would be design boundaries was considered. Calculating preload and elongation length was pivotal in creating these boundaries. Understanding the layout of a metric bolt is important when trying to replicate the conditions of running ring fasteners. Figure 18 show the representation of the layout of a metric bolt.

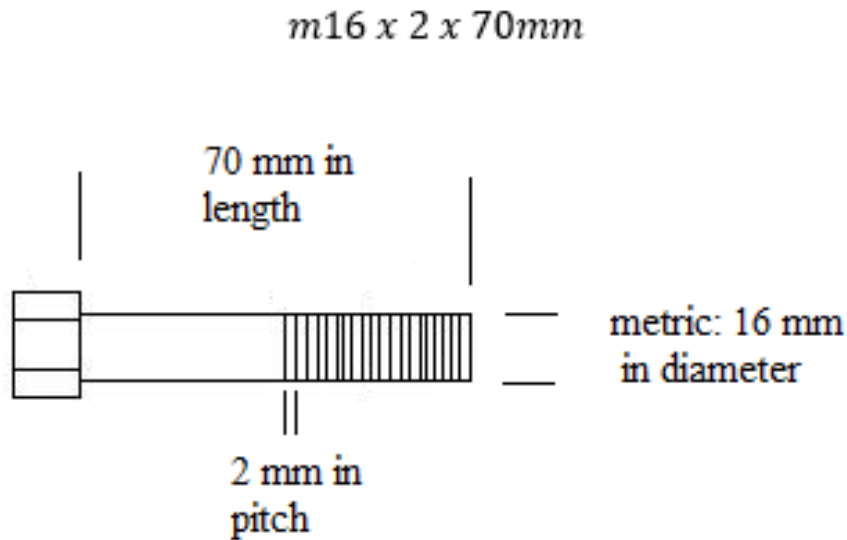


Figure 18: Description of metric bolt [25].

With the bolt properties determined through Manitoba Hydro engineering drawings, the bolt properties can be calculated, which are shown in TABLE XI [9].

TABLE XI: MANITOBA HYDRO M16X2X70MM BOLT PROPERTIES

Elastic Modulus for ASTM A193 B7 [11] (Pa)	Yield Strength of ASTM A193 B7 [5](Mpa)	Thread Pitch (mm)	Bolt Diameter (mm)	Bolt Length (mm)	Thread Length (mm)	Bolt body length (mm)	Threads in contact (mm)	Threads exposed (mm)	Bolt head length (mm)
2.0477E+11	723.95	2	16	70	44	26	24	20	16

Firstly, effective lengths were determined using equations (2.3.5) and (2.3.6), which are seen below.

$$L_b = \frac{L_{bh}}{2} + L_{bb} \quad L_t = \frac{L_{bc}}{2} + L_{bf}$$

$$L_b = \frac{16}{2} + 26 \quad L_t = \frac{24}{2} + 20$$

$$L_b = 34 \text{ mm} = 0.034 \text{ m} \quad L_t = 32 \text{ mm} = 0.032 \text{ m}$$

Once the effective lengths have been found, the area in which force acts on was calculated through equations (2.3.7) and (2.3.8), which can be seen below.

$$A_b = \frac{\pi}{4} D^2 = \frac{\pi}{4} 16^2 = 201.06 \text{ mm}^2 = 0.000201 \text{ m}^2$$

$$A_t = \frac{\pi}{4} (D - 0.938P)^2 = \frac{\pi}{4} (16 - 0.938(2))^2 = 156.68 \text{ mm}^2 = 0.000157 \text{ m}^2$$

Preload was then verified using the elongation length. Preload is determined by applying equation (2.3.9).

$$F_p = \sigma_{yld} \times A_t \times 0.6 = 723.95 \times 10^6 \times 0.000157 \times 0.6 = 87335.27 \text{ N}$$

With all of the unknowns quantified, the elongation length can be determined, which is used to verify the preload from equation (2.3.4).

$$\Delta L = F_p \left( \frac{L_b}{EA_b} + \frac{L_t}{EA_t} \right)$$

$$\Delta L = 87335 \left( \frac{0.034}{2.047 \times 10^{11} \times 0.000201} + \frac{0.032}{2.047 \times 10^{11} \times 0.000157} \right)$$

$$\Delta L = 0.000160 \text{ m}$$

These results are shown in TABLE XII.

TABLE XII: CALCULATED M16X2X70MM BOLT PROPERTIES

Elongation length (mm)	Effective stress on threads $A_s$ (mm <sup>2</sup> )	Cross sectional area of bolt body $A_b$ (mm <sup>2</sup> )	Effective body length $L_b$ (mm)	Effective Thread Length $L_t$ (mm)	Inverse of stiffness of bolt body (m)	Inverse of stiffness of bolt threads (m)	Preload $F_p$ (N)
0.00016	156.67	201.06	34	32	1.06E-09	7.77E-10	87335
in (inch)							lbs
0.0063							19633

By applying the short form equation of the relation of torque to preload, the nut factor can be determined, which is show below.

$$K = \frac{T}{F D}$$

Until the test is performed, the applied torque cannot be determined nor verify the preload. However, these properties can be used to begin modelling. By replicating these conditions from the running ring in the design, an accurate nut factor can be determined.

### 3.3.2 Nut Factor Conceptual Design

By applying the design methodology, preliminary designs can be conceptualized, which improved versions are built upon them, until one design meets all of the customer requirements for a final conceptual design.

Preliminary designs and sketches were influenced by criteria outlined in the design methodology, which include but do not only pertain to ease of use and cost.

**C1.1.1a Initial design 1:** By torquing the nut and bolt down to the needed load, a micrometer can be used to validate the results. Therefore, a simple design such as shown in Figure 19 would solve the goal of measuring the elongation length and determining the nut factor K.



Figure 19: Concept C1.1.1a sketch side view [26].

- C1.1.1b** Concerns about how one hole may affect another on the apparatus during testing, or how the apparatus is going to be supported (clamped, free standing), needed to be addressed. Additional concerns regarding manufacturability, mainly, the thickness of the metal, repeatability, and strength of the test, are going to be considered. Economically, using more than one block of steel makes sense, because blocks of metal are typically more expensive than thick sheet metal. Taking these concerns into consideration, the design evolved, which can be seen in Figure 20.

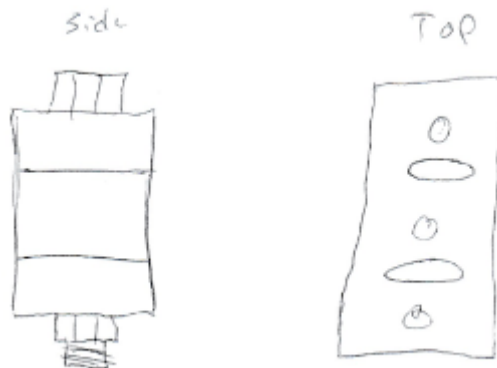


Figure 20: Concept C1.1.1b side and top view [27].

- C1.1.1c** In C.1.1.1b, the side view of the material has been divided up to allow for ease of manufacturing and cost. On the top view, slots that have been created to keep clamping forces from interfering with each other by increasing the distance that the force must travel. In Figure 21 below, flanges were added to support and secure the apparatus.

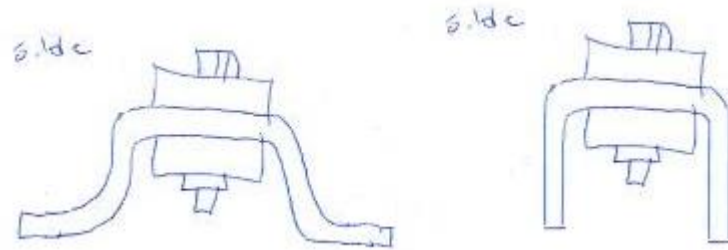


Figure 21: Concept C1.1.1c stabilizing design side views [28].

**C1.1.1d** The stability of the apparatus was further secured by adding locations for possible bolts to go through and provide mounting; this design can be seen in Figure 22.

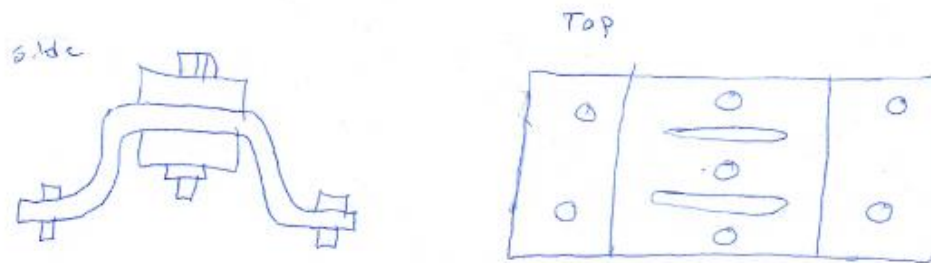


Figure 22: Concept C1.1.1d side and top view [29].

**C1.1.2** In Figure 23, repeatability is to be achieved by making the apparatus larger to allow for more holes, which also increased the ease of access to the bolts.

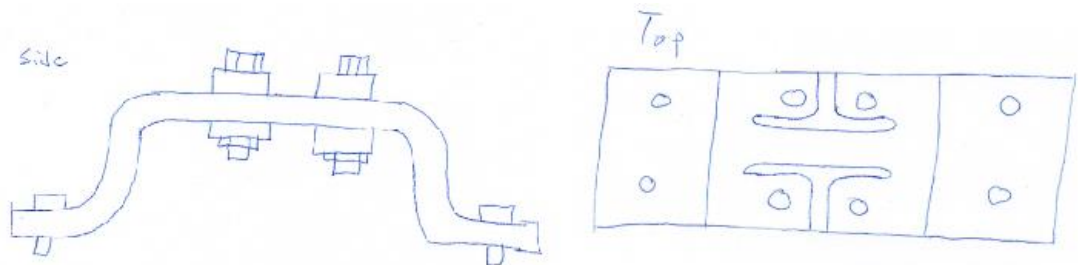


Figure 23: Design C1.1.2: Side and top view [30].

**C1.1.3** Building off the previous design C1.1.1d, the ease of access to the bolt for measuring and torqueing was considered. In Figure 24, by splitting the apparatus into halves, this allows for easier access but restricts the apparatus from standing alone.

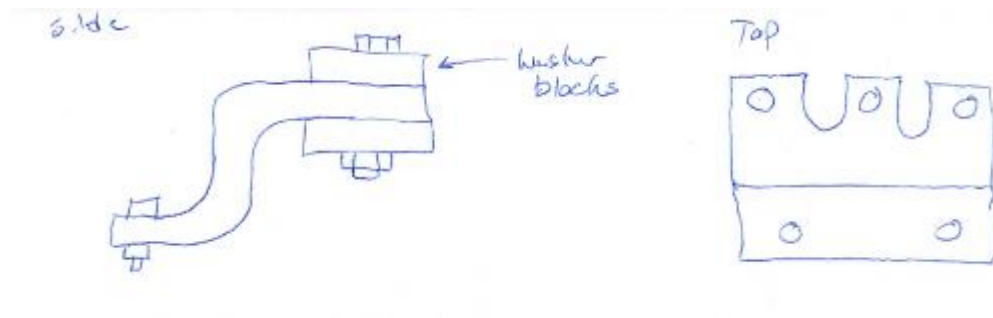


Figure 24: Design C1.1.3: Side and top view [31].

### 3.4 Concept Generation Summary

In summary, the concepts developed were to focus on three distinct areas, indicated by the appropriate customer need ID:

1. Running ring deformation (CN5): focusing on the alignment issues with the running ring deforming due to its own weight, two key methods of addressing this are:
  - a. Increasing the moment of inertia (A1): a total of four concepts were generated, A1.1 through A1.4, each with different cross-sectional shapes and features on the running ring, proposed to increase the bending stiffness.
  - b. Increasing the modulus of elasticity (A2): 14 different materials with high moduli of elasticity are considered to increase the bending stiffness. This will need to be integrated with the corrosion resistant concepts to choose a material that meets all of the customer needs.
2. Running ring corrosion (CN6): with the running ring undergoing circumferential corrosion, a variety of methods for increasing the resistivity against corrosion are proposed:
  - a. Use of coatings (B1): metallic coatings (B.1.0) and a variety of non-metallic coatings (B.1.2-B.1.9) are considered to be added to the surface of the running ring to act as a shield for the main running ring material.
  - b. Material change (B2): changing the material of the running ring also can improve the corrosion resistance; four materials (B.2.1-B.2.4) are being proposed. The stiffness of the material must also be considered to address CN5.

- c. Electro-chemical methods (B3): including anodic and cathodic protections in place can increase the corrosive resistivity. Concepts B.3.1a, B.3.1b, and B.3.2 are proposed.
  - d. Environmental changes (B4): making the environment the running ring is operating less corrosive also can improve the corrosive resistivity; concepts B.4.1 through B.4.3 are proposed.
3. Bolt testing concepts (CN10): to determine the nut factor for given fasteners, an apparatus and corresponding procedure must be designed. A total of six concepts are proposed, with the first four being derivatives of each other.

With the concepts now generated and qualitatively defined, they can be assessed against the other customer needs to determine which to proceed into detailed design with.

## 4 Concept Analysis and Selection

With the concepts now outlined, each will be taken through selection matrices which will facilitate a systematic method of ending with potential solutions to invest detailed design into.

### 4.1 Addressing Running Ring Deformation (CN5)

The first analysis will score the concepts developed to address the running ring deformation, specifically regarding the geometry and material.

#### 4.1.1 Methods of Increasing Moment of Inertia (A1)

Before in depth analysis was performed to determine optimal dimensions for any of the designs, the seven preliminary were narrowed down to three. This was done through the use of a selection matrix. Specifically, the criteria were used in the selection matrix were:

1. **Changes to seal components (CN8):** the new design for the running ring should result in minimal changes to the mating components of the shaft seal. This criterion is a measure of the level of changes that will be required to be made to mating components of the running ring should the design be implemented.
2. **Added complexity to installation process (CN7):** One of the major aspects of the running ring redesign is to shorten the lengthy installation time. The running ring assembly is currently congested, and adding additional design features to the design can limit space and make the installation process more complex.
3. **Manufacturability (CN9):** Manufacturability is an important selection criterion as any design that is created must be possible to create in a machine shop with standard manufacturing processes. It may be possible to create an intricate design that satisfies the problem statement, however having the design being possible to manufacture is critical to consider.
4. **Cost (CN1):** Cost of implementing a design must always be considered in any engineering application. However, in this case, the cost of the turbine downtime is so great that if the installation time can be reduced, then having an excessive cost of implementing a design will be justified.
5. **Weight (CN6 and CN7):** As previously mentioned, since the running ring is deforming under its own weight, having a lighter design for a given material will result



in less deformation. Although the moment of inertia of the running ring is to be increased and the weight of the design will likely be greater than the original design, the redesigned running ring will be optimized to encompass the lightest weight possible.

6. **Increased moment of inertia (CN7):** Increasing the moment of inertia is the main objective of changing the geometry of the running ring. Although the magnitude of the increase in the moment of inertia cannot be determined without performing calculations, a general idea of how much each design will increase the moment of inertia value can be estimated.

In order to determine how each of these criteria should be weighted, they were formatted into what is known as a criteria weighting matrix. This involves each criterion being compared directly to every other criterion to determine which is more crucial in producing a design that can achieve the problem statement. The weighting of each criterion is then based on the importance of said criterion when compared to others. This criteria weighting matrix can be seen in TABLE XIII.

**TABLE XIII: DM A1: INCREASING MOMENT OF INERTIA CRITERIA WEIGHTING MATRIX**

		Changes to seal components	Added complexity to installation process	Manufacturability	Cost	Weight	Increased moment of inertia
		a	b	c	d	e	f
Changes to seal components	a		a	a	a	a	f
Added complexity to installation process	b			b	b	b	f
Manufacturability	c				c	c	f
Cost	d					e	f
Weight	e						f
Increased Moment of inertia	f						
Total Hits		4	3	2	0	1	5
<b>Weight:</b>		<b>0.27</b>	<b>0.20</b>	<b>0.13</b>	<b>0.00</b>	<b>0.07</b>	<b>0.33</b>

Since the cost criterion was not deemed more important than any other criterion, it resulted with a weighting of zero. For this reason, this criterion will no longer be considered for evaluating concepts related to increasing the moment on inertia.

Once the weightings for each criterion were determined, each design was given a rank on each criterion. These ranking ranged from a value of 1, if it was felt the design would perform poorly in that category, to 4 if it was predicted that it would have exceptional performance in the given area. The rankings of each design for each selection criteria can be seen in TABLE XIV.

**TABLE XIV: DM A1: INCREASING MOMENT OF INERTIA SELECTION MATRIX**

Selection Criteria	Weight	Increased Thickness	Increased Flange Dimensions	Added Flange	Ribbed
Changes to Seal Components	0.27	2	3	4	4
Added complexity to installation process	0.20	3	3	2	3
Manufacturability	0.13	3	3	3	2
Weight	0.07	2	4	3	3
Increased Moment of Inertia	0.33	3	1	2	2
Total	1	2.67	2.40	2.73	2.80
Ranking		2	4	1	4
Continue?		YES	NO	YES	Yes

The selection matrix indicated that the three best designs on which to perform further analysis are the running ring with the increased thickness, with the added flange, and the ribbed design. These three designs will proceed into detailed design which will ultimately determine the best one. It may be found that one of these concepts may not be able to achieve a sufficiently large moment of inertia value, and the ideal design may be a combination of these concepts.

#### 4.1.2 Methods of Increasing the Modulus of Elasticity (A2)

Having 14 potential materials to considered is excessive, and therefore the considered materials were screened for their feasibility in order to eliminate concepts that are impractical to implement for various reasons. The feasibility screening can be seen in TABLE XV.

**TABLE XV: DM A2.1: MATERIAL FEASIBILITY SCREENING**

ID	Design Idea	Feasibility Screen (Pass/Fail)	Justification
A2.1.1	Stainless Steel (302)	Pass	
A2.1.2	Titanium Alloy (TI-6AL-4V)	Pass	
A2.1.3	Nickel Alloy (625)	Pass	
A2.1.4	Brass	Pass	
A2.1.5	Copper	Pass	
A2.1.6	Gray Cast Iron	Fail	Casting cost not justified for number of parts required
A2.1.7	Nickel	Pass	
A2.1.8	Steel, Structural ASTM-A36 (Reference)	Pass	
A2.1.9	Beryllium	Fail	Excessive Cost
A2.1.10	Diamond	Fail	Excessive Cost
A2.1.11	Graphene	Fail	Excessive Cost
A2.1.12	Molybdenum	Fail	Excessive Cost
A2.1.13	Sapphire	Fail	Excessive Cost
A2.1.14	Tungsten	Fail	Excessive Cost

Each selection criteria are compared to each other to determine their priority. This is shown in TABLE XVI.

**TABLE XVI: DM A2.2: WEIGHING MATRIX FOR MATERIAL**

		Modulus of Elasticity	Density	Economics	Manufacturability
		a	b	c	d
Modulus of Elasticity	a		a	a	d
Density	b			b	d
Economics	c				c
Manufacturability	d				
Total Hits		2	1	1	2
Total Possible		6	6	6	6
Weight:		0.33	0.17	0.17	0.33

Once the criteria were weighted appropriately, each material was ranked on each criterion on a scale of 1 to 4, similarly to TABLE XIV. The completed selection matrix can be seen in TABLE XVII.

**TABLE XVII: DM A2.2: MATERIAL SELECTION MATRIX**

Selection Criteria		Stainless Steel (302)	Titanium Alloy	Nickel Alloy	Brass	Copper	Nickel	Steel
	Weight	Value	Value					
Modulus of Elasticity	0.33	2	1	4	1	1	2	3
Density	0.17	2	4	2	2	2	2	2
Economics	0.17	4	2	2	2	2	2	4
Manufacturability	0.33	4	3	3	3	3	3	4
<b>Total</b>		<b>3.00</b>	<b>2.33</b>	<b>3.00</b>	<b>2.00</b>	<b>2.00</b>	<b>2.33</b>	<b>3.33</b>

As seen in the results above, the current material and structural steel are the most favorable for reducing the deformation in the running ring. However, there are other materials that received scores close to that of structural steel that are likely to improve corrosion resistant properties, which will be addressed in section 4.2.

## 4.2 Addressing Running Ring Corrosion (CN6)

To narrow the many potential concepts associated with corrosion resistance, a feasibility matrix has been created to pre-screen the different concepts and determine the feasibility of each concept, which is shown in TABLE XVIII.

**TABLE XVIII: DM B.0: FEASIBILITY SCREEN ON CORROSION METHODS**

Design idea	Feasibility screen (pass or fail)	Justification
Corrosion resistant coating	Pass	Depends on material
Corrosion resistant material	Pass	Most important
Electro-chemistry	Fail	Hard to apply power supply or add sacrificial anode
Changing the operating variables	Pass	Depends on material
Remove corrosion constituents	Fail	Difficult to remove the ion from the water without adding chemicals to the river
Use of inhibitors	Fail	Contaminates the water

There are three design ideas which will be considered. Changing the material is the most important design idea of the project as the other design ideas are based on the material. Once the

material is decided, a protective coating may then be selected. Changing the operating variables will also be an additional consideration.

The following criteria are considered for selecting the material which can be demonstrated by TABLE XIX.

**TABLE XIX: DM B4.2.1 CORROSION CONCEPT SELECTION CRITERIA**

<b>Selection Criterion</b>	<b>Relevant need</b>	<b>Justification</b>
Cost	Affordable	The design has to be economical.
Safe to environment	Less damage to environment	The design should not cause any pollution or contamination to the environment.
Endurance time	Lifespan/maintenance cycle	The design should last as long as possible
Maintainability	Easy to maintain	The running ring should be easy to maintain during regular maintenance time
Manufacturability	Easy to manufacture	The running should be easy to be manufactured
Installation	Easy to install	The weight of the material should be as light as possible for easy installation

A list of materials is considered during this selection to determine whether or not to pursue. The material which are being considered are stainless steel, titanium, nickel alloy and tantalum. The original material carbon steel is also listed as a reference in TABLE XX.

**TABLE XX: DM B4.2.1: CORROSION PRELIMINARY CONCEPT SCREENING**

<b>Selection Criterion</b>	<b>Stainless steel</b>	<b>Titanium alloy</b>	<b>Nickel alloy</b>	<b>Tantalum</b>	<b>Carbon Steel (reference)</b>
Cost	-	-	-	-	0
Safe to environment	+	+	+	-	0
Endurance time	+	+	+	+	0
Maintainability	+	+	+	+	0
Manufacturability	-	-	-	-	0
Installation	+	+	-	-	0
<b>TOTAL</b>	2	2	0	-2	0
<b>Rank</b>	1	1	2	3	3
<b>Pursue?</b>	Yes	Yes	Yes	No	

By performing the above matrix, tantalum is out of consideration due to its negative score. The next step is to compare the various selection criteria to determine weighted scores. This criteria weighting matrix can be seen below in TABLE XXI.

TABLE XXI: DM B4.2.2: CORROSION CRITERIA WEIGHING MATRIX

	A	B	C	D	E	F
Cost (A)		B	C	A	A	A
Safe to environment(B)			B	B	B	B
Endurance time(C)				C	C	C
Maintainability(D)					D	D
Manufacturability(E)						E
Installation(F)						
<b>TOTAL</b>	<b>3</b>	<b>5</b>	<b>4</b>	<b>2</b>	<b>1</b>	<b>0</b>
<b>Weight</b>	<b>0.2</b>	<b>0.33</b>	<b>0.26</b>	<b>0.13</b>	<b>0.06</b>	<b>0</b>

TABLE XXII is used to determine the score of each material with 1 being the worst scenario and 5 being the best scenario.

TABLE XXII: DM B4.2.2 WEIGHT CONCEPT SCORING FOR MATERIAL

Criterion	Weight	Stainless steel		Titanium alloy		Nickel alloy		Carbon Steel(ref)	
		Rat.	Sc.	Rat.	Sc.	Rat.	Sc.	Rat.	Sc.
Cost	0.2	4	0.8	1	0.2	3	0.6	5	1
Safe to environment	0.33	4	1.32	5	1.65	4	1.32	2	0.66
Endurance time	0.26	4	1.04	4	1.04	3	0.78	0	0
Maintainability	0.13	4	0.52	4	0.52	4	0.52	3	0.39
Manufacturability	0.06	4	0.24	4	0.24	3	0.18	5	0.3
Installation	0	3	0	5	0	3	0	4	0
<b>Total</b>		<b>3.92</b>		<b>3.65</b>		<b>3.4</b>		<b>2.35</b>	

From the above matrix, the stainless steel is the material with the highest score and will be selected for the material. After the material is selected, the next step is to select the best coating material for the stainless steel.

There are two types of coatings; metallic and non-metallic. TABLE XXIII is created to screen the considered coatings for stainless steel.

**TABLE XXIII: DM B4.1.1 FEASIBILITY MATRIX FOR METALLIC AND NON-METALLIC COATINGS**

Design idea	Feasibility screen (pass or fail)	Justification
Metallic coating	Fail	Doesn't apply to stainless steel
Non-metallic coating	Pass	

As previously mentioned, the running ring is exposed to water and abrasion due to friction between the packing and the running ring. Besides the existing selection criteria, the coating would require additional criteria which will be introduced in TABLE XXIV.

**TABLE XXIV: ADDITIONAL COATING SELECTING CRITERIA**

Selection Criterion	Relevant need	Justification
Adhesion	The coating should have enough adhesion with stainless steel	If coating fails to adhere to running it could cause damage to the packing
Compatibility	The coating should be compatible with the packing	May affect the hardness or surface finish of the packing in order to create a running surface

With the additional criteria added, a new criteria weighing matrix is performed to determine the weight of each criterion which can be shown by the following TABLE XXV.

**TABLE XXV:DM B4.1.2 CRITERIA WEIGHING MATRIX**

	A	B	C	D	E	F	G	H
Cost (A)		B	C	A	A	A	G	H
Safe to environment (B)			B	B	B	B	B	H
Endurance time(C)				C	C	C	C	H
Maintainability(D)					D	D	E	E
Manufacturability (E)						E	E	H
Installation(F)							G	H
Adhesion(G)								H
Compatibility(H)								
<b>TOTAL</b>	<b>3</b>	<b>6</b>	<b>5</b>	<b>2</b>	<b>4</b>	<b>0</b>	<b>2</b>	<b>6</b>
<b>Weight</b>	<b>0.11</b>	<b>0.21</b>	<b>0.18</b>	<b>0.07</b>	<b>0.14</b>	<b>0</b>	<b>0.07</b>	<b>0.21</b>

A weighted scoring matrix is created to choose the best non-metallic coating which can be shown by TABLE XXVI. The running ring uses two sets of epoxy coating; hence it is listed as a reference.

**TABLE XXVI: DM B4.1.2 WEIGHTED CONCEPT SCORING RESULTS FOR COATING**

Criterion	Wt.	Oil-base		Alkyd		Chlorinated rubber		Silicone aluminum		Vinyl		Urethane		Epoxy (reference)	
		Rat.	Sc.	Rat.	Sc.	Rat.	Sc.	Rat.	Sc.	Rat.	Sc.	Rat.	Sc.	Rat.	Sc.
Cost	0.11	5	0.55	4	0.44	3	0.33	4	0.44	4	0.44	5	0.55	5	0.55
Safe to environment	0.21	4	0.84	4	0.84	5	1.05	3	0.63	5	1.05	4	0.84	4	0.84
Endurance time	0.18	2	0.36	3	0.54	4	0.72	3	0.54	4	0.72	5	0.9	4	0.72
Maintainability	0.07	4	0.28	3	0.21	3	0.21	5	0.35	3	0.21	5	0.35	4	0.28
Manufacturability	0.14	5	0.7	4	0.56	4	0.56	5	0.7	4	0.56	5	0.7	5	0.7
Adhesion	0.07	4	0.28	3	0.21	4	0.28	5	0.35	4	0.28	5	0.35	5	0.35
Compatibility	0.21	4	0.84	4	0.84	3	0.63	4	0.84	3	0.63	5	1.05	5	1.05
<b>Total</b>		<b>3.85</b>		<b>3.64</b>		<b>3.78</b>		<b>3.85</b>		<b>3.89</b>		<b>4.74</b>		<b>4.49</b>	

From the scoring matrix, urethane is a strong choice and can be applied to a stainless steel finish. A urethane finish coating would require zinc rich primer and pre-treatment [21]. Additionally, using a combination of coatings should be also being taken into consideration.

Lastly, there are certain number of variables that can be modified to decrease the corrosion rate of the material. A feasibility matrix is created to determine the feasibility of changing each variable.

**TABLE XXVII: B4.4.1 FEASIBILITY MATRIX FOR OPERATING VARIABLES**

Design idea	Feasibility screen (pass or fail)	Justification
Change the velocity of the water	Pass	
Change the temperature of the water	Fail	The temperature of the river water is already relatively low.



Design idea	Feasibility screen (pass or fail)	Justification
Change the pH of the water	Fail	The PH of the river water is considered to be neutral

Easily passivated materials such as stainless steel and titanium are more corrosion resistant when the velocity of the medium is high [8]. Therefore, the corrosion rate will be reduced if the velocity is increased. As previously mentioned, most of the corrosion happens during the shut-down period while the unit is sitting in the water. Having the seal water supply on during shut down period will circulate the water between the running ring and lantern ring instead of having stagnant water. However, the extremely high velocity should always be avoided.

From the corrosion resistant perspective, stainless steel with urethane coating is chosen. Having seal water supply on during shut down would be an option to modify operating variables in order to reduce corrosion rate.

### 4.3 Bolt Testing (CN10)

Before scoring the concepts outlined in Section 3.3, the metrics are first weighed by comparing them to each other, determining the priorities of the design, as shown in

TABLE XXVIII.

TABLE XXVIII: DM C1.1 NUT FACTOR METRIC WEIGHTING

		Simplicity	Weight	Repeatability	Structurally Sound	Manufacturability	Cost	Ease of use and analysis
		a	b	c	d	e	f	g
Simplicity	a		a	c	d	e	f	g
Weight	b			c	d	e	f	g
Repeatability	c				c	c	c	g
Structurally Sound	d					d	f	g
Manufacturability	e						f	g
Cost	f							g
Ease of use and analysis	g							
Total Hits		1	0	5	3	2	4	6
Total Possible		21	21	21	21	21	21	21
Weight:		0.05	0.00	0.24	0.14	0.10	0.19	0.29

From the weighting criteria, we can see that repeatability and ease of use and analysis were the two most important criteria. These important criteria gained the highest rankings, because they are necessary for achieving the objective of this project in determining the nut factor K. The scoring matrix with the associated weights is shown in TABLE XXIX.

**TABLE XXIX: DM C1.1 NUT FACTOR DESIGN SCORING MATRIX**

Selection Criteria		C1.1.1d	C1.1.2	C1.1.3
	Weight	Value	Value	Value
Simplicity	0.05	4	2	4
Weight	0.00	4	3	4
Repeatability	0.24	2	4	4
Structurally Sound	0.14	4	3	1
Manufacturability	0.10	4	4	4
Cost	0.19	3	3	3
Ease of use and analysis	0.29	4	4	4
<b>Total</b>		<b>3.33</b>	<b>3.57</b>	<b>3.38</b>

From the scoring matrix, the second design (C1.1.2) has been favoured. This design has been selected due to its high repeatability and ease of use, even though it may have been scored poorly in simplicity.

Once a sketch to move further with had been chosen, outlining boundaries to what was needed in the design could be considered. Since the running ring fasteners have 70 mm of length in tension from the bottom of the bolt head to the end of the nut, this would be a good starting place. We also know that hole diameter for the bolts should be 16 mm. When measuring an M16x2 nut, a thickness of 14.5 mm was specified. Subtracting the nut thickness from the initial 70 mm in tension yields a remaining thickness of 55.5 mm.

$$70 \text{ mm} - 14.5 \text{ mm} = 55.5 \text{ mm} = 2.185 \text{ in}$$

Both sides of the main plate will likely have washer blocks to achieve the necessary elongation length, which can be seen in Figure 23. Both of these blocks should be equal in thickness for simplicity sake. If a generic 1-inch washer plate is used on each side of the main plate, 0.185 in is remaining of plate to choose from. The closest sheet metal to 0.185 in is 7 gage (0.1793 in) and in this stage of the design will be used as the main material. 7-gage has a bend radius of

0.203 in and will be bent outside the material to allow for tolerance. Taking into account all these considerations has yielded Figure 25.

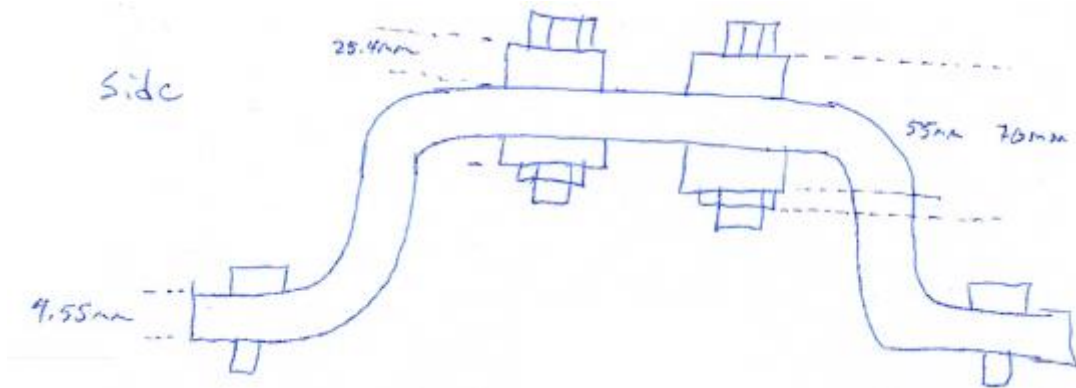


Figure 25: Final preliminary design side view [32]

Once a design is confirmed, modelling will commence to ensure the ideas generated are feasible. Moving forward in design, clearances for tools above and below the bolt were considered. The strength of the material was also verified, which is used as the main structure, which may incur loads such as clamping and buckling. Error may accumulate when friction occurs between the bolts and plates, both inside the holes and on the surfaces of contact. Therefore, ISO standards will provide guidance for testing throughout and try to minimize criteria that will create error within the test. With a conceptual design based on the theory and processes outlined in the design methodology of the nut factor, a CAD model can be created.

#### 4.4 Concept Selection Summary

In summary, concepts were passed through decision matrices based on the customer needs to determine which to proceed into detailed design with. This can be separated into three distinct areas:

1. Running ring deformation (CN5): focusing on the alignment issues with the running ring under its own weight, two key methods of addressing this are:
  - a. Increasing the moment of inertia (A1): the four original concepts were passed through DM A1.1, resulting in three concepts to develop: A.1.1, A.1.3, and A.1.4.
  - b. Increasing the modulus of elasticity (A2): all 14 materials were first passed through a pass/fail decision matrix, DM A2.1, narrowing the selection to seven materials. Then they were passed through DM A2.2, narrowing the material to

stainless steel. This will be integrated into the corrosion resistive methods selection.

2. Running ring corrosion (CN6): with the running ring undergoing circumferential corrosion, a variety of methods for increasing the resistivity against corrosion are proposed. All methods were compared against each other in DM B.0, where the resulting concepts to examine were use of coatings, material change, and changes to environmental aspects.
  - a. Use of coatings (B1): the coatings were first passed through DM B4.1.1 which ruled out metallic coatings. Then seven non-metallic coatings were passed through DM B4.1.2, where urethane is the best coating option.
  - b. Material change (B2): the proposed materials were first passed through DM B4.2.1 which ruled out tantalum as a choice. Then the materials were passed through B4.2.2, which favored stainless steel. This option is suitable as it lines up with the material choice made for improving the stiffness of the material as well.
  - c. Environmental changes (B4): the three proposed changes to the environment were passed through a pass/fail matrix DM B4.1.1, where changing the flow velocity was the only concept to pass.
3. Bolt testing concepts (CN10): the three proposed concepts were passed through DM C.1, which favoured concept C1.1.2 to begin development.

With the concepts now narrowed down and selected, detailed design can begin to quantitatively define the designs and come to a final design that meets the customer requirements.

## 5 Detailed design

Final design details include analysis, implementation, and presentation. These can now be developed from the concepts that have been narrowed down and selected. Detailed design brings the concepts into real design space with quantitative results.

### 5.1 Running Ring Optimization

The running ring now has potential cross-sections to explore as well as a material to proceed with. The running ring will be brought into detailed analysis to achieve the desired tolerance while using stainless steel. The goal is to present final engineering drawings with the intent that the client proceeds on fabrication for an optimized running ring for installation.

#### 5.1.1 FEA Analysis and Validation on Running Ring

In order to determine an optimized design, Generation Solutions must determine the amount of deformation the current running ring is experiencing to determine how much the second moment of inertia will need to be increased. The installation process of the running ring indicates that the running ring must be concentric to the turbine shaft within a tolerance of 0.005". Generation Solutions is planning to reduce the change in vertical diameter of the running ring below this tolerance.

Using equation (2.1.4) a change in vertical diameter of 0.594 mm or 0.0234" was obtained. This corresponds to a moment of inertia value of  $1.186 \times 10^{-6} \text{ m}^4$ . The current running ring design was then modelled in SolidWorks and subjected to a Finite Element Analysis (FEA) to verify the accuracy of the analytical calculations. The SolidWorks model of the running ring can be seen in Figure 26.

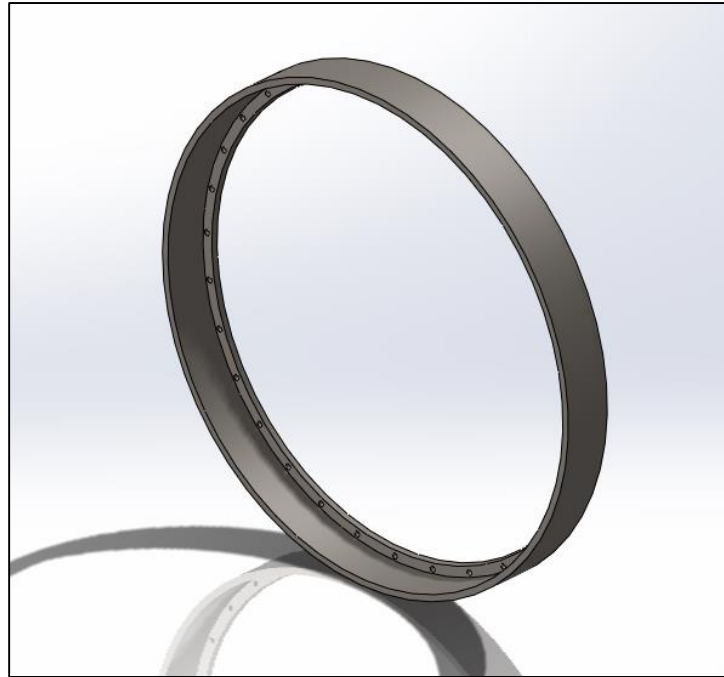


**Figure 26: SolidWorks model of running ring.**

A small base was extruded from the bottom of the running ring in order to simulate the running ring sitting on the ground. This face was then fixed, which can be seen below in Figure 27.

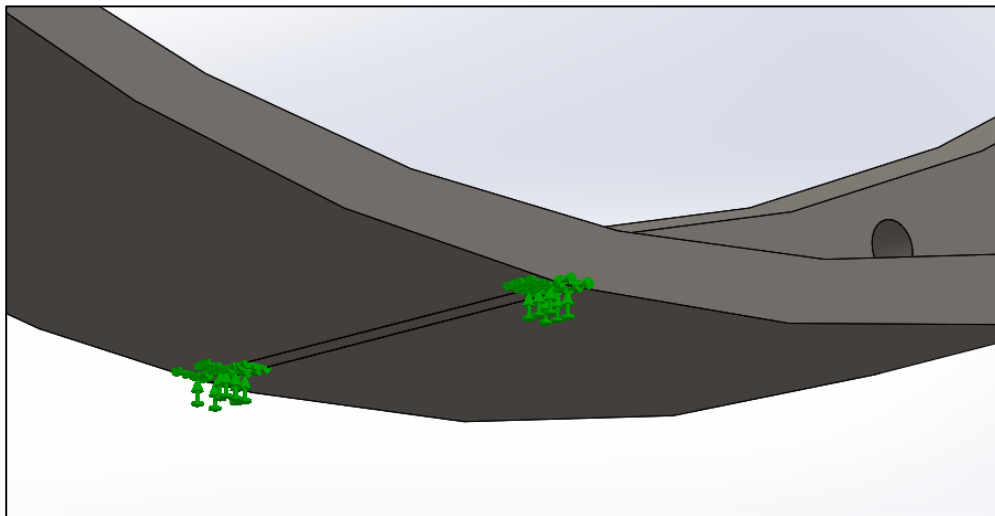


**Figure 27: Running ring base fixture.**

Gravity was then applied as an external force with a value of  $9.81 \text{ m/s}^2$ . An h-adaptive mesh refinement was used in order to prove convergence of strain energy. This mesh type increases element size in regions of low stress and increases the element size in area of high stress. The system will refine the mesh a certain number of iterations until the strain energy is within 3% of the previous iteration. The deformation of the running ring can be seen in Figure 28.

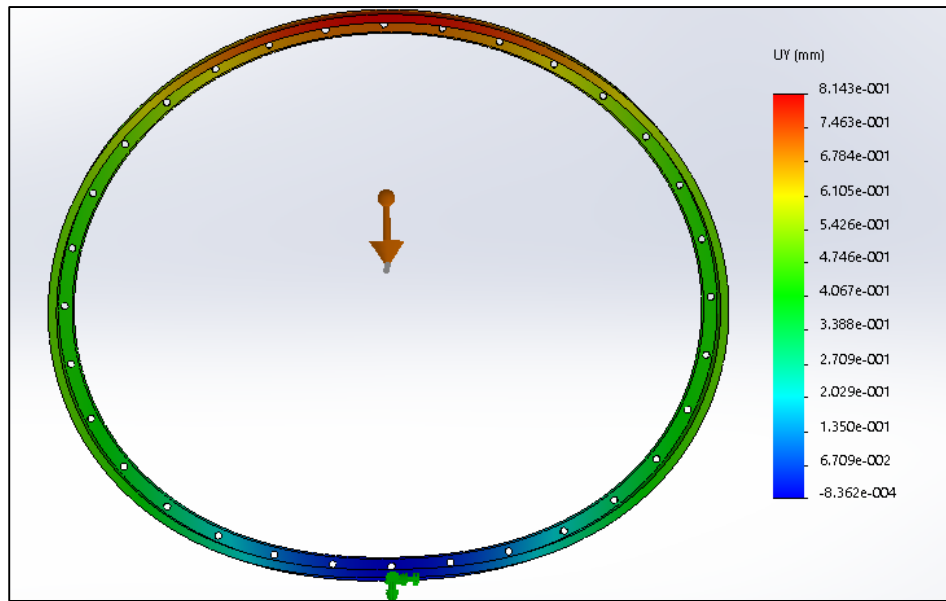


**Figure 28: Deformation of current running ring design.**

The maximum deflection in the vertical direction, which corresponds to the change in vertical diameter, is 0.814mm. This is slightly larger than the calculated value of 0.594mm, with a percent error of 27%. However due to the complex geometry of the running ring and the omission of the mounting holes in the hand calculations, Generation Solutions concludes that the analytical calculations confirms the accuracy of the FEA analysis. Additionally, before the credibility of the FEA analysis can be confirmed, the convergence of the strain energy must be investigated. A convergence plot for the strain energy as well as the maximum von Mises Stress can be seen below in Figure 29.

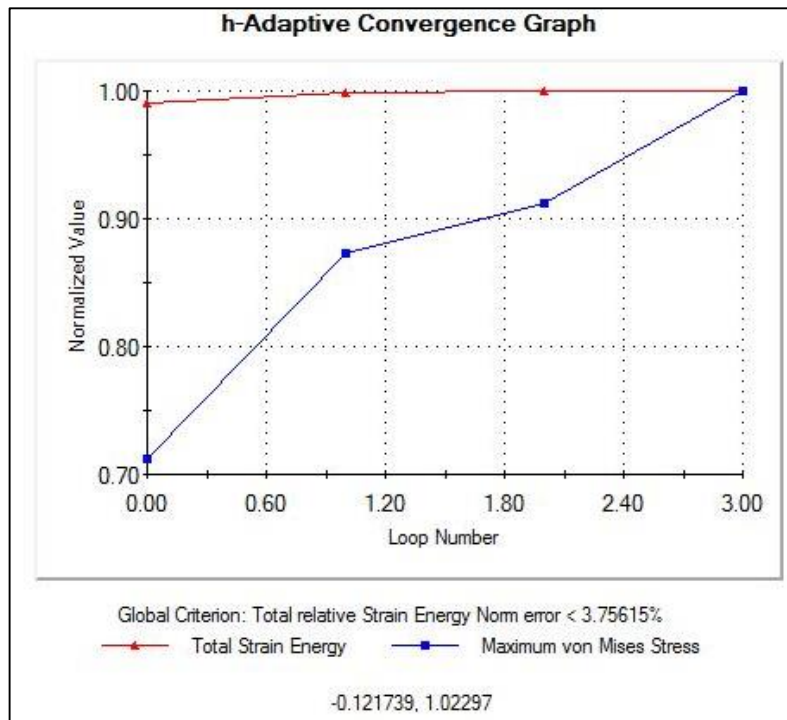


Figure 29: Convergence plot of FEA analysis of current running ring.

After three iterations of mesh refinement, the total strain energy converges. However, it can also be seen that the maximum value of von Mises stress does not converge. This is due to the sharp edges introduced at the base that were necessary in order to apply a base fixture to the running ring. The mesh in this region will become increasingly fine with each iteration creating stress values converging to infinity. The fine mesh in the base fixture region can be seen in Figure 30.

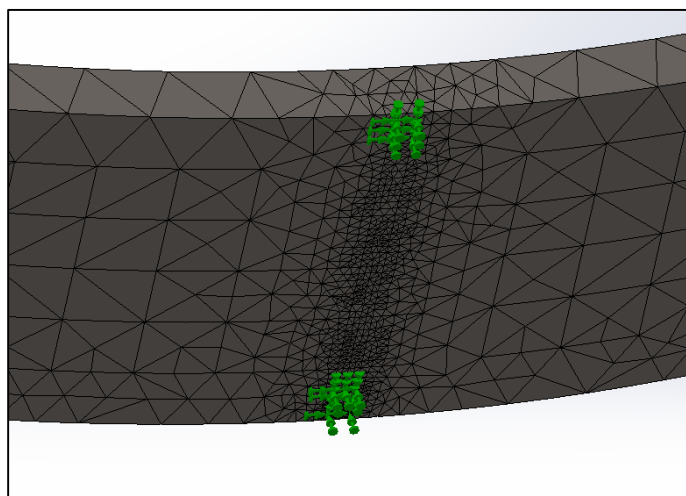
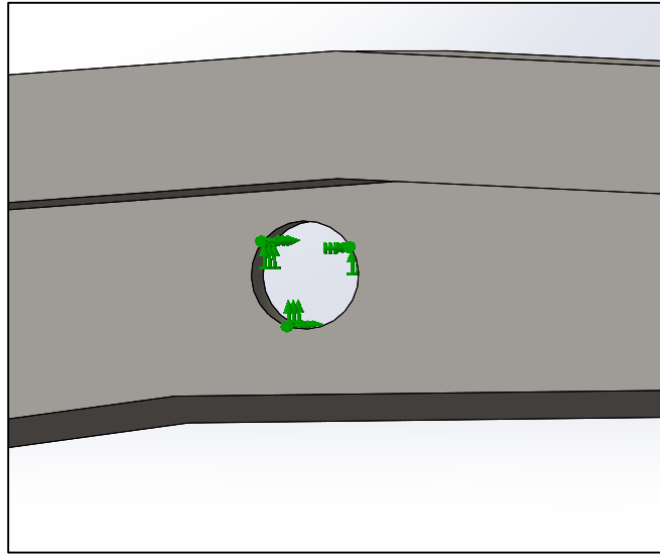


Figure 30: Fine mesh in region of base fixture.



Once the accuracy of our FEA was confirmed, the actual loading scenario was modelled in order to determine the amount of deflection experienced by the running ring during the current installation process. An approach similar to that of the previous analysis was used with the exception of how the fixture was applied. Rather than a fixture being applied at the base, the inner face of the mounting bolt hole at the top of the running ring was fixed. This can be seen in Figure 31.



**Figure 31: Bolt hole fixture**

The generated deflection from this analysis can be seen in Figure 32.

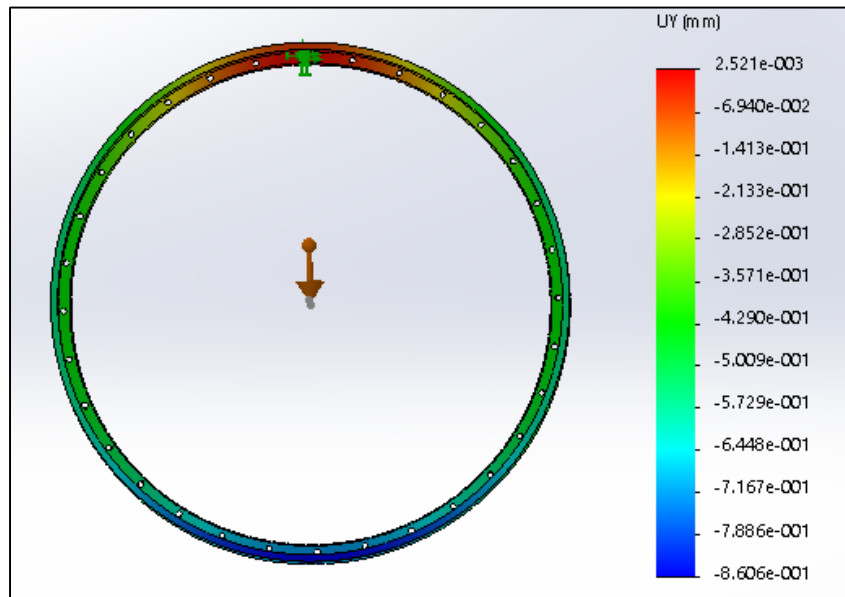


**Figure 32: Deflection of current running ring under actual loading conditions.**

This analysis indicates that the actual loading conditions yield a slightly larger change in vertical diameter with a value of 0.8606mm or 0.033". The validity of this analysis must also be confirmed by investigating the convergence of strain energy. A convergence plot for the strain energy as well as the maximum von Mises stress can be seen below Figure 33.

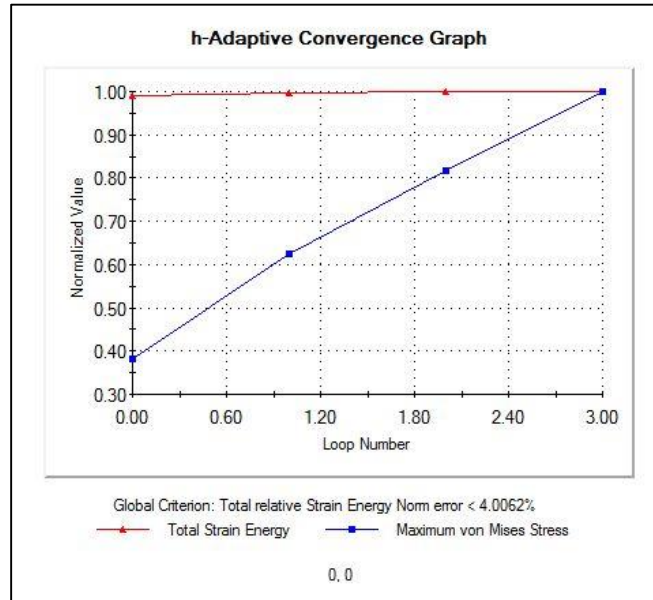


**Figure 33: Convergence plot for actual loading scenario of current design.**

Similar to the last analysis, the strain energy of the system quickly converges, but the maximum von Mises stresses trend towards infinity. Again, this is due to a singularity located at the sharp edges near the fixture of the bolt hole at the top of the ring. This singularity will cause increasingly fine mesh along with increasing stress values. The fine mesh in the fixed bolt hole region can be seen in Figure 34.

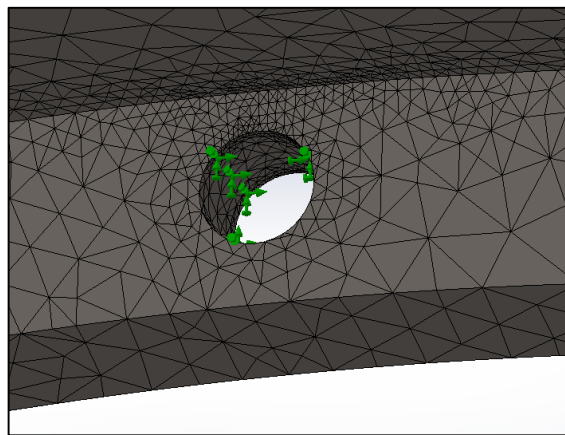


**Figure 34: Fine mesh in fixed bolt hole region.**

This analysis indicates that the actual loading scenario will yield slightly higher deflection values than the calculated scenario. As previously stated, Generation Solutions is planning to reduce this deflection value to 0.005 inches. Reducing the deflection to a value this small will require a significant increase in moment of inertia in order to increase the stiffness of the running ring.

The selection matrix performed to narrow down possible design solutions had indicated that the ribbed design may be an ideal solution. Upon further review, it was determined that this design would help keep the flange perpendicular to the main ring, but would not cause a significant improvement in the deformation of this ring. This is due to the ribs not significantly increasing the moment of inertia through the whole running ring.

Therefore, Generation Solutions decided to move forward with the added flange, increased flange dimensions, and increased thickness designs. It is assumed that a combination of these three designs will be required due to the significant moment of inertia value that will be required to reduce the deflection. The new cross section will have the general shape shown below in Figure 35.

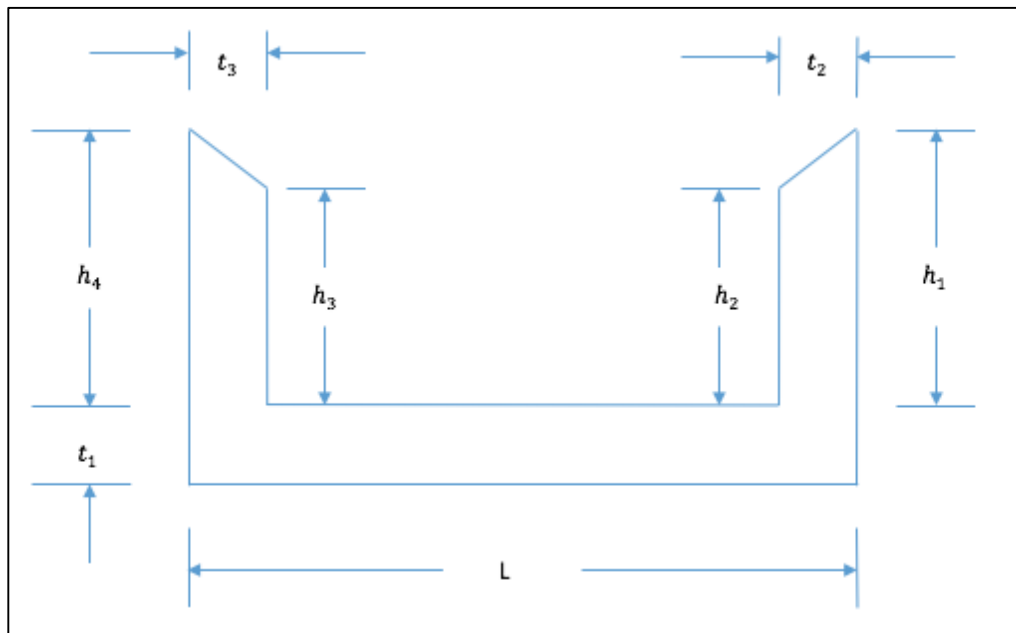


**Figure 35: General shape of optimized cross section.**

All dimensions shown above with the exception of the length,  $L$ , will have to be optimized through the use of the calculations done previously. The length is required to remain constant as several neighbouring components would be affected if this dimension were to be changed. It can

be observed that the flanges are chamfered on the ends. The functionality of this chamfer is to guide any escaped water back into the shroud on the bottom half on the running ring, and to help retain the water in the shroud on the top half of the running ring. For this reason, the flange that is bolted to the turbine shaft must be chamfered, however a chamfer on the added flange is not necessary. This idea is shown in Figure 36.

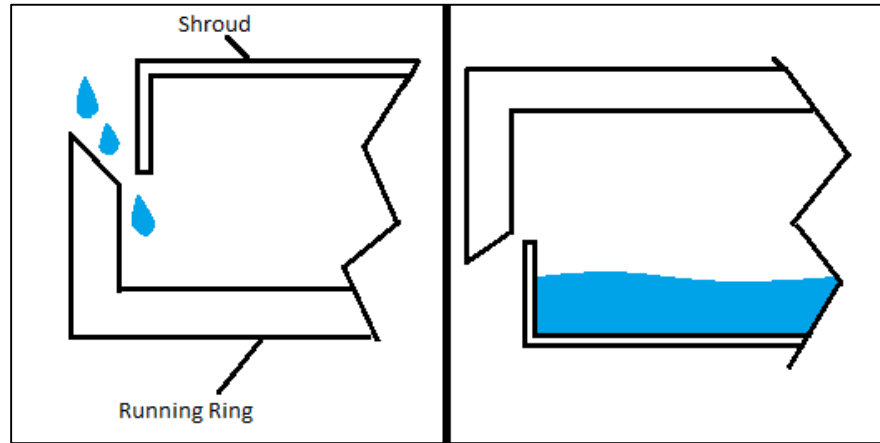


Figure 36: Flange chamfer functionality.

Although the calculations from having the ring being supported by its own weight on a small base at the bottom, are not for the actual loading scenario of the running ring, basing the redesign from this analysis will give a good starting point that can be further optimized through Finite Element Analysis. These dimensions will be optimized through the use of an Excel Solver. The current Running ring dimensions along with other design variables and their constraints can be seen in TABLE XXX.

TABLE XXX: CURRENT RUNNING RING DIMENSIONS AND DESIGN CONSTRAINTS

Parameter	Symbol	Value	Units	Constraint	Value
Length	L	190	mm	Constant	N/a
Outside flange height	h1	40	mm	Max	60
Inside flange height	h2	45	mm	Max	65
Added flange inside height	h3	N/a	N/a	Max	65
Added flange outside height	h4	N/a	N/a	Max	65
Base thickness	t1	24.78	mm	Max	30
Flange thickness	t2	20	mm	Max	20
Added flange thickness	t3	N/a	N/a	Max	30
Modulus of Elasticity	E	200	GPa	Constant	N/a
Moment of inertia	I	$1.186 \times 10^{-6}$	$m^4$	N/a	N/a

Parameter	Symbol	Value	Units	Constraint	Value
Weight per unit circumference	w	411.83	$\frac{N}{m}$	N/a	N/a
Density	$\rho$	7850	$\frac{kg}{m^3}$	Constant	N/a
Mass	m	538	lbs	Max	TBD
Change in vertical diameter	$\Delta D_v$	0.594	mm	Target	min

The Excel Solver was then implemented in order to minimize the deflection while keeping the constraints under the allowable values outlined above. The deflection was set as the target cell, while the heights and thicknesses of the flanges were set as the variable cells. The solver was then able to provide dimensions that will produce the desired deflection value while holding the dimensions and the mass to the constraints listed in TABLE XXX. The dimensional constraints are due to the limited space within the current shaft seal assembly. The constraints were implemented as maximum values that will fit in the current assembly with allowable clearances. The theoretical added flange as well as the assembly dimensions that governed the maximum increased dimensions can be seen in Figure 37.

TABLE XXXI: MASS VS DEFLECTION DECREASE

Mass (lbs)	Change in Vertical Diameter generated by solver(in)
537.3 (original)	0.0234
650	0.0110
700	0.0079
750	0.0074
800	0.0072
850	0.0070

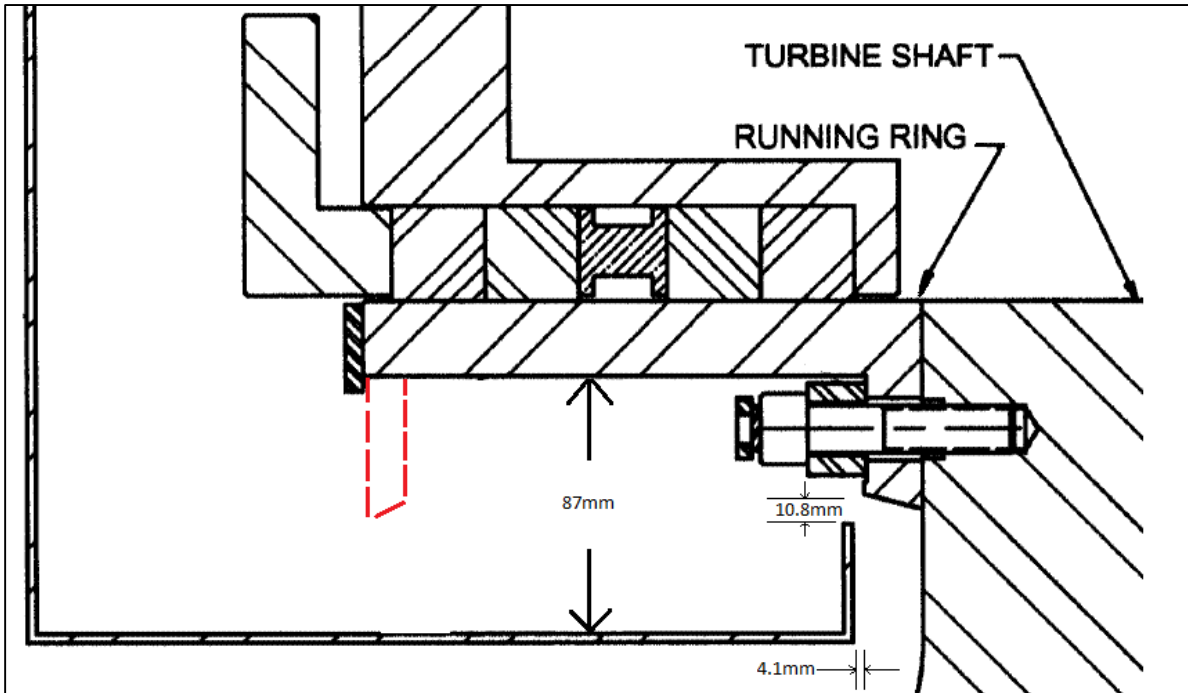


**Figure 37: Theoretical added flange and space constraints**

The last variable that must be controlled is the total mass of the running ring. Due to the tight assembly tolerances associated with the running ring, having a design with a small mass is desirable to promote easy handling. The solver program was implemented using incremental masses to determine an optimal mass that would come closest to achieving the goal of a change in vertical diameter of 0.005” without becoming too heavy. The results of this process are shown in TABLE XXXI.

By analyzing the results of the above table, the reduction in diameter change did not justify the added mass after 750 lbs. For this reason, a maximum mass of 750lbs was chosen. The original dimensions and properties are compared to that of the optimized cross section in TABLE XXXII. In addition to optimizing the dimensions of the running ring for improved deflection, the material was also changed to improve corrosion resistance. As mentioned in section 0, stainless steel 410 was chosen due to its corrosion resistance properties and relatively high stiffness. For the optimized cross section, material properties of stainless steel 410 were used.

**TABLE XXXII: ORIGINAL VS. OPTIMIZED RUNNING RING PROPERTIES**

Parameter	Symbol	Original	Optimized	Units
Length	L	190	190	mm
Outside flange height	h1	40	60	mm

Parameter	Symbol	Original	Optimized	Units
Inside flange height	h2	45	65	mm
Added flange inside height	h3	N/a	65	mm
Added flange outside height	h4	N/a	65	mm
Base thickness	t1	24.78	24.78	mm
Flange thickness	t2	20	20	mm
Added flange thickness	t3	N/a	27.7	mm
Modulus of Elasticity	E	200	210	GPa
Moment of inertia	I	$1.186 \times 10^{-6}$	$4.931 \times 10^{-6}$	$m^4$
Weight per unit circumference	w	411.83	574.89	$\frac{N}{m}$
Density	$\rho$	7850	7850	$\frac{kg}{m^3}$
Mass	m	537.3	750	lbs
Change in vertical diameter	$\Delta D_v$	0.594	0.189	mm

The solver generated dimensions that minimized the deflection to a value of 0.189mm or 0.0074 inches. Although this value is incrementally larger than the assembly tolerance, the redesigned running ring will be significantly more rigid and will reduce installation time.

The optimized geometry was then modelled using SolidWorks, where a Finite Element Analysis was performed in order to verify the calculated deflection value. The optimized running ring model can be seen below in Figure 38.

Similar to the previous analyses, gravity was applied as an external load and an h-adaptive mesh was used. The ring was also fixed by the bolthole at the top of the ring, however, an additional hole was added to the new flange and was also fixed to promote stability. The resulting vertical deflection from this analysis can be seen in Figure 39.

In Figure 39, the running ring experiences a 0.1946 mm, or 0.0077 inches, change in vertical diameter, this is extremely close to the calculated value of 0.1885 mm, a percent difference of about 3%. Although these values are nearly identical, the convergence of the strain energy and maximum von Mises stress had to first be investigated before the accuracy of the FEA analysis can be confirmed. The convergence plot for the strain energy and the maximum von Mises stress can be seen in Figure 40. Comparing the deflection values obtained by the FEA analysis for the original and improved cross sections, an improvement of 77.38% can be observed.



Figure 38: Optimized running ring geometry.

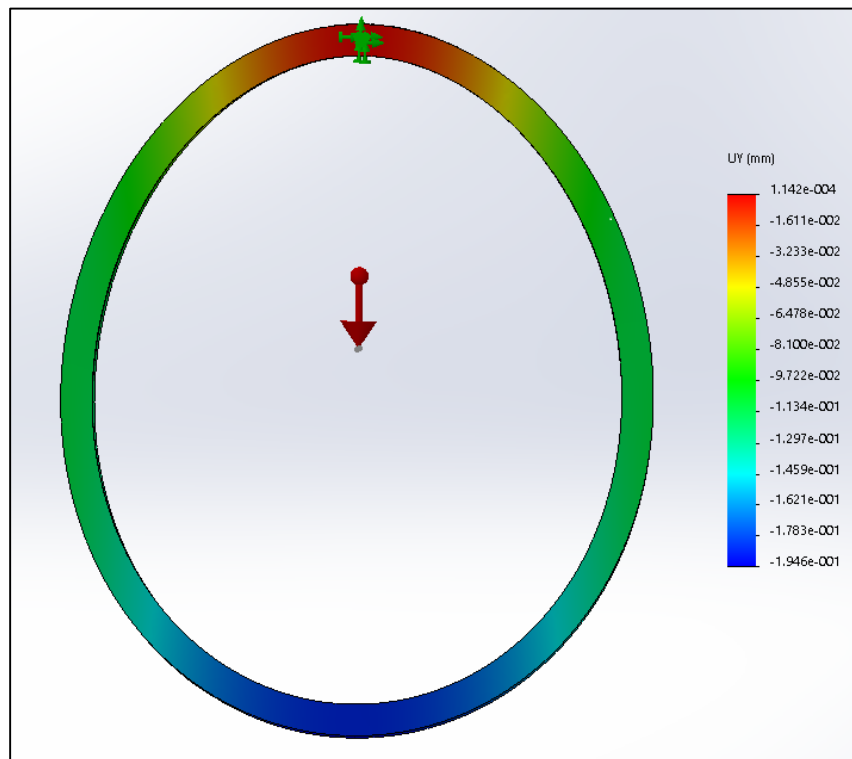
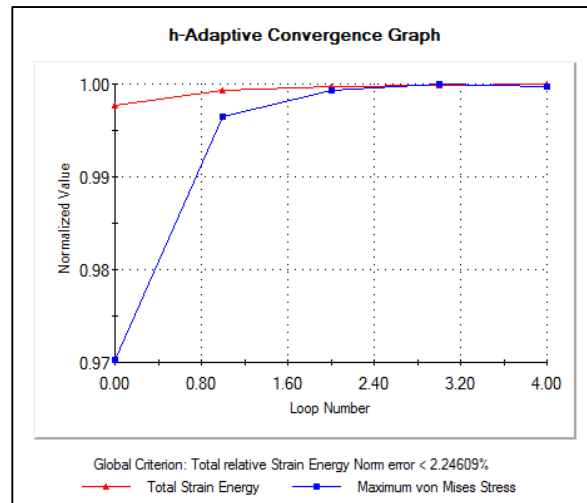


Figure 39: Optimized geometry vertical deflection.





**Figure 40: Optimized geometry convergence plot.**

The strain energy of the system and the maximum von Mises stress both converge after four loops of h-adaptive mesh refinement. The running ring mesh at the end of the fourth loop can be seen below in Figure 41. The combination of the convergence on the strain energy and maximum von Mises stress combined with the similar deflection values between the FEA and the calculations proves that the analysis performed is accurate.

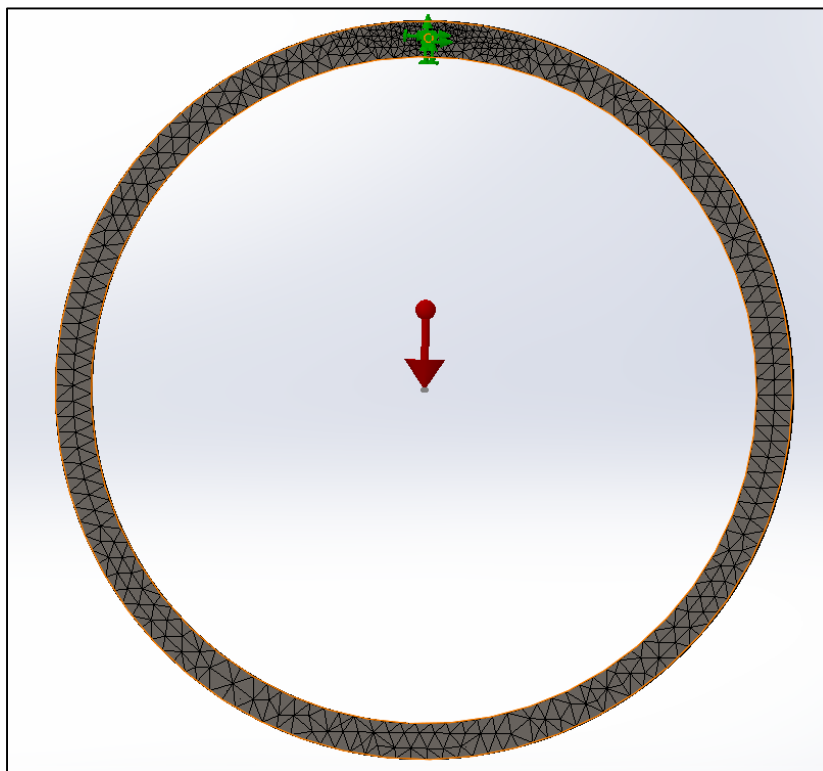


**Figure 41: Geometry mesh at the end of fourth loop of optimization.**

Generation Solutions then integrated the new running ring geometry into the current shaft seal assembly in order to validate its compliance. As can be seen in Figure 42, the optimized running ring geometry does not experience any interference in the current shaft seal assembly. This meets the customer need that the mating components of the shaft seal must remain unchanged.

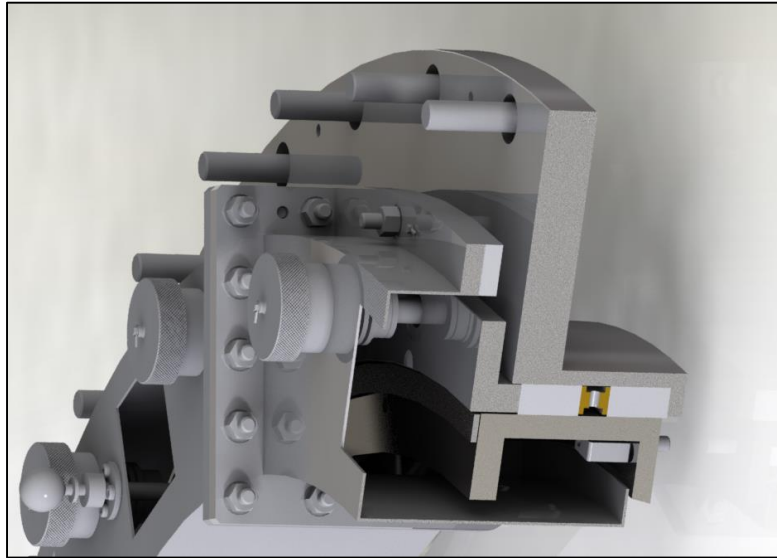


**Figure 42: Optimized running ring geometry in shaft assembly.**

From these new optimized geometries that propose an increase in stiffness to meet the tolerance requirements originally outlined in the customer requirements, combined with the new material of the running ring to also address the corrosion concerns, this design can now be detailed through final models and engineering drawings, along with a cost and resource estimate.

### **5.1.2 Loading on Fasteners**

The current running ring design has been in operation for several years without any performance issues, and therefore failure of the running ring itself is not a major concern. However, since the running ring dimensions have increased resulting in a heavier mass, it must be determined how the loading of the running ring is transmitted to the fasteners connecting the running ring to the turbine shaft. The amount of load transmitted to the fasteners will govern how much preload is required in the joint and ultimately the amount of torque that will be needed to be applied. The loads on the running ring that will be considered are: gravity, friction between the packing and the running ring, centrifugal due to rotation of the turbine shaft, compression from the packing, and pressure spikes due to the water inlets.

The first major force on the fasteners to consider is gravity due to the weight of the running ring. It can be calculated through the equation (5.1.2.1):

$$F_g = mg \quad (5.1.2.1)$$

where:

$m$  is the mass of the running ring

$g$  is the gravitational acceleration

The second force on the fasteners to consider is the centrifugal force, applied outward radially due to the rotation of the turbine shaft. It can be calculated using the equation (5.1.2.2):

$$F_c = m\omega^2 r \quad (5.1.2.2)$$

where:

$\omega$  is the angular velocity of the running ring

$r$  is the radius of the running ring

The third force on the fasteners to consider is the compression force that the packing is exerting on the running ring. The packing is compressed during installation and due to the Poisson effect, expanding against the running ring therefore exerting a force. This idea is illustrated below in Figure 43.

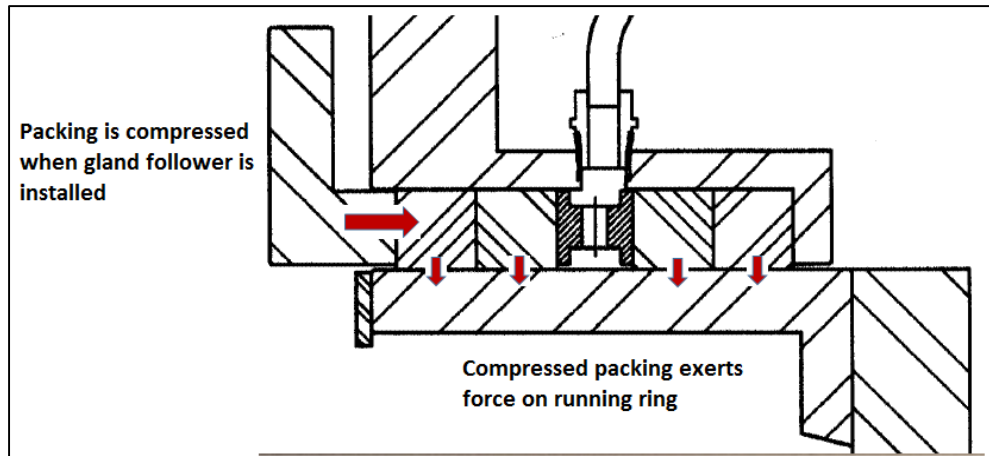


Figure 43: Packing compression.

The amount of force that the gland follower applied to the packing can be determined by finding the amount of preload in the gland follower fasteners. Rearranging equation (2.3.10) the preload can be found

$$F = \frac{T}{DK}$$

During installation, a torque of 66 N-m is applied to the stud and a K value of 0.14 was assumed for a stud with a thread locking compound applied. Once the preload is the joint is determined the pressure applied to the packing can be determined through the following equation:

$$P_p = \frac{F_p}{A_p} \quad (5.1.2.3)$$

where:

$P_p$  is the pressure of the gland follower on packing

$A_p$  is the total cross-sectional area of the packing

$F_p$  is the force exerted on the packing

The resulting pressure on the running ring from a single strand of packing can then be determined by manipulating Poisson's ratio:

$$\nu = \frac{\varepsilon_y}{\varepsilon_x} = \frac{E\sigma_y}{E\sigma_x} = \frac{\sigma_y}{\sigma_x} \quad (5.1.2.4)$$

where:

$\nu$  is Poisson's ratio

$\varepsilon_y$  and  $\varepsilon_x$  are the strain values experienced in y and x directions respectively

$\sigma_y$  and  $\sigma_x$  are the stress values experienced in the y and x directions respectively

$E$  is the modulus of elasticity

A Poisson's ratio value of 0.5 was assumed for packing materials, this value was suggested by Manitoba Hydro as they have done similar analyses with the same material. The stress exerted on the running ring can then be converted back to a force by dividing by the area, which will then be multiplied by four as there are four strands of packing.

The fourth force to consider is friction on the fasteners due to the contact between the packing and the running ring resisting the rotation of the turbine shaft. The friction force can be determined through the following equation:

$$F_f = F_N \mu \quad (5.1.2.5)$$

where:

$F_f$  is the frictional force applied on the running ring

$F_N$  is the compressive force the packing exerts on the running ring

$\mu$  is the coefficient of friction between the running ring and the packing; A value of 0.25 was assumed for the packing material

The final force to consider are the pressure spikes since there are 3 water supply inlets that provide water to the packing for cooling and lubrication. A cross sectional view of a water inlet can be seen in Figure 44.

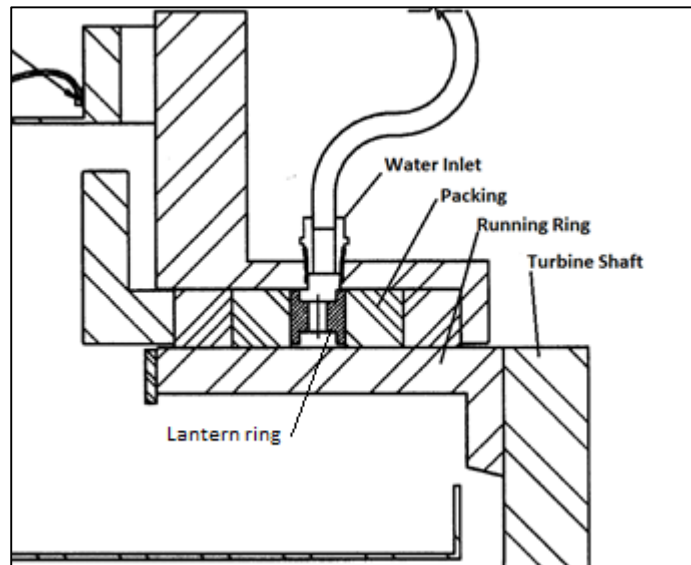


Figure 44: Water supply inlet.

The water supply inlets cause pressure spikes on the running ring, some of which will be transferred to the fasteners. A turbine unit at Jenpeg was monitored in order to determine the magnitude of these pressure spikes. This investigation determined that there was one large pressure spike at the inlet located at top dead center, and two smaller spikes at the two other inlet locations. The water pressure at these locations is summarized in TABLE XXXIII.

TABLE XXXIII: INLET WATER PRESSURE

Location	Pressure (psi)
Average large spike	33.8
Average small spike	27.3
Minimum pressure	23.2

A visual representation of these pressure spikes can be seen below in Figure 45.

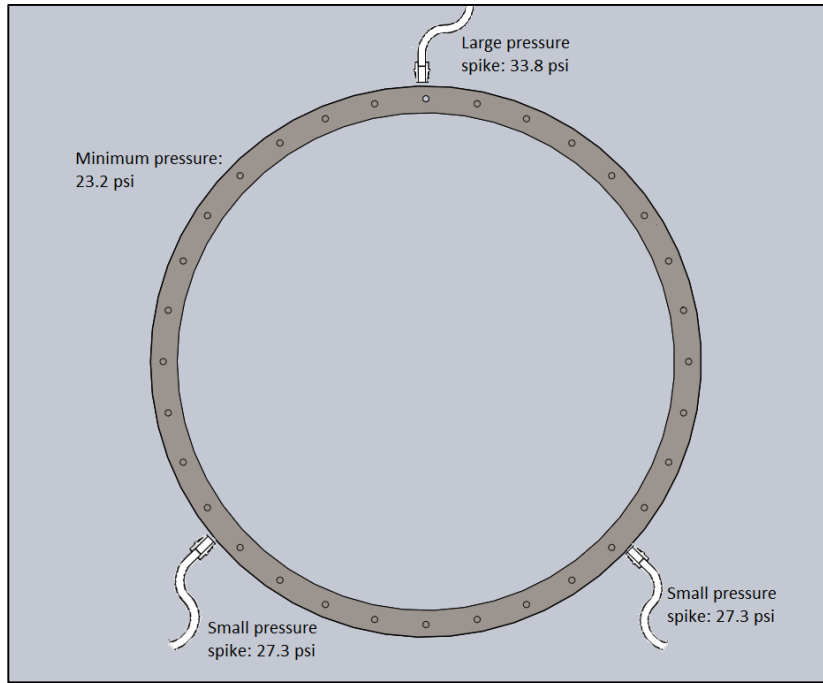


**Figure 45: Running ring water pressure spikes.**

These loads will be investigated to determine their effect on the fatigue life of the fasteners. The first step in doing this is to determine the amount of force generated on the running ring from the water pressure. This can be done using the equation below:

$$F_{ps} = P_{ps}A_{ps} \quad (5.2.2.6)$$

where:

$F_{ps}$  is the force from the pressure spike

$P_{ps}$  is the water pressure

$A_{ps}$  is the area that the pressure is acting on

The only variable needed to determine the force is the area. The water is injected onto the packing through the lantern ring, and the pressure is applied across the square area with a 20mm side length, shown below in Figure 46.

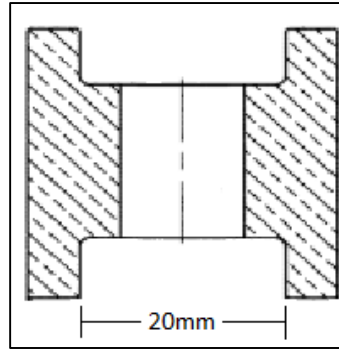


Figure 46: Lantern ring cross section

### 5.1.3 Total Loading

To determine the complete loading on a single fastener, all of the loads were summed up and then divided by 32 as this is the total number of fasteners on the running ring. It will then be determined how the loads on the running ring are transmitted to the fasteners in order to determine the required preload and ultimately the required torque. The loading on each fastener is summarized in TABLE XXXIV.

TABLE XXXIV: RUNNING RING FASTENER LOADING

Force	Value per fastener(N)
Gravity	103.8
Centrifugal	823.6
Compression	15713
Friction	3928.4
Pressure Spikes	Max: 93.23 Min: 64.05

The gravitational, centrifugal, compressive and pressure spike loads were assumed to be applied at the midpoint of the running ring in order to simplify the analysis. The frictional force is a shear force that will be transmitted directly to the fastener. The loading the running ring will not be constant as the ring will be rotating. For this reason, two extreme loading cases will be considered: at top and bottom dead center. These loading scenarios are shown in Figure 47 and Figure 48.

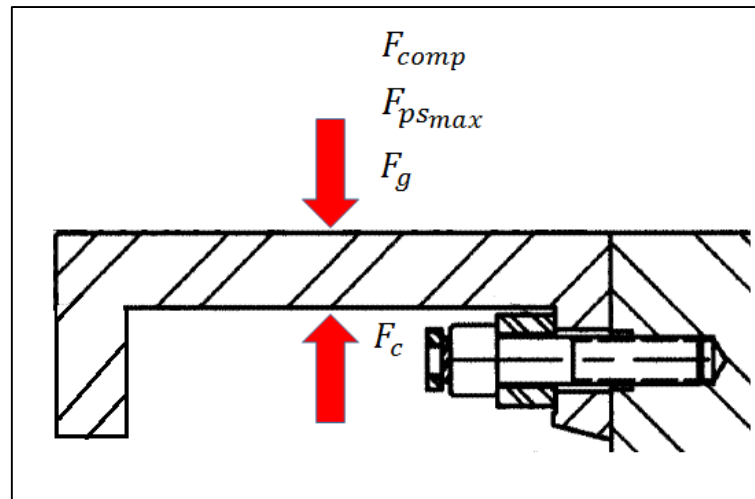


Figure 47: Loading conditions at top dead center.

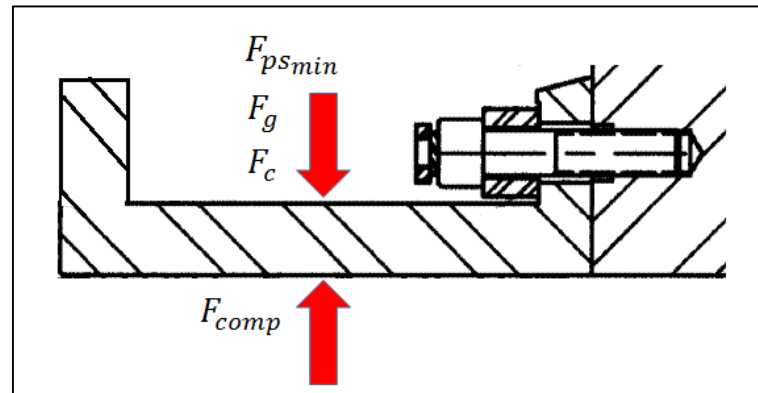


Figure 48: Loading conditions at bottom dead center.

Once the loading was known at the two extreme conditions, the forces were summed to determine the net force. The net forces at these two locations are shown in TABLE XXXV.

TABLE XXXV: NET FORCES ON FASTENERS

Location	Net Force (N)	Direction
Top Dead Center	15085.88	Downwards
Bottom Dead Center	14722.16	Upwards

Once the net forces were determined, it was necessary to determine how the loads were transmitted to the running ring fastener, which was done using the free body diagram in Figure 49.



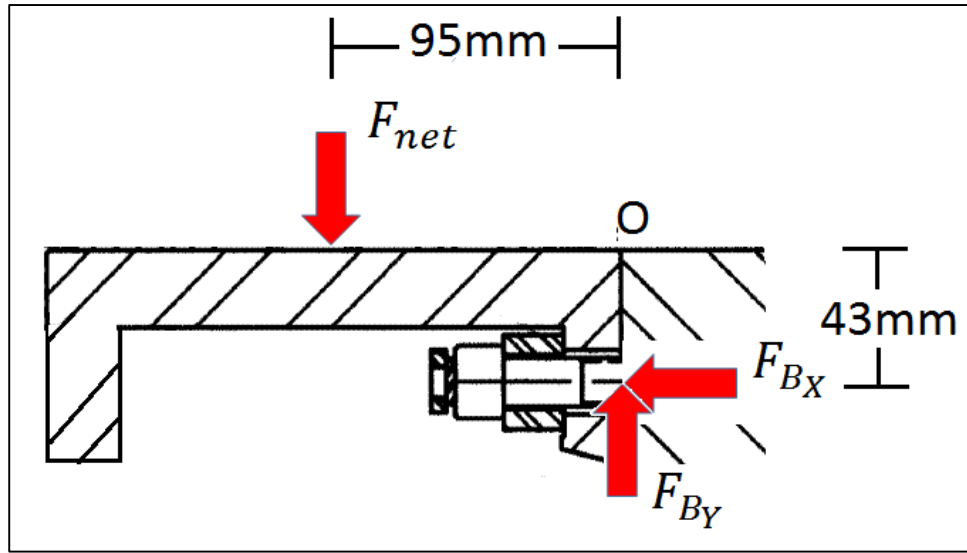


Figure 49: Free body diagram of running ring at top dead center.

The reaction forces were then determined through the following equations:

$$F_{By} = F_{net} \quad (5.1.3.1)$$

$$F_{Bx} = F_{net} \cdot \frac{95}{43}$$

These resulting forces for the two scenarios are shown in TABLE XXXVI.

TABLE XXXVI: REACTION FORCES

Location	$F_{By}$ [N]	$F_{Bx}$ [N]
Top Dead Center	15085.88↑	33329.29←
Bottom Dead Center	14722.16↓	32525.70←

The amount of preload required by the joint is determined by two criteria:

1. The joint must sufficient preload to prevent shear slippage:  $F_i \geq \frac{F_s}{\mu}$

Where  $F_i$  is the preload in the joint,  $F_s$  is the shear force acting on the bolt and  $\mu$  is the coefficient of friction between the two mating surfaces.

2. The joint must have sufficient preload to prevent joint separation:  $F_i \geq F_a$

Where  $F_a$  is the axial force acting on the bolt.

To ensure the first requirement is satisfied, the total shear force must first be determined. The total shear stress will be a combination of the previously determined reaction force and the friction force, which is shown in Figure 50.

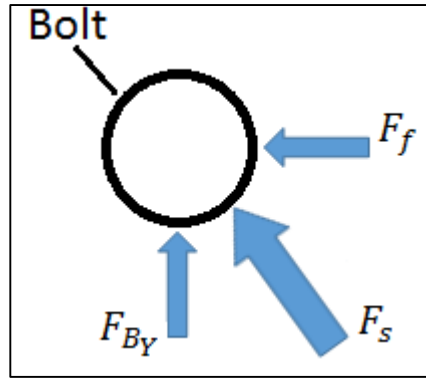


Figure 50: Shear forces on bolt.

$$F_s = \sqrt{F_f^2 + F_{By}^2} \quad (5.1.3.2)$$

$$F_s = 15588.97 \text{ N}$$

A friction coefficient of 0.5 was assumed for a steel on steel connection [33] . This value was taken as a dry value, due to the fact that the flange is cleaned and Loctite is applied before the running ring is installed. The two criteria then become:

1.  $F_i \geq 31177.94 \text{ N}$ , due to shear force.
2.  $F_i \geq 33329.29 \text{ N}$ , due to axial force.

Taking the larger of these two values the required preload in the joint is 33329.29N. The joint is currently torqued 160Nm. Using the nut factor K determined through the performed testing (detailed in section 5.4 Bolt Test Results), it was determined that the joint is currently experiencing approximately 58,800N of preload. Comparing this to the calculated preload this resulted in a factor of safety of 1.76.

### 5.1.4 Fatigue on Fasteners

Because the running ring and associated fasteners are in rotation while the turbine is in service, these components will undergo cyclic loading. Cyclic loading requires that fatigue failure must be investigated. Fatigue is defined as the evolution of damage at the microstructural level that ultimately leads to the formation of cracks and failure. Since the running ring has been in operation for many years and all dimensions have either increased or remained constant, a fatigue analysis on the running ring is not required. However, increasing dimensions will change the loading on the bolts fastening the running ring to the turbine shaft. Therefore, a fatigue analysis on these fasteners must be performed to ensure an infinite fatigue life.

The loading of the running ring was investigated in the previous section and an appropriate torque value was specified. This torque value ensures that the fasteners only experience axial loading so that they do not experience the cyclic loads of the running ring. However, this assumes a perfectly stiff joint. In reality, the fastener will experience additional tension due to the loading of the running ring.

In order to determine what portion of the running ring loads will be carried by the fasteners, the relative stiffness of both the joint and the fastener must be determined. Using previously defined variables, the bolt stiffness,  $k_b$ , can be found through the following equation:

$$k_b = \frac{A_b A_t E}{A_b l_t + A_t l_b} \quad (5.1.4.1)$$

The joint stiffness can then be determined using the following equation:

$$k_m = EdAe^{\frac{Bd}{t}} \quad (5.1.4.2)$$

Where A and B are constants, their values are 0.78715 and 0.62873 for steel. The stiffness constant of the joint can then be determined, this value represents the portion of the applied load that will be carried by the bolt or fastener. It is calculated using equation (5.1.4.3):

$$C = \frac{k_b}{k_b + k_m} \quad (5.1.4.3)$$

The results of these equations are summarized below in TABLE XXXVII.

**TABLE XXXVII: BOLT AND JOINT STIFFNESS**

Parameter	Value
$k_b$	$5.484 \times 10^8$
$k_m$	$2.581 \times 10^9$
$C$	0.1753

The total load on the fastener can then be calculated using the following equation:

$$F_b = CP + F_i \quad (5.1.4.4)$$

where:

$P$  is the applied load to the running ring

$F_i$  is the preload in the fastener

Once the loading in the fastener is known, the stress amplitude can be determined:

$$\sigma_a = \frac{F_{b_{max}} - F_{b_{min}}}{2A_t}$$

Where  $F_{b_{max}}$  and  $F_{b_{min}}$  are the maximum and minimum total loads experienced by the bolt.

This equation can then be simplified by substituting equation (5.2.6):

$$\begin{aligned}\sigma_a &= \frac{(CP_{max} + F_i) - (CP_{min} + F_i)}{2A_t} \\ \sigma_a &= \frac{C(P_{max} - P_{min})}{2A_t}\end{aligned}\quad (5.1.4.5)$$

The mean stress can be determined using a similar method:

$$\begin{aligned}\sigma_m &= \frac{F_{b_{max}} + F_{b_{min}}}{2A_t} \\ \sigma_m &= \frac{(CP_{max} + F_i) + (CP_{min} + F_i)}{2A_t} \\ \sigma_m &= \frac{C(P_{max} + P_{min})}{2A_t} + \frac{F_i}{A_t}\end{aligned}\quad (5.1.4.6)$$

$P_{max}$  represents the  $F_{B_x}$  value at top dead center and  $P_{min}$  represents the  $F_{B_x}$  at bottom dead center. Using these calculating values as well as the preload currently experienced by the bolt, the stress amplitude and mean stress were calculated, their values are shown in TABLE XXXVIII.

TABLE XXXVIII: AXIAL STRESS ON FASTENERS

Variable	Value
Stress Amplitude	0.4495 MPa
Mean Stress	412.28 MPa

Once the alternating and mean stresses in the fastener are known, the fatigue performance can be determined. This is done using a Goodman Analysis, which involves plotting the stress amplitude on the vertical axis and the mean stress on the horizontal axis. The endurance limit of the specimen with applicable stress concentration factors is then plotted on the vertical axis and the ultimate tensile strength was plotted on the horizontal axis. An endurance limit of 129 MPa for the stud material was assumed. This endurance limit is incorporating all applicable modifying factors [34]. A line was then drawn connecting these two points, this is referred to as the Goodman line. The Goodman line allows for certain combinations of stress amplitude and mean stress to be above the yield strength of the bolt, which is unacceptable in this application. For this reason, an additional line connecting the endurance limit on the vertical axis and the yield strength on the horizontal axis, this is known as the safe line. Combinations of mean and alternating stress that lie below the safe line are considered to be safe. Next, the load line was drawn. This line starts at the applied preload and increases linearly with a slope of  $\sigma_a/(\sigma_m - \sigma_i)$ , where  $\sigma_i$  is the preload stress. The maximum alternating and mean stress values will be at the intersection point load line and the safe line.

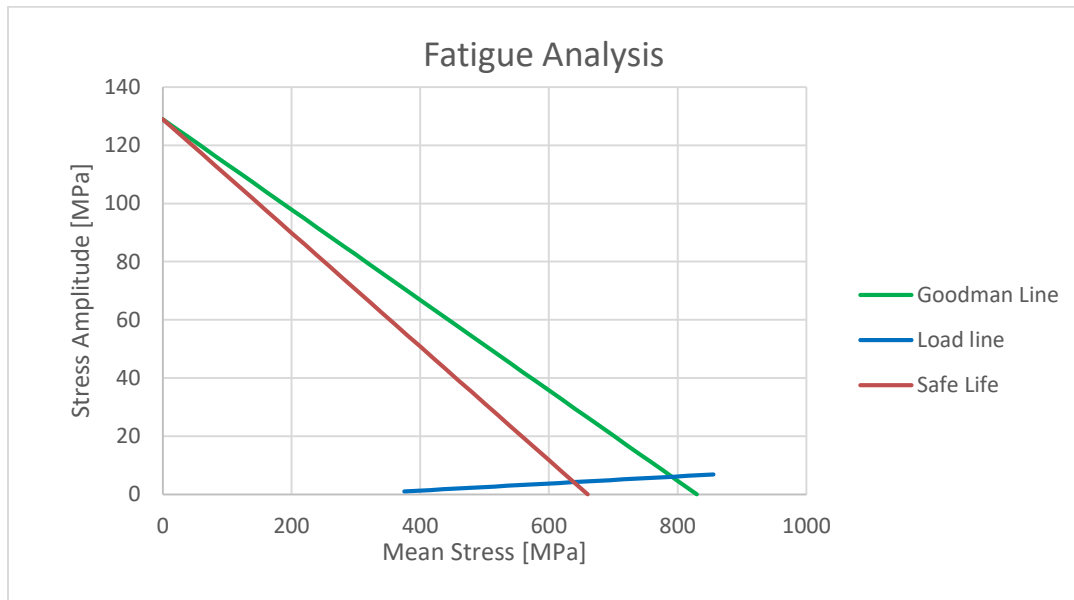


**Figure 51: Goodman fatigue analysis.**

Figure 51 Indicates that the maximum values for stress amplitude and mean stress are approximately 643MPa and 3.30Mpa.

A factor of safety can be calculated for the axial stresses in fatigue using the following equation:

$$n_f = \frac{\sigma_e(\sigma_{yld} - \sigma_i)}{\sigma_a(\sigma_{yld} + \sigma_e)} \quad (5.1.4.7)$$

where:

$n_f$  is the factor of safety

$\sigma_e$  is the endurance limit of the fastener

$\sigma_{yld}$  is the yield strength of the fastener

$\sigma_i$  is the preload applied to the fastener

$\sigma_a$  is the stress amplitude

Using the Goodman factor of safety criteria, the fasteners have a factor of safety of 103.5. The extremely high factor of safety can largely be attributed to the small stress amplitude. The axial loads transferred to the fastener are near constant indicating that fatigue due to the axial loads is not a concern. However, this only validates that the fasteners will not fail due to fatigue from the axial loads. Analysing the shear stresses applied to the bolt it becomes apparent that fatigue failure is more likely to occur from these stresses. For this reason, it was necessary to perform a separate Goodman analysis to analyse fatigue failure due to shear stresses. This was done using a method as the previous analysis. However, rather than having a load line intersecting with a safe line, a safe zone can then be created by connecting the endurance limit of the bolt on the vertical axis to the yield stress on the horizontal axes. Additionally, the yield stress must be adjusted for shear stresses. Typically, the yield strength of a material in shear will be 57.7% of the yield strength due to axial stresses [34]. Combinations of mean stress and stress amplitude below the safe zone line are considered safe. The Goodman plot can be seen in Figure 52.

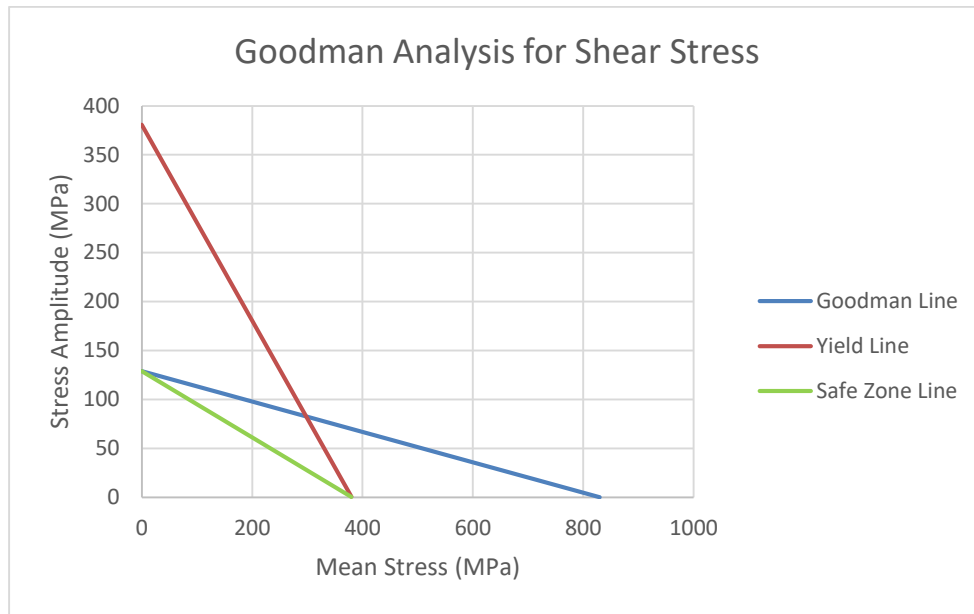


**Figure 52: Goodman analysis for shear stress.**

Assuming a worst case scenario, it is assumed that all of the experienced shear will be transmitted to the fastener. Although the shear loads are fully reversed, the fasteners are also rotating and therefore the direction of the load on the fastener remains almost constant. This will result in a high mean stress and low stress amplitude. The mean stress and stress amplitude were then calculated to ensure they are within the safe zone. Their values are shown in TABLE XXXIX.

**TABLE XXXIX: SHEAR STRESS ON FASTENERS**

Stress	Magnitude (MPa)
Stress Amplitude	0.904
Mean Stress	74.16

Analysing these values, it becomes clear that they are well within the safe zone. A factor of safety for the fasteners with respect to fatigue due to shear stresses can then be calculated.

$$\frac{\tau_a}{\sigma_e} + \frac{\tau_m}{\sigma_{yld}} = \frac{1}{n} \quad (5.1.4.8)$$

where:

$\tau_a$  is the shear stress amplitude

$\tau_m$  is the mean shear stress

$n$  is the factor of safety

Solving for  $n$ , a factor of safety with respect to shear stresses in fatigue of 4.32. Similar to the axial stresses, the shear stresses applied are near constant and the low stress amplitude results in the high factor of safety. Upon completion of this fatigue analysis, it can be concluded that the running fasteners are not under risk of fatigue failure.

### 5.1.5 Comparison of Materials and Optimization

Stainless steel has been chosen to be the material, which will be pursued for fabrication. There are four important aspects that needs to be considered to deal with deformation and corrosion aspects, which are Young's modulus, density, general corrosion resistance in a water environment, and galvanic corrosion due to the lantern ring.

Commonly used stainless steel Young's modulus and density are listed in TABLE XL. ASTM A516 Grade 70 steel is also listed since this is the material used for the existing running ring.

**TABLE XL: MECHANICAL PROPERTIES OF VARIOUS MATERIALS**

Material	Young's Modulus (GPa)	Density (kg/m <sup>3</sup> )
Steel ASTM A516 Grade 70	204	7850
Stainless Steel - Grade 304	203	8060
Stainless Steel - Grade 410	210	7850
Stainless Steel - Grade 316	205	8070

From TABLE XL, it can be shown that Grade 410 is the only type of stainless steel which is more rigid and less dense than the original material. Thus Grade 410 is the best choice for stainless steel to reduce deformation.

For increased corrosion resistance, a list of commonly used stainless steels' corrosion resistance can be shown by the following TABLE XLI.

**TABLE XLI: CORROSION PERFORMANCE OF VARIOUS MATERIALS [8]**

Material	Corrosion Resistance
Steel ASTM A516 Grade 70	U
Stainless Steel - Grade 304	G
Stainless Steel - Grade 410	G
Stainless Steel - Grade 316	G

\*G ≤ 20 Mils Penetration/Year; U ≥ 50 Mils Penetration/Year



From the TABLE XLI. For Grade 304, 410 and 316 stainless steel, the penetration rates are under 20 Mils (thousands of inch) per year comparing to the existing material with more than 50 Mils per year.

For the risk of galvanic corrosion, the electric potential difference is the major contributor to galvanic corrosion. The bigger electrical potential difference between two metals, the galvanic corrosion will more likely to occur. The following Figure 53 summarizes galvanic series of various common metals.

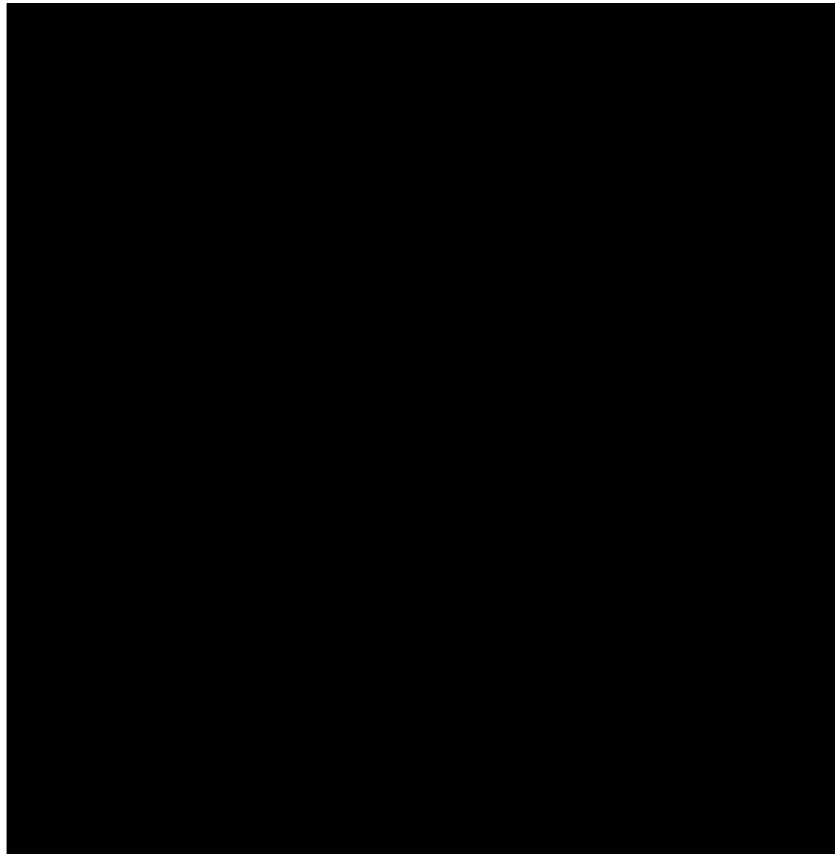


**Figure 53: Simplified galvanic series [35].**

From the figure above, the existing running ring with carbon steel is at the active side of the chart while the brass is less active than carbon steel, which will cause galvanic corrosion. Since the new proposed material of stainless steel is a passive metal, it will be protected if there is galvanic corrosion. Also, the lantern ring, which is made of yellow brass is also safe from galvanic corrosion since brass is fairly corrosion resistant due to a passivation layer.

Figure 54 also verifies the galvanic corrosion effect will be reduced.

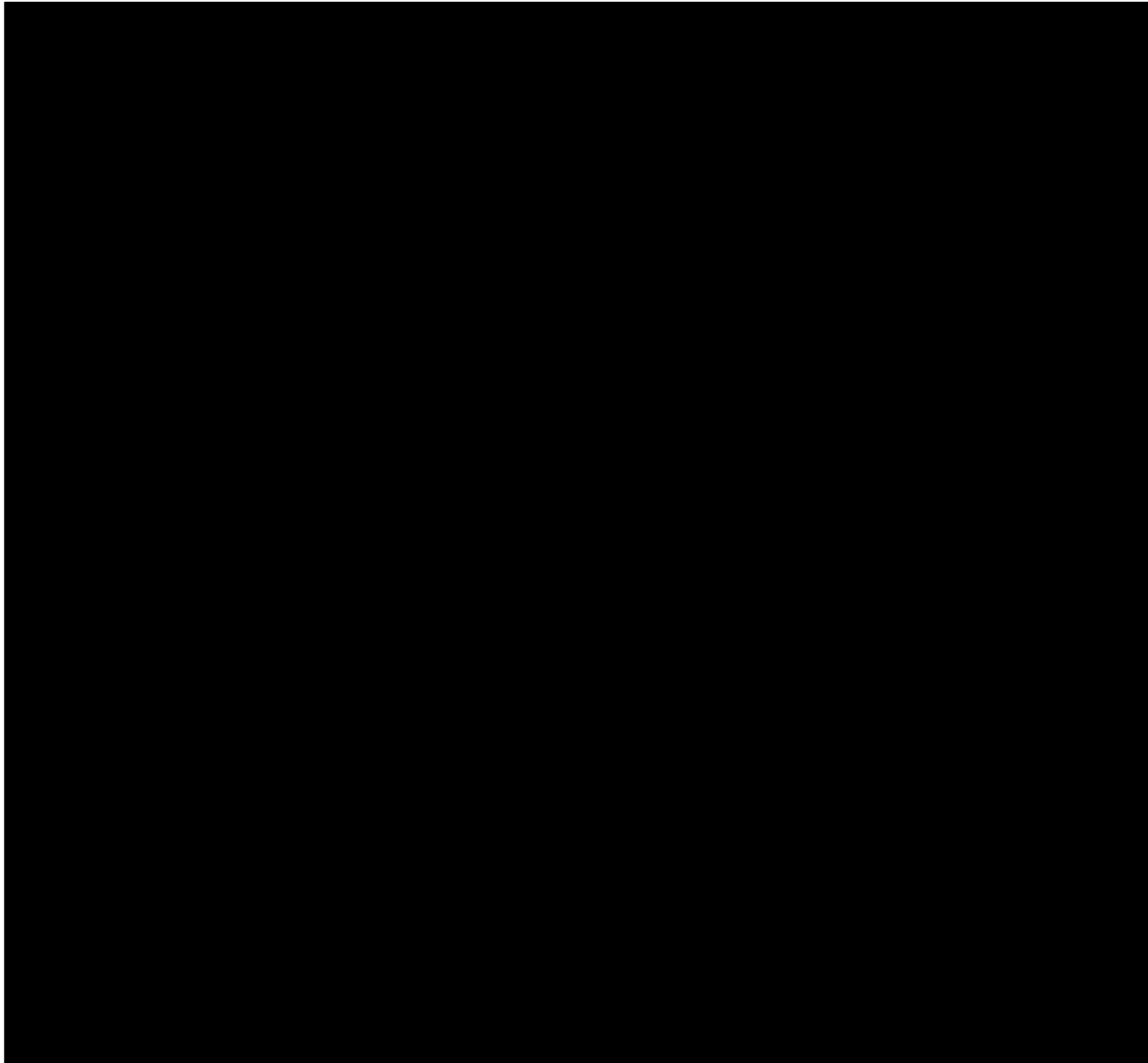


**Figure 54: Risk of corrosion from bimetallic contact in neutral electrolytes [35].**

With the proposed stainless steel running ring, there will be less corrosion when compared to the original material.

The cost of the material and manufacturing of the new running ring geometry must be considered. One day of downtime for a single turbine cost Manitoba Hydro approximately \$20,000 in lost generating opportunities. Approximate manufacturing and material costs for the

proposed 410 stainless steel compared to the original running ring material can be seen below in TABLE XLII.

**TABLE XLII: MATERIAL COST BREAKDOWN [36]**

Material	Manufacturing costs	Approximate Material Costs
ASTM A516 Gr 70	\$17,000	\$2,100.00
410 Stainless Steel	\$17,000	\$9,100.00

TABLE XLII illustrates that the manufacturing costs will be constant for the two materials, however the 410 stainless steel is significantly more expensive. Although the stainless steel is more expensive, the increased cost can be justified by the drastic improvement in corrosion resistance.

Due to the increased stiffness, reduced density, significant improvement in corrosion resistance, and justification for the increased cost, it was determined that 410 stainless steel is the best suited material for this application. However, since the price of materials were not obtained locally, the values that they represent are arbitrary and will need to be revisited upon ordering.

For the coating that was mentioned in concept generation, the team has approached a local coating company regarding the coating suggestions on stainless steel. The team has been advised that the coating application procedures for stainless steel differs from carbon steel. It must be kept in mind that if surfaces are not prepared properly, if coatings are not correctly applied, or if there is a localized breakdown of the coating system, the rate of corrosive attack in that localized area can be higher and more severe. Besides that, due to the physical contact with the packing it would require certain adhesion on the coating in order to prevent it from scraping off. The team assessed that there are certain risks of applications of coating which will cause significant failure to the packing assembly. Thus, Generation Solutions decided to pursue the design with plain stainless steel without any coating.

## **5.2 Running Ring Final Design**

The running ring final design will describe the final cross section, material change and features of the improved design. Now that the stiffness of the running ring has been increased, the installation procedure will be changed. Lastly, the running ring design and performance will be compared to the customer needs to evaluate the proposed design.

### 5.2.1 Final Cross-section, Material and Features

The final design of the running ring will be using Grade 410 stainless steel which has a slightly larger modulus of elasticity and a similar density as the original material, however with significant increase in corrosion resistance performance. With this grade 410 stainless steel, the anticipated penetration rate is assumed to be less than 20 thousandths of inch per year, compared to more than 50 thousandths of inch per year with the existing carbon steel material.

In order to reduce the deformation of the running ring due to gravity and to make the installation process easier, another flange is added to the other side of the running ring. The cross-section of the new running design can be shown by Figure 55.

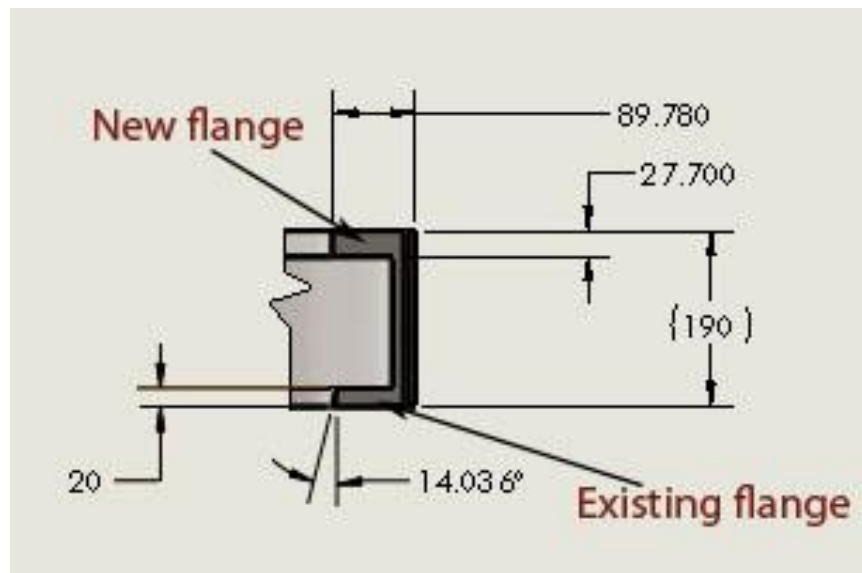


Figure 55: Cross section of the new running ring.

The dimensions of the new flange can be seen and the length of old flange is also increased in order to achieve a higher moment of inertia. The thickness of the running ring is kept the same since it will not affect the moment of inertia much because it is close to the neutral axis. For more details of the actual design, there is a whole set of new running ring design drawings which can be seen in Appendix G: Updated Running Ring Final Drawings.

With the additional flange in place, an FEA analysis generated a change in vertical diameter of to 0.1946mm compare to 0.8606mm with the old design. The new design makes the running ring more rigid and decreases the deformation by 77.3%.

## 5.2.2 Updated installation procedure

The installation procedure with the new running ring geometry will remain the same as the current process. However, Generation Solutions was informed that the running ring alignment tool called out in the installation of the running ring is often not used. This is due to maintenance staff determining that it is less time consuming to align the running ring by hand rather than using the alignment tool. Since the expected deflection of the running ring is expected to decrease significantly, it is predicted that the installation of the running ring will become significantly less cumbersome and time consuming for maintenance staff.

## 5.2.3 New Running Ring Design Comparison to Customer Needs

Several customer needs were developed during the project definition phase, the redesigned running ring was able to meet or exceed all customer needs, with the exception of the reduced deflection. Although the deflection that the running ring expected to see is slightly higher than assembly tolerances, a 77% improvement was observed. Customer needs relating to maintenance and labour hours of installation time are only estimates as the new design is yet to be manufactured or installed. That being said, our team assumes that the 77% reduction in deflection will correspond to a reduction in installation time of at least 50% of the running ring.

TABLE XLIII: RUNNING RING CUSTOMER NEEDS COMPARISON

Metric	Units	Marginal Value	Actual Value	Justification/notes
<b>Labour, material and machining costs</b>	CAD\$	\$37000	\$26,000*	Estimate only; obtaining a quote from a local machine shop is recommended.
<b>Stress on running ring</b>	MPa	factor of safety of 3	>>3	Stresses on running ring are relatively insignificant.
<b>Time between maintenance cycles</b>	years	1 year	1 year	Improved corrosion resistance reduces need for maintenance.
<b>Maintenance time</b>	days	4 days	2 days*	Increased stiffness will significantly lower installation time.
<b>Rate of corrosion</b>	inches /month	0.005 in/month	>0.002 in/month	Material change to 410 stainless steel will significantly improve corrosion resistance.

<b>Installation runout from hole centers</b>	inches	< 0.005 in	0.0077 in	Marginal value was unable to be met due to excessive size of running ring; reduction in deflection is still a significant improvement.
<b>Labour hours of installation</b>	Hours	192	96*	Increased stiffness will decrease the required time for installation.
<b>Did we change the assembly</b>	Pass / Fail	none	Pass	Optimized running ring design will fit into current shaft seal assembly without interference.
<b>Running ring is not too heavy</b>	lbs	800 lbs	750 lbs	Running ring mass is light enough for efficient installation.
<b>Components were manufactured locally</b>	Pass / Fail	none	Pass	A local machine shop has machined all running ring parts in the past and will likely do them in the future.

\*Anticipated Values

### 5.3 Bolt Testing Finalization

Now that the bolt testing apparatus has been conceptualized and narrowed to a single configuration, the details on the apparatus design and experiment can be fully developed. With a fully developed apparatus, Generation Solutions can begin fabrication, with which testing will soon follow. With testing data, Generation Solutions will obtain results to analyze and conclude with.

#### 5.3.1 Bolt Testing Experimental Design

Once the apparatus was conceptualized, the detailed experimental design needed to be developed. The complete and finalized test procedure can be accessed in Appendix C: Bolt Test Procedure, which will be referenced throughout this discussion.

With the intent of retrieving values of nut factor ‘K’ and understanding its high variance nature due to many areas of error, the experiment needs to be repeatable and consistent. Because the fasteners to be tested have a specific application, the experiment will be designed to simulate the conditions of fasteners on the running ring of the turbine shaft. Doing so will assist designers with knowing the nut factor for this particular application.

Using ASTM and SAE test standards as templates on what to include in the experimental design, the first part was to fully develop the scope, which is to determine the nut factor ‘K’ intended for stud-bolts fastened with two nuts on either end. From here, an introduction to background and theory is required to guide the user to understand how this value is determined, specifically with the proposed method of measuring the elongation length as an indirect measurement of verifying preload, leading to a nut factor.

A key part of experimental design is to understand sources of error and how to lead to meaningful conclusions while understanding that there will be statistical variations. Therefore, statistical tools are introduced in the background to characterize the distribution of the results and lead to a conclusion of the experiment.

Before any results are achieved, the sample size must be taken into consideration. The difficulty is having a sample size large enough to make strong conclusions, while making it small enough that it does not become too resource intensive, especially given the time constraint of the project. Details of determining the exact sample size are provided in the procedure, which was determined to be 31 specimens, using equation (5.4.1.1):

$$n = \left( \frac{zs}{ME} \right)^2 \quad (5.4.1.1)$$

where:

$n$  is the sample size,

$z$  is z-score related to the desired confidence interval,

$s$  is the standard deviation,

$ME$  is the margin of error.

A limitation of this sample size is that it is dependant on the standard deviation, a value that is not known in advance. So an estimate was made, and once the results are obtained, a discussion will guide the user to revisit the sample size and determine if the assumption was valid or needs to be adjusted.

Additional statistical tools introduced such as p-value, mean, standard deviation, and 85% confidence interval of the mean, will assist the user with describing the shape and spread of the results, intended to lead towards a conclusion on a nut factor to use in design.

With the background now communicated with the user, a procedure is established, ensuring that it is well defined and repeatable. This begins with a list of required items: the main test plate, washer plates, torque wrench, simple wrench, digital micrometer, and the test fasteners with corresponding nuts. The user is directed to proceed into a pre-test setup, mainly concerning the verification of dimensional specifications, and ensuring that contact surfaces are clean and smooth.

The main test procedure is relatively simple, adding convenience to the user, who must repeat the bolt test many times for the sample size. Basically, the user fastens the test bolt into the main test plate, sandwiching the three washer plates in between to increase the elongation length. Then the user is instructed to hold the bottom nut stationary, while using the torque wrench to tighten the fastener until the specified torque. Once achieved, the user removes the wrenches, and uses the digital micrometer to measure the elongation length, which is shown in Figure 56.

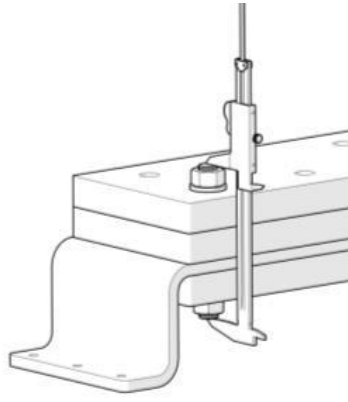


**Figure 56: Measuring the elongation length of the bolt after torquing.**

Once the elongation lengths are measured for the sample size, the user inputs this data into the Excel spreadsheet ‘Nut Factor Analysis’ which will automatically calculate the nut factor per trial. These results will also be imported into a Minitab spreadsheet to obtain a statistical summary report, displaying the p-value, shape, center, and spread of the results. An example of this summary report is shown in Figure 57.



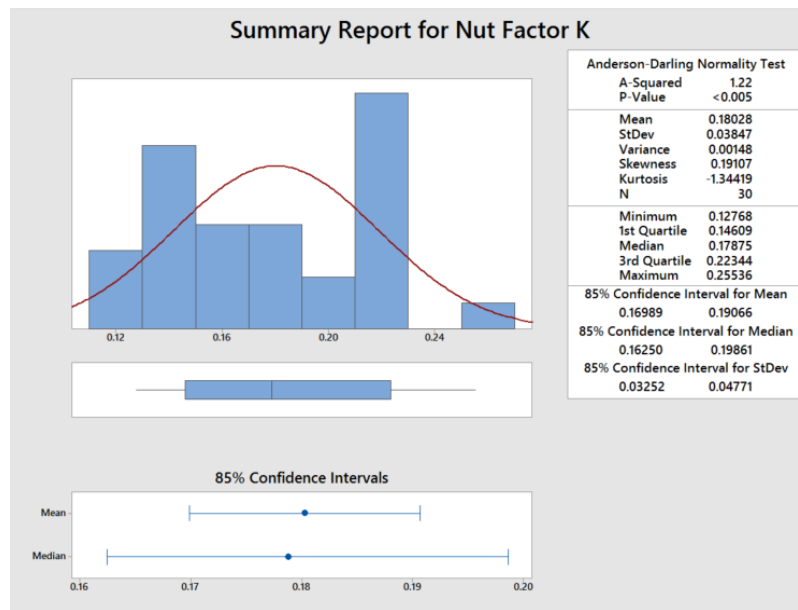


**Figure 57: Sample data results in Summary Report from Minitab.**

Lastly, a discussion guides the user to critically analyze the results that were obtained and determine the validity. The experiment ends by asking the user to specify a final nut factor that designers can use and justify why it is a reliable and safe value to use.

### 5.3.2 Optimized Test Apparatus

Building off of conceptual design enabled us to further optimize our design based on limitations set out by the project. In the following, this progression can be seen through designs and the thought processes behind decisions. The goal of this apparatus was to determine the Nut factor. This was done by verifying a given preload, based upon the measurement of elongation length and torque, while considering cross sectional area of the threads, elastic modulus of the material and the effective length that the bolts are under.

The initial goal for the nut factor apparatus was to create an apparatus, which was able to achieve an accurate nut factor that could be related to the current fasteners on the running ring. We were also tasked with creating a simple procedure to outline how to perform the test, along with a data acquisition calculator, to analyze the Nut factor from raw data. Having deliverable drawings and models was also a goal for the project.

With respect to simulating a similar environment to what is currently on the running ring, the type of fastener must be determined, along with the length at which they are tensioned at. Referencing to the Manitoba Hydro running ring drawings, the fasteners were created from

ASTM A193 B7 steel, while the turbine and spacers were mainly made of A516 Grade 70. Additionally, the fasteners have 70mm in tension due to them being threaded straight into the turbine.

Through the progress of the design, the scope shifted from determining the Nut factor of the running fasteners, to determining a repeatable Nut factor for a given fastener situation. This was due to potential testing costs of replicating the environment of the current running ring fasteners, and the goal of creating a standard Nut factor test for Manitoba Hydro.

Figure 58 and Figure 59 presents the concepts that were proposed in section 3.3 Bolt Testing Concepts (CN10). In the model, the design achieved 2.18" in tension excluding the nuts; typically, M16 nuts are 0.55" thick, so the total length in tension of the bolt would be 2.68", which amounts to 68 mm. Since the intent was to replicate running ring conditions, the remaining 7 mm that the running ring fasteners see can be achieved with washers.

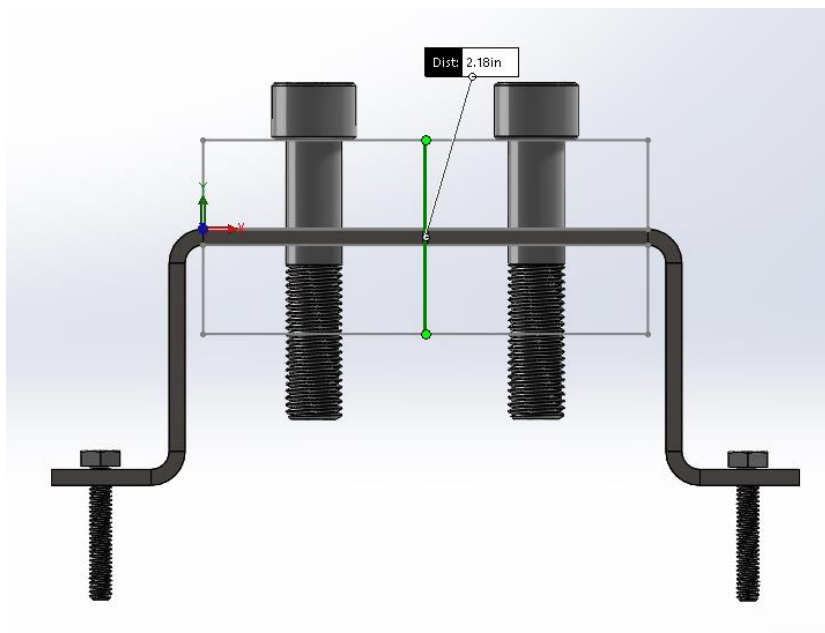


Figure 58: 7 Gage plate apparatus side view [37].

Slots were initially created for the test plate, which are demonstrated in Figure 59, to negate the effects of potential localized deformation being incurred on one hole from another. Holes on the outer flanges added areas to secure the test. Upon consulting with a local machine shop, it was determined that the bend radius of 7 gage is 0.203". The test apparatus as a whole was made fairly compact.

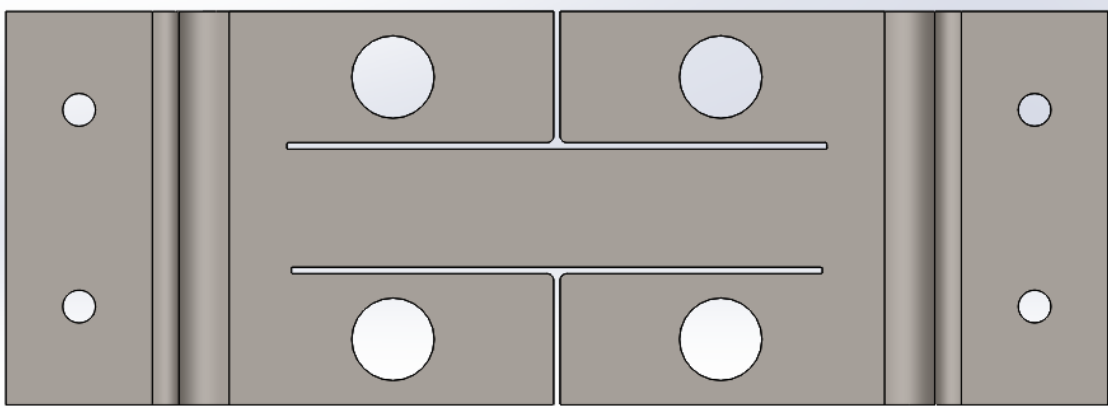


Figure 59: 7-Gage plate [38].

It was determined that a thicker metal for the apparatus should be used to negate potential negative effects while torquing the fasteners. The thicker metal was also chosen to help increase the effective length. Making the platform of the test procedure bigger, was key in increasing ease of access and potential clamping load redistribution along with a sturdier test apparatus. In Figure 60, the apparatus also began to evolve with the creation of spacer plates. Simple blocks were originally created because they were thought to be affordable, easy to make from sheet metal, and expendable. Two blocks 0.875" thick were finally chosen as the block thickness, which would achieve 2.75" corresponding to 70 mm, which the current running ring fasteners are under tension.

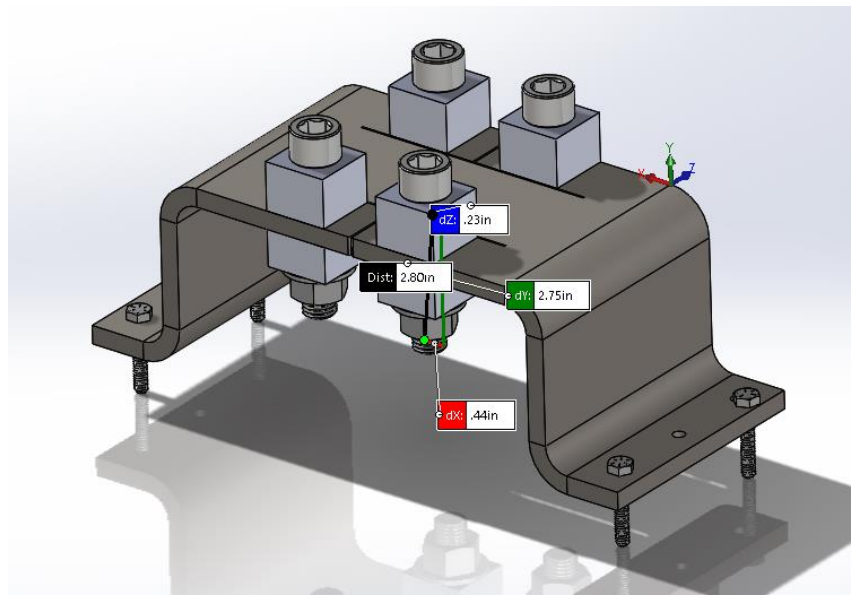


Figure 60: 3/8" Plate apparatus isometric view [39].

An increase in plate thickness created the necessity for an increase in plate length to compensate for an increase in bending radius, which shifted the flanges for clamping. The bending radius was determined to be 0.47". These features can be seen in Figure 61. Not only did the test sheet increase in length, but also in width, which was to allow for the centre load bearing connecting piece to be less susceptible to any types of load.

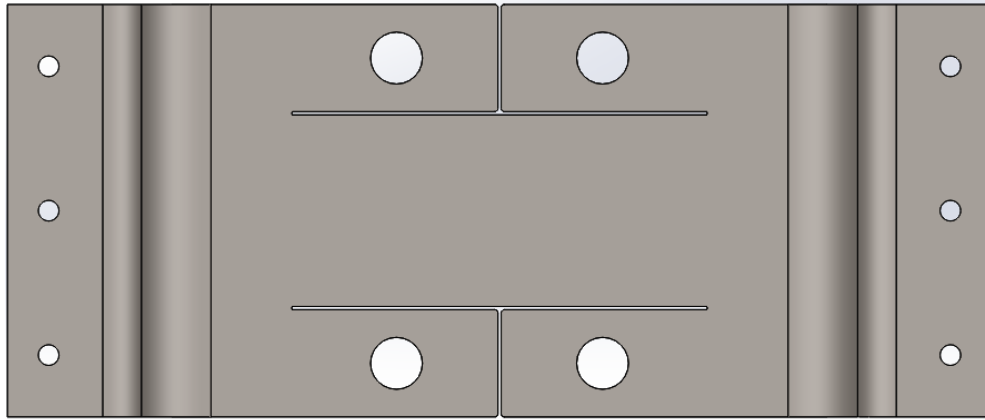


Figure 61: 3/8" Plate [40].

Towards the end of design optimization, the test plate was becoming larger through each phase. This was due to a larger apparatus providing more room to move freely, allowing it to be unsusceptible to failure under loading conditions, and for the addition of further holes, adding more repeatability to the test. The washer plates were also made bigger to allow for more surface area to clamp to. In this last phase of optimization, the focus was on creating an apparatus, which would be able to achieve larger elongation lengths, deviating from the initial goal of the running ring environment.

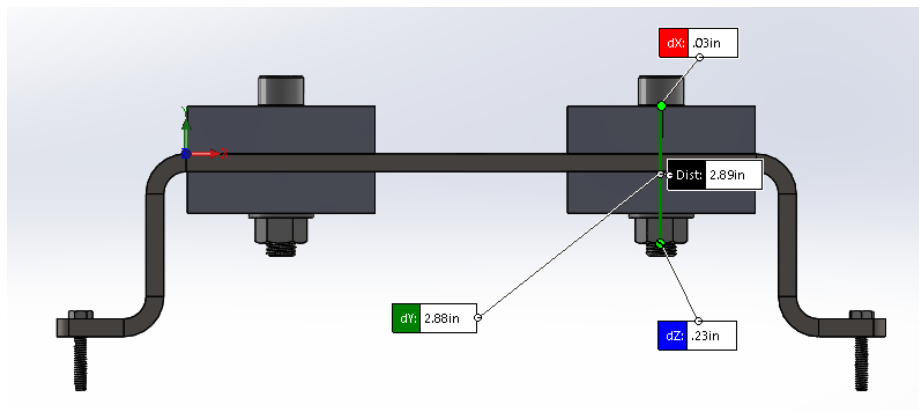


Figure 62: 3/8" Plate apparatus 2 side view [41].

Slots were determined to potentially be limiting the clamping area in which the bolts act through. In order to achieve an adequate clamping load, the slots were removed, and the holes were moved at least 1.5 hole diameters in from the edge, which is a common criterion for achieving suitable clamping area [11]. As a precautionary measure to act as a safety factor, the holes were moved 2-hole diameters.

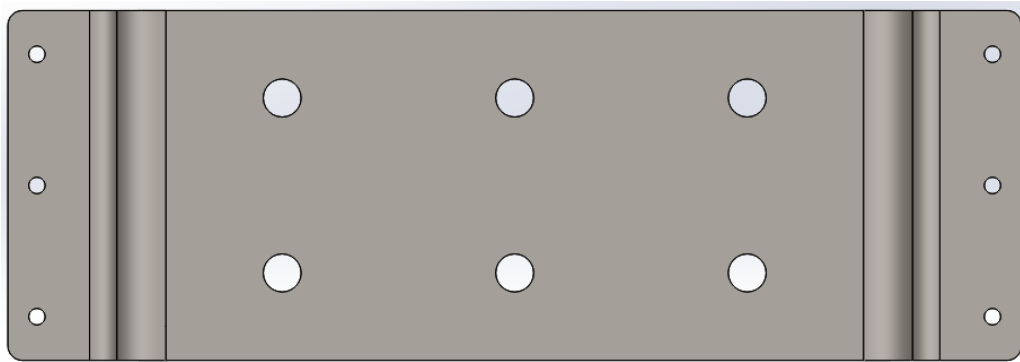


Figure 63: 3/8" Plate 2 [42].

Singular plates were originally created, with the intent to be easily discarded should they become damaged. However, two-hole or six-hole spacer plates were also considered, for they can limit the amount of shifting between plates, Figure 64 illustrates these plates.

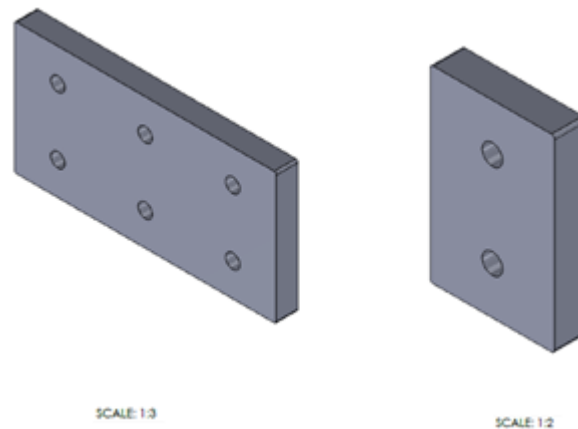


Figure 64: 1" Spacer plates with two and six holes [43].

The 6-hole space plate was eventually chosen because it allowed for easier installation. The potential galling or wear of the plate was contemplated and was determined to be negated through the use of washers.

In the final assembly, fully threaded fasteners were used due to the affordability and simpler to measure, since they have two smooth surfaces on top and bottom. This makes the test functional

for both stud-type and head-screw type fasteners. Instead of trying to replicate the conditions of the current running ring fasteners, 0.01” elongation length is the planned target, while applying a stress of 70% of the yield. Since 0.01”, is a standard for stretch length of fasteners at Manitoba Hydro. Because the measurement equipment for elongation length can vary in measurements by up to 0.002”, increasing the elongation length helps in the verification process by reducing the amount of potential error.

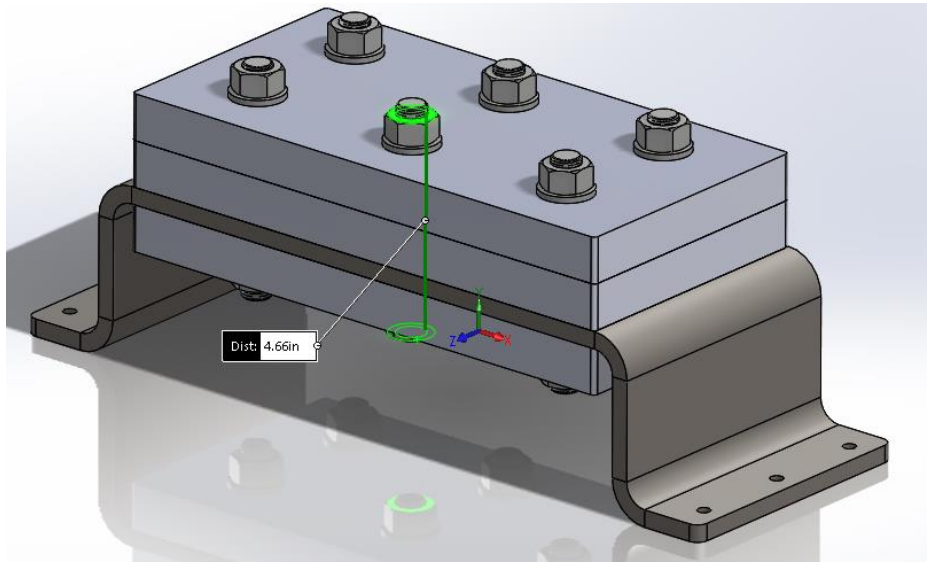


Figure 65: Final apparatus isometric view [44].

## 5.4 Bolt Test Results

Once a final test apparatus had been chosen, we began coordinating the fabrication of the test, along with the development of a test procedure and calculator. Once all tasks were completed, testing was performed and data was acquired, which was then analyzed to find the nut factor  $K$ .

### 5.4.1 Manufacturing Details

When design optimization was completed, we began the fabrication process. The fabrication started with communication, between the team and the client. Ensuring that they approved of the design was our goal. Once confirmation was given from the client on the design, communication with a machine shop started. This involved the exchange of drawings, procedures, material types, quantities, expected lead times, completion times, and quotes. Initially, a similar test environment of current running ring fasteners was the intent on the test, which composed of the A516 Grade 70 steel apparatus. However, it was found that this option was expensive, with a larger lead time due to its availability. The machine shop proceeded to recommend the use of

A36 steel which was similar in mechanical properties and was readily available. Additionally, the machine shop proposed the use a large block of steel, which was readily available in their inventory. This large block of steel could be fabricated into something similar to the proposed apparatus for a very affordable price, since the material was readily available. Since the option offered benefits such as decreased lead time and cost, the test apparatus was fabricated out of the block and which was tested on, seen below in Figure 66.

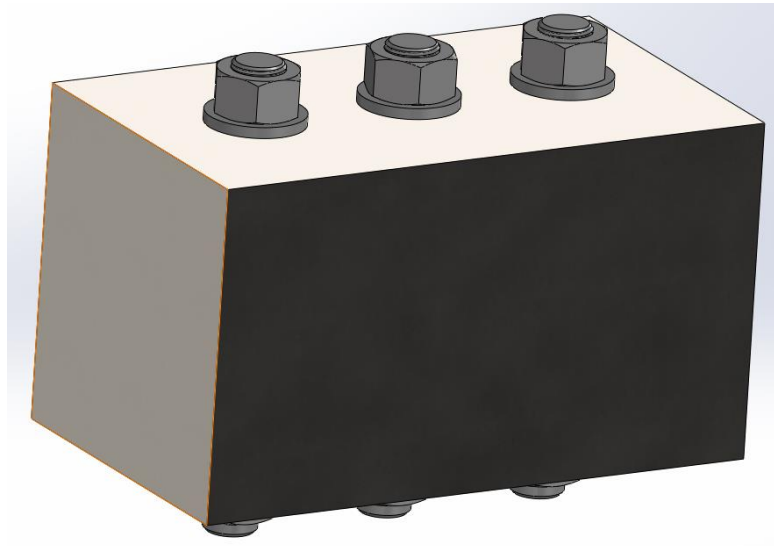


Figure 66: 4x4 Block testing apparatus [45].

Although the block looks different from the proposed apparatus design, it achieves the same objective. Typically, the availability of a stock steel with these dimensions is not common and for this reason, Generation Solutions would still recommend creating the apparatus proposed earlier. Special attention may be needed when ordering and manufacturing parts for the apparatus, because sheet metal can have defects. For instance, 1-inch-thick sheet metal may vary in thickness from one area to another. Keeping the surfaces planar is a consideration that must be accounted for in the testing of our bolts because any external forces or unaccounted length will contribute to the error of the test. To reduce this error, these plates would have to have both sides ground to achieve a finish dimension within 0.001”.

### 5.4.2 Observations

Bolt testing was performed on November 28<sup>th</sup> 2016 at a local machine shop. Initiation of the testing procedure had begun with the cleaning of purchased nuts and bolts with solvents, this can be seen in Figure 67.





**Figure 67: Bolt cleaning [46].**

The team worked in parallel during the cleaning process to use time efficiently and began prepping the test area. Preparation of the test area entailed cleaning of the test apparatus and securing it to the test table with a clamp. After the apparatus was secured, a test was simulated and inspected, which found that stud and apparatus clearance would only allow for one nut on each side of the stud without any washers, which is illustrated by Figure 68.

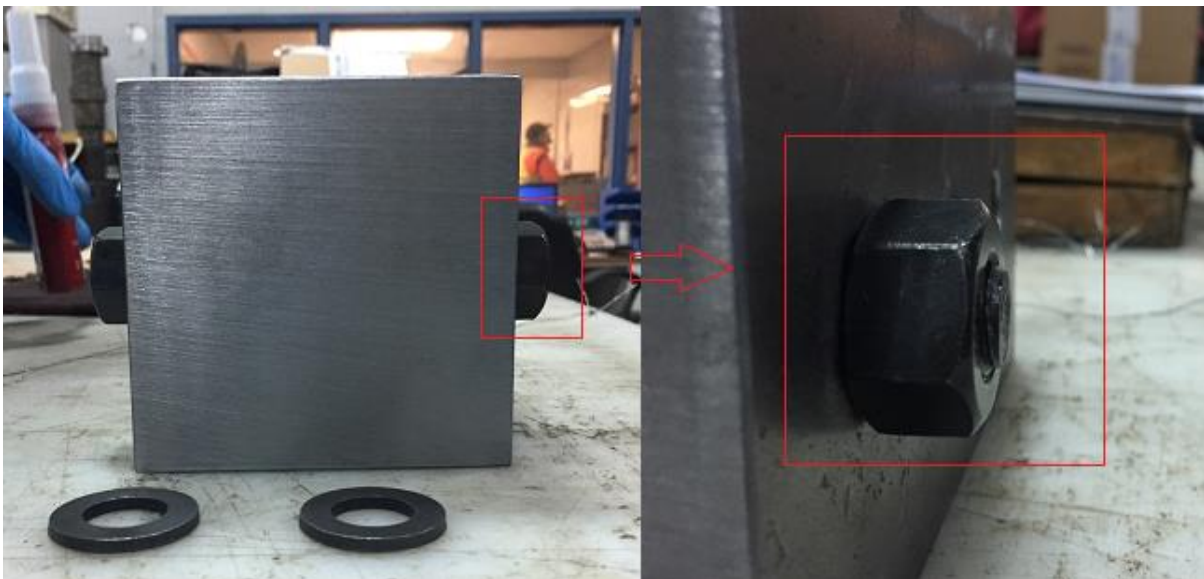


**Figure 68: Nut clearance during test [47].**



The clearance issue meant that potential wear of the apparatus could occur and for this reason was monitored before, during and after the test. When testing concluded it was found that wear had created a loss of 0.003” of the apparatus material at the test location. This observation was noted within the results.

The testing procedure was conducted as follows:

- Studs were put into the three holes of the apparatus.
- 2 Nuts were added and snugged up on each side of the stud, ensuring that there was an equal amount of threads on both sides of the stud.
- Measurements of the stud length were taken, along with the length between each outside face of the nuts (effective length).
- The nuts were taken off.
- 9 Drops of Loctite was applied to one side of each stud by rotating 120 degrees for every three drops.
- 2 Nuts were re added and snugged up on each side of the stud, ensuring that there was an equal amount of threads on both sides of the stud.
- The torque wrench was dialed to 120 ft-lbs and was applied to the side of the stud with Loctite, while a breaker bar held the opposing nut. This is apparent in Figure 69.



Figure 69: Test run through torque application [48].

- When the torque wrench reached its mark, the wrenches were removed.
- Measurement of the stud was taken again while in tension, which is shown in Figure 70.



**Figure 70: Test run through measurement [49].**

- Measurement data was collected and analyzed.
- Nuts were backed off and the apparatus was inspected prior to another trial.

During the testing of the studs, certain events were observed:

- It was realized that the studs being used were of two separate finishes and were noted within the results. A change in finish can alter the amount of friction between threads and for this reason was monitored during data collection and analysis.
- After 12 trials, it was realized that studs had an uneven finish at each end, leading to greater variation within elongation measurement. In order to try and control the variable, the team filed down each end of the stud. Data from the previous 12 trials were discarded.
- 31 trials of bolt testing were performed after the original 12 trials.
- The 31 trials of bolt testing contributed to the final data and analysis.

### 5.4.3 Final Results

From the data collected, where the full results can be seen in Appendix E: Bolt Test Results, the results can be summarized using the *MiniTab* graphical summary, as shown in Figure 71.

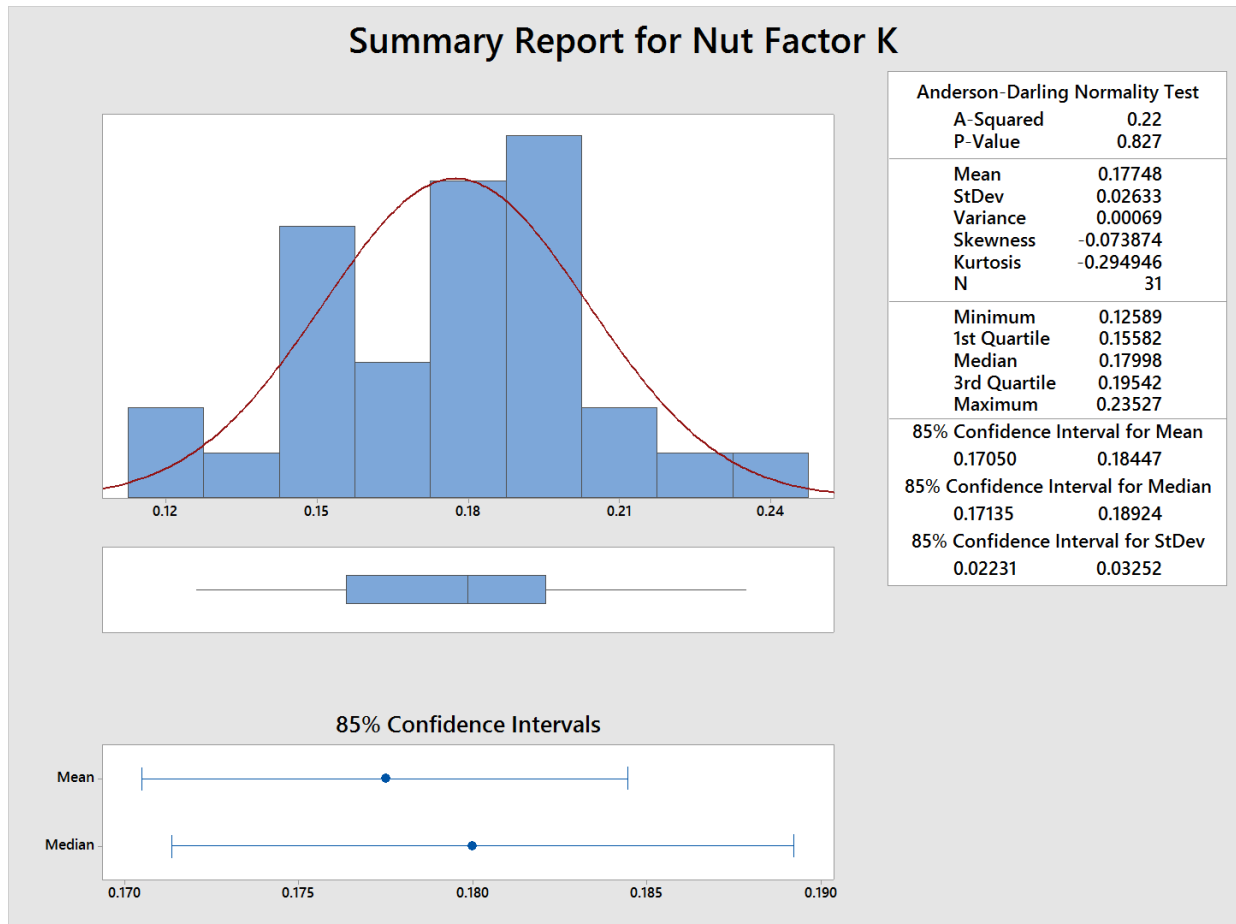


**Figure 71: Minitab graphical results of Nut Factor K testing.**

These results describe the shape, center, and spread of the results, including the p-value, mean, and standard deviation.

### 5.4.4 Discussion and Compare to CN's

From the results obtained, Generation Solutions has determined that a 5/8" stud under 4.66" length in tension with blue Loctite applied will incur a Nut factor value of 0.177, with a confidence level of 85%.

For the scope of this project, it was determined a sample size of 31 was adequate in reaching a large enough confidence level for the client. This was taking availability of materials, and time constraints into consideration. With the standard deviation now known, the sample size can be

constraints into consideration. With the standard deviation now known, the sample size can be recalculated using equation (5.4.1.1). Keeping the margin of error at 0.0053 and an 85% confidence interval constant, a new sample size of 51 is obtained. This means that to carry out an experiment with these assumptions, 20 more specimens would need to be tested. Furthermore, if the test were to only have 31 specimens, the data will result in either a new margin of error of 0.0068, or a new confidence interval of around 72%.

Commenting on the shape, center, and spread, the results follow an approximate normal distribution. Referring to Figure 71, the p-value is 0.827, which is much greater than 0.1, the established minimum p-value, where any smaller than 0.1 would reject the null hypothesis. In this case, it is concluded that we fail to reject the null hypothesis meaning the results of the bolt testing cannot be confirmed or denied that they do follow a normal distribution.

In terms of application of the results, Generation Solutions would recommend using a nut factor value of 0.177 for a 5/8" fastener under 4.66" of tension at a confidence level of 85%.

Expected sources of error during the test are:

- The torque wrench used was calibrated, but it is known that the torque value can vary from friction, jerk or change in operator. All known areas of error within the torque wrench should be accounted for in the sample size.
- The measurement of the micrometer can vary due to the surface areas of measurement along with the method an operator follows.
- Friction between washers and plates creates error due to slipping.
- Loss of load due to friction within the bolt and head was also a source of error.
- Loctite application may vary from one individual to another, creating a range of lubrication and friction.
- Surface finish of the bolts, but upon completion of analysis, it was determined that the difference of surface finish of the bolts had little to no affects within results.

The objective of the Nut factor apparatus and procedure had originally been to determine the Nut factor value for fasteners on the running ring. The scope of the project needed to change in order to allow for fabrication and testing. 5/8" x 5" Studs were used instead of M16x70mm socket head screws, changing both the diameter of fastener and length of tension. Although the Nut factor was determined to a 5/8" x 5" stud, it provides confidence into a range of Nut factor

values for the corresponding M16 socket head screw. TABLE XLIV shows how customer needs were altered to achieve the new scope of the project and why.

**TABLE XLIV: NUT FACTOR K CUSTOMER NEEDS COMPARISON**

Metric	Units	Marginal Value	Actual Value	Why
Distance of elongation length represents 60% yield of bolt while in tension	inch	0.0063 + 10%	0.01	The scope of the project changed, to make testing more affordable.
Does the test apparatus replicate running ring conditions	Pass / fail	None	Fail	Since the scope of the project changed, we tried to create a standardized test that was able to determine an accurate and repeatable nut factor K.
Torque and preload relationship is found with little standard deviation	Factor margin of error from nominal K value	+/- 10%	+/-14% (standard dev.)	Results had a higher standard deviation than planned; this is expected due to the many uncontrolled sources of error related to fastener testing.
Number of tests for design life	number	5000 tests	30	30 tests have been completed without any issue with the test apparatus.
Procedure steps allow for accurate performance	pass / fail	none	Pass	Although the scope of the project changed, we were still able to deliver a well-defined and informational procedure
Is the test easy to perform	pass / fail	none	Pass	The test was easier than expected, due to testing being performed on a 4x4 block.

## 6 Conclusion

In conclusion, the team has learned more about the engineering design process, and was privileged enough to experience implementation and testing. Despite the team's best efforts, some recommendations can be made to further enhance the quality of the design that the team advises future users to consider if full implementation were to take place.

### 6.1 Recommendations for Running Ring

As previously mentioned, Generation Solutions' goal of reducing the change in vertical diameter below 0.005 inches was not achieved, as our team achieved a value slightly larger at .0077 inches. One major limitation in this project was the restriction to changes on mating components of the running ring. The existing flange on the original running ring design is extremely close to the shroud portion of the shaft seal when assembled. For this reason, the thickness of this flange was limited to its current thickness as it could not be increased without interfering with the shroud. Increasing this thickness would help increase the moment of inertia of the running ring and would therefore help to further reduce the change in vertical diameter. However, increasing this thickness would require the shroud design to be changed. Our team decided to pursue an increased flange thickness due to the added cost of changes shaft seal mating components. If a lower deflection value was desired, increasing this thickness and redesigning the shroud would further reduce the change in vertical diameter.

The restriction of changes to mating components of the running ring limited the generation of design concepts as they had to fit into the current assembly. If the deflection value achieved by our design was found to be insufficient, allowing for other shaft seal components to be redesigned would allow for a variety of additional design concepts that would potentially further reduce the deflection.

With respect to the corrosion concerns, there are a few suggestions that can be made to further decrease the corrosion rate. For the material, the stainless steel is selected under multiple design parameters. However, other materials still can be considered such as titanium alloy because it is the second highest score in the scoring matrix. Titanium alloy was discarded as an option due to excessive cost.

Another suggestion can be made to increase corrosion resistance is to have the seal supply water during a turbine shutdown period instead of turning it off. As previously mentioned, the

corrosion happened mostly while the water was stagnant. According to the team's research, the circulating water environment will likely reduce the corrosion effect comparing it to the stagnant water environment. The suggestion for the seal running water is to have it on with the same set-up as it would be on during regular operation

## **6.2 Recommendations for Bolt Testing**

It is our recommendation that testing be performed in the exact same environment as the running ring fasteners, by having the same effective length, type of fastener being used, and clamping material. By performing the testing in a more similar environment, nut factor K results will resemble the running ring fasteners nut factor more closely. Other bolt testing methods should be explored, such as destructive testing, or the use of different equipment such as load cells to verify pre-load. When manufacturing the apparatus that was designed, ensuring the fabrication process does not yield defects is also important. Having uniform faces on fasteners will allow for more accurate readings with tools such as the micrometer. Keeping suitable lead time scheduled for fabrication would be advisable. Modifications to the procedure and analysis software may need to be made if the apparatus or test was changed in any way.

## **6.3 Design Lessons Learned from Team**

The team found that working together with active communication was pivotal in completing deliverable material on time with the highest level of quality. The team engaged in dynamic work sessions and meetings, including many virtual, offline, and in-person meetings with the client for regular consultation and decision making. This open communication with the client made the team more productive as this meant meaningful feedback, advice, and guidance. Furthermore, the team was able to learn about manufacturing constraints, and learn how to communicate with fabricators to ensure that the part that is designed, is the part that is made. One key lesson learned is to be accountable for the tasks that are assigned and to communicate realistic challenges that may hinder a team member's delivery. Another is that the task delegation could have been more fair to share the workload effectively; dialogue when a team member feels overworked is recommended to allow other members to offer help, if they can. Finally, while the best efforts were made on delivering this project, the team feels that it would be more advantageous for the client to investigate the running ring and fasteners in two separate

projects, as our team believes more depth could have been covered. Nonetheless, the team is very proud of the final design and hopes that Manitoba Hydro will implement it in the future.

## **6.4 Design Summary and Recommendations**

From this design project, the team as a whole has gained valued experience in an engineering process. Generation Solutions has created a running ring with more rigid geometry to assist with deformation concerns, along with an adjusted material to help counteract the effects of corrosion. The team has also created a standard test apparatus, procedure and analysis for determining the Nut factor  $k$  of fasteners.

Following the completion of a rigorous design process and finite element analysis Generation Solutions has successfully increased the stiffness of the running ring. The vertical deformation of the running ring was reduced to 0.007" from 0.033". Generation Solutions and Manitoba Hydro were hoping to achieve a deflection value of 0.005" in order to conform to assembly tolerance, however the achieved value will significantly reduce the deflection despite not meeting our goal.

Research conducted by Generation Solutions determined that changing the material of the running ring from ASTM A516 Gr 70 steel to 410 stainless steel will reduce the corrosion concerns significantly, by more than a factor of 2 every year.

Through extensive detailed design and optimization, we have created a procedure for how to use the apparatus to determine the Nut factor, along with its corresponding analysis program. We have received acceptable results from our apparatus, with an average Nut factor value of 0.177 for a 5/8" x 5" stud under 5.2" of tension with Loctite applied undergoing 0.010" elongation length with a standard deviation of 0.0263 and a confidence level of 85%.

Although some of the initial design scope was modified due to project constraints, Generation Solutions has completed the objective of the project through hard work and determination. In doing so, we have completed on our deliverables, that both we and the client are happy with. We have enjoyed our time working on this project and look forward to working with Manitoba Hydro again in the future.

- Generation Solutions



## 7 Bibliography

- [1] "Jenpeg Generating Station," Hydro.mb.ca, [Online]. Available: [https://www.hydro.mb.ca/corporate/facilities/gs\\_jenpeg.shtml](https://www.hydro.mb.ca/corporate/facilities/gs_jenpeg.shtml). [Accessed 16 September 2016].
- [2] "Machining Solution: Repairing Cracked Turbine Shafts at Jenpeg," Hydroworld, 2011. [Online]. Available: <http://www.hydroworld.com/articles/hr/print/volume-30/issue-7/articles/machining-solutions-repairing-cracked-turbine-shafts-at-jenpeg.htm>. [Accessed 19 September 2016].
- [3] W. C. Y. a. R. G. Budynas, Roark's Formulas for Stress and Strain, New York: McGraw-Hill, 2002.
- [4] E. Morrish, Artist, *Running ring variables*. [Art]. University of Manitoba, 2016.
- [5] The Engineering Toolbox, "Young Modulus of Elasticity for Metals and Alloys," 2016. [Online]. Available: [http://www.engineeringtoolbox.com/young-modulus-d\\_773.html](http://www.engineeringtoolbox.com/young-modulus-d_773.html). [Accessed 24 October 2016].
- [6] The Engineering Toolbox, "Modulus of Rigidity of some Common Materials," [Online]. Available: [http://www.engineeringtoolbox.com/modulus-rigidity-d\\_946.html](http://www.engineeringtoolbox.com/modulus-rigidity-d_946.html). [Accessed 24 October 2016].
- [7] "Corrosion," Wikipedia, 24 October 2016. [Online]. Available: <https://en.wikipedia.org/wiki/Corrosion>. [Accessed 8 October 2016].
- [8] M. G. Fontana, Corrosion engineering, McGraw Hill Education, 2005.
- [9] M. Hydro, *Units 1-6 Turbine Shaft Seal Assembly*, Winnipeg, 2012.
- [10] A. Skorpád, Artist, *Illustration of tensile load applied through fastener actual and simplified*. [Art]. University of Manitoba, 2016.
- [11] J. H. Bickford, Introduction to the Design and Behavior of Bolted Joints, Boca Raton: CRC Press, 2006.
- [12] E. Morrish, Artist, *Original running ring cross-section*. [Art]. University of Manitoba, 2016.
- [13] E. Morrish, Artist, *Original versus concept A1.1.1: increased thickness*. [Art]. University of Manitoba, 2016.
- [14] E. Morrish, Artist, *Original versus resulting A1.1.1 concept turbine flange hole pattern*. [Art]. University of Manitoba, 2016.
- [15] E. Morrish, Artist, *Original versus concept A1.1.2: increased flange dimensions*. [Art]. University of Manitoba, 2016.
- [16] E. Morrish, Artist, *Running ring flange cap screw*. [Art]. University of Manitoba, 2016.
- [17] E. Morrish, Artist, *Original versus concept A1.1.3: added flange*. [Art]. University of Manitoba, 2016.
- [18] E. Morrish, Artist, *Original versus concept A1.1.4 ribbed*. [Art]. University of Manitoba, 2016.
- [19] E. Toolbox, "Densities of Solids," [Online]. Available: [http://www.engineeringtoolbox.com/density-solids-d\\_1265.html](http://www.engineeringtoolbox.com/density-solids-d_1265.html). [Accessed 25 October 2016].

- [20] "Stainless steel," Wikipedia, [Online]. Available: [https://en.wikipedia.org/wiki/Stainless\\_steel](https://en.wikipedia.org/wiki/Stainless_steel). [Accessed 8 October 2016].
- [21] E. Bardal, Corrosion and Protection, Manchester: Springer, 2003.
- [22] "Cathodic Protection," JOTUN, [Online]. Available: <http://www.slideshare.net/mujiqc/13-cathodic-protection>. [Accessed 8 October 2016].
- [23] "Offshore cathodic Protection 101," cathodic Protection 101, 2013. [Online]. Available: <http://www.cathodicprotection101.com/>. [Accessed 8 October 2016].
- [24] "Anodic protection," Wikipedia, 15 October 2016. [Online]. Available: [https://en.wikipedia.org/wiki/Anodic\\_protection](https://en.wikipedia.org/wiki/Anodic_protection). [Accessed 8 October 2016].
- [25] A. Skorpad, Artist, *Description of Metric Bolt*. [Art]. University of Manitoba, 2016.
- [26] A. Skorpad, Artist, *Initial Sketch Side View*. [Art]. University of Manitoba, 2016.
- [27] A. Skorpad, Artist, *Evolution 1 of Design Side and Top View*. [Art]. University of Manitoba, 2016.
- [28] A. Skorpad, Artist, *Evolution 2 Stabilizing Design Side Views*. [Art]. University of Manitoba, 2016.
- [29] A. Skorpad, Artist, *Design 1 side and top View*. [Art]. University of Manitoba, 2016.
- [30] A. Skorpad, Artist, *Design 2 side and side and top view*. [Art]. University of Manitoba, 2016.
- [31] A. Skorpad, Artist, *Design 3 side and top view*. [Art]. University of Manitoba, 2016.
- [32] A. Skorpad, Artist, *Final Optimized Design Side View*. [Art]. University of Manitoba, 2016.
- [33] "Friction and Friction Coefficients," [Online]. Available: [http://www.engineeringtoolbox.com/friction-coefficients-d\\_778.html](http://www.engineeringtoolbox.com/friction-coefficients-d_778.html).
- [34] J. K. N. Richard G. Budynas, Shigley's Mechanical Engineering Design, Ninth Edition ed., McGraw-Hill.
- [35] R. Francis, "Bimetallic Corrosion," DTI, 1982.
- [36] OnlineMetals.com, [Online]. Available: <http://www.onlinemetals.com/>. [Accessed 6 12 2016].
- [37] A. Skorpad, Artist, *7 Gage plate apparatus side view*. [Art]. University of Manitoba, 2016.
- [38] A. Skorpad, Artist, *7 Gage plate flat pattern*. [Art]. University of Manitoba, 2016.
- [39] A. Skorpad, Artist, *3/8" Plate apparatus isometric view*. [Art]. University of Manitoba, 2016.
- [40] A. Skorpad, Artist, *3/8" Plate flat pattern*. [Art]. University of Manitoba, 2016.
- [41] A. Skorpad, Artist, *3/8" Plate apparatus 2 side view*. [Art]. University of Manitoba, 2016.
- [42] A. Skorpad, Artist, *3/8" Plate 2 flat pattern*. [Art]. University of Manitoba, 2016.
- [43] A. Skorpad, Artist, *1" Spacer plates with two and six holes*. [Art]. University of Manitoba, 2016.
- [44] A. Skorpad, Artist, *Final apparatus isometric view*. [Art]. University of Manitoba, 2016.
- [45] A. Skorpad, Artist, *4x4 Block testing apparatus*. [Art]. University of Manitoba, 2016.
- [46] A. Skorpad, Artist, *Bolt cleaning*. [Art]. University of Manitoba.

- [47] A. Skorpad, Artist, *Nut clearance during test*. [Art]. University of Manitoba.
- [48] A. Skorpad, Artist, *Test run through torque application*. [Art]. University of Manitoba, 2016.
- [49] A. Skorpad, Artist, *Test run through measurement*. [Art]. University of Manitoba, 2016.
- [50] "Stress corrosion cracking," Wikipedia, [Online]. Available: [https://en.wikipedia.org/wiki/Stress\\_corrosion\\_cracking](https://en.wikipedia.org/wiki/Stress_corrosion_cracking). [Accessed 20 October 2016].
- [51] E. Morrish, Artist, *Neutral axis of running ring cross section*. [Art]. University of Manitoba, 2016.
- [52] "Material Property Data," 1995-2016. [Online]. Available: <http://www.suppliersonline.com/propertypages/A51660.asp>.
- [53] "Stainless Steel - Grade 304 (UNS S30400)," azo material, [Online]. Available: <http://www.azom.com/properties.aspx?ArticleID=965>.
- [54] "Stainless Steel - Grade 316 (UNS S31600)," azo material, [Online]. Available: <http://www.azom.com/article.aspx?ArticleID=863>.
- [55] "Stainless Steel - Grade 410 (UNS S41000)," azo material, [Online]. Available: <http://www.azom.com/properties.aspx?ArticleID=970>.
- [56] E. Inox, "stainless steel in contact with other metallic materials," 2009. [Online]. Available: [http://www.worldstainless.org/Files/issf/non-image-files/PDF/Euro\\_Inox/Contact\\_with\\_Other\\_EN.pdf](http://www.worldstainless.org/Files/issf/non-image-files/PDF/Euro_Inox/Contact_with_Other_EN.pdf).
- [57] "Friction and Friction Coefficients," [Online]. Available: [http://www.engineeringtoolbox.com/friction-coefficients-d\\_778.html](http://www.engineeringtoolbox.com/friction-coefficients-d_778.html).

## Appendices

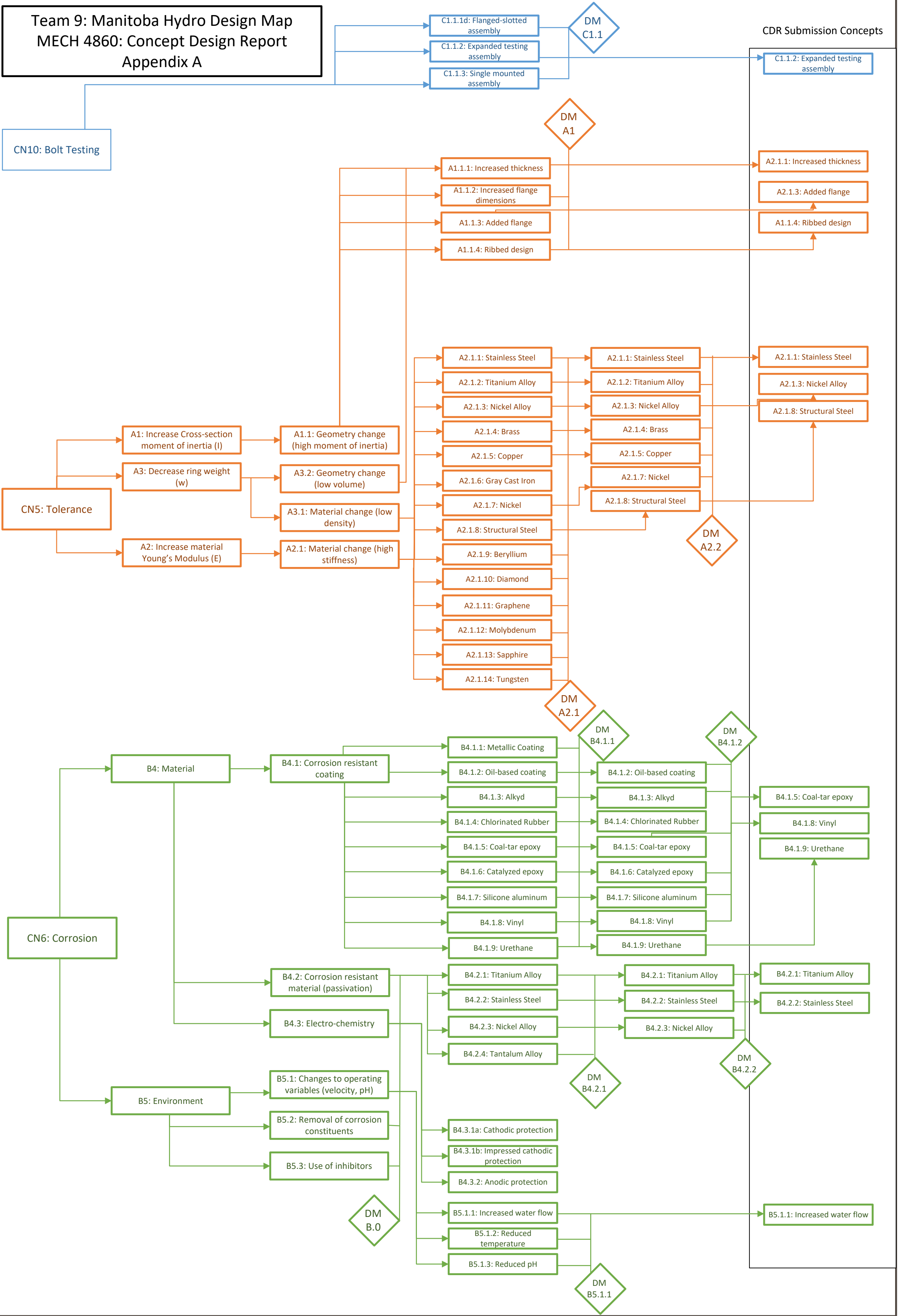
Appendix A: Design Map .....	2
Appendix B: Updated Gantt Chart.....	3
Appendix C: Bolt Test Procedure .....	4
Appendix D: Test Apparatus Final Drawings.....	5
Appendix E: Bolt Test Results.....	6
Appendix F: Test Results MiniTab Analysis.....	7
Appendix G: Updated Running Ring Final Drawings .....	8

## **Appendix A: Design Map**

Team 9: Manitoba Hydro Design Map  
MECH 4860: Concept Design Report  
Appendix A

CN10: Bolt Testing

CDR Submission Concepts



## **Appendix B: Updated Gantt Chart**

ID	Task Name	Durati	Start	Finish	Finish1	% Complete	Pred	Resource Names																																
									September 06 09 12 15 18 21 24 27 30 2016 October 03 06 09 12 15 18 21 24 27 30 2016 November 02 05 08 11 14 17 20 23 26 29 2016 December 02 05 08 11																															
1	Shaft Seal and Fasteners Capstone Project	60 day	'16 Sep 12	'16 Dec 05	'16 Dec 07	100%																																		
2	1. Planning and Research	24 day	'16 Sep 12	'16 Oct 13	'16 Nov 06	100%																																		
3	1.1 Team Building	6 days	'16 Sep 12	'16 Sep 18	'16 Sep 18	100%		M James Harper																																
4	1.2 Project Charter Development	6 days	'16 Sep 19	'16 Sep 25	'16 Sep 27	100%	3	M James Harper																																
5	Project Charter Approved	0 days	'16 Sep 26	'16 Sep 26	'16 Sep 27	100%	4	M James Harper																																
6	1.3 PDR Development	6 days	'16 Sep 26	'16 Oct 02	'16 Oct 02	100%		Team																																
7	PDR Submission	0 days	'16 Oct 03	'16 Oct 03	'16 Oct 03	100%	6																																	
8	1.4 Shaft seal research	3 days	'16 Oct 03	'16 Oct 05	'16 Oct 10	100%		Eric Morrish																																
9	1.5 Research of material and corrosion	6 days	'16 Oct 06	'16 Oct 13	'16 Oct 18	100%		Yang Qin,Shenghui Zao																																
10	1.6 Research of fastener testing methods	6 days	'16 Oct 06	'16 Oct 13	'16 Oct 18	100%		Andrew Skorpad																																
11	2. Redesign of Running Ring	31 day	'16 Oct 14	'16 Nov 25	'16 Nov 28	100%																																		
12	2.1 Concept Generation (running ring)	4 days	'16 Oct 14	'16 Oct 19	'16 Oct 21	100%	9,10	Eric Morrish																																
13	2.2 Concept design development (running ring)	3 days	'16 Oct 20	'16 Oct 23	'16 Oct 24	100%	12	Eric Morrish,Yang Qin,Shenghui Zao																																
14	2.3 Concept screening and assessment (running ring)	4 days	'16 Oct 24	'16 Oct 27	'16 Oct 27	100%	13	Eric Morrish,Shenghui Zao,Yang Qin																																
15	CDR Submission	0 days	'16 Oct 28	'16 Oct 28	'16 Oct 28	100%	14																																	
16	2.3 Design modelling	6 days	'16 Oct 28	'16 Nov 04	'16 Nov 18	100%	14	Eric Morrish																																
17	2.4 Design analysis	6 days	'16 Nov 05	'16 Nov 11	'16 Nov 25	100%	16	Shenghui Zao,Yang Qin																																
18	2.5 Optimization	6 days	'16 Nov 14	'16 Nov 21	'16 Nov 27	100%	17	Eric Morrish,Shenghui Zao,Yang Qin																																
19	2.6 Final Design	6 days	'16 Nov 19	'16 Nov 25	'16 Nov 28	100%	18	Eric Morrish,Shenghui Zao,Yang Qin																																
20	3. Fastener Testing	36 day	'16 Oct 14	'16 Dec 02	'16 Dec 03	100%																																		
21	3.1 Concept Generation (Fastener)	4 days	'16 Oct 14	'16 Oct 19	'16 Oct 19	100%	10	Andrew Skorpad																																
22	3.2 Concept design development (fasteners)	3 days	'16 Oct 20	'16 Oct 23	'16 Oct 19	100%	21	Andrew Skorpad																																
23	3.3 Concept screening and assessment	4 days	'16 Oct 24	'16 Oct 27	'16 Oct 23	100%	22	Andrew Skorpad																																
24	3.4 Design of test apparatus and process	6 days	'16 Oct 28	'16 Nov 04	'16 Nov 14	100%	23	Andrew Skorpad																																
25	3.5 Fabrication of test components	6 days	'16 Nov 05	'16 Nov 11	'16 Nov 25	100%	24	Andrew Skorpad,Eric Morrish																																
26	3.6 Perform tests	6 days	'16 Nov 12	'16 Nov 18	'16 Nov 28	100%	25	Team																																
27	3.7 Test results analysis	7 days	'16 Nov 19	'16 Nov 26	'16 Nov 30	100%	26	Andrew Skorpad,M James Harper																																
28	3.8 Test conclusions	6 days	'16 Nov 27	'16 Dec 02	'16 Dec 03	100%	27	Andrew Skorpad,M James Harper																																
29	4. Finalize	9 days	'16 Nov 22	'16 Dec 05	'16 Dec 07	100%																																		
30	4.1 FDR Development	7 days	'16 Nov 22	'16 Nov 30	'16 Dec 06	100%	18	Team																																
31	4.2 Poster and presentation development	2 days	'16 Dec 01	'16 Dec 02	'16 Dec 07	100%	30	M James Harper																																
32	FDR Submission	0 days	'16 Dec 05	'16 Dec 05	'16 Dec 07	100%	31																																	
Appendix A2 Project: MB Hydro Capstone Project Date: '16 Dec 07		Task	<div></div>	Project Summary	<div></div>	Manual Task	<div></div>	Start-only	<div></div>	Deadline	<div></div>																													
		Split	<div></div>	Inactive Task	<div></div>	Duration-only	<div></div>	Finish-only	<div></div>	Progress	<div></div>																													
		Milestone	<div></div>	Inactive Milestone	<div></div>	Manual Summary Rollup	<div></div>	External Tasks	<div></div>	Manual Progress	<div></div>																													
		Summary	<div></div>	Inactive Summary	<div></div>	Manual Summary	<div></div>	External Milestone	<div></div>		<div></div>																													
Page 1																																								



## **Appendix C: Bolt Test Procedure**

 <b>UNIVERSITY OF MANITOBA</b>	<b>Experimental Determination of Nut Factor</b>	Author: A. Skorpad M.J. Harper  Published: 11/24/2016
---	---	--

## Introduction

This document establishes an experimental method in determining the nut factor ‘K’ intended for stud-bolts fastened with two nuts on either end. This will aid designers in determining the torque specification for fasteners that provides the adequate clamping force through the relationship with the nut factor.

## Background

The relationship between the clamping force the bolted joint provides and how much torque is applied to the bolt is shown by equation (1)

$$T = KFD \quad (1)$$

where:  $T$  is the maximum torque applied to the fastener, ft-lb

$K$  is the nut factor

$F$  is the amount of clamping force the fastener applies to the bolted joint, lb

$D$  is the nominal diameter of the fastener, ft

In a bolted joint, this relationship is used to specify to how much torque should be applied when fastening the bolt to provide enough clamping force. The amount of clamping force can be determined by measuring the initial and final lengths of the stud-bolt (elongation) as well as knowing the material of the bolt, by equation (2):

$$F = \frac{EA\Delta L}{L} \quad (2)$$

Where:  $E$  is Young’s Modulus of the material of the bolt, ksi

$A$  is the nominal cross-sectional area of the bolt, in<sup>2</sup>

$L$  is the initial length of the bolt, in

$\Delta L$  is the elongation length of the bolt when in tension, in

The nut factor ‘K’ is usually conservatively estimated as it is not well understood in most bolted joints, making most bolted joints over-designed for their intended purpose. This is because the nut factor is heavily influenced by friction due to the many surfaces that are in contact. Debris, surface finishes, tolerances, and other sources of error change the nut factor ‘K’ making it specific to every application.

Due to the statistical nature of this experiment, more variables to characterize the size, spread, and shape of the distribution of specimen results are required. Firstly, a reasonable sample size is required; enough to specify a small margin of error, but small enough to be economically feasible. Sample size is calculated using equation (3):

$$n = \left( \frac{zS}{ME} \right)^2 \quad (3)$$

Where:  $n$  is the sample size,

$z$  is z-score related to the desired confidence interval,

$s$  is the standard deviation,

$ME$  is the margin of error

Equation (3) only is valid for sample sizes greater or equal to 30; any sample size below requires a t-score rather than a z-score, which is more involved to analytically determine. Additionally, we cannot know the standard deviation in advance, so this value is estimated. Consider a nominal nut factor 'K' of 0.206. Then assume the standard deviation is 10% of nominal, making it equal to 0.0206. Suppose the results are to reflect 85% of all fasteners of that type; this corresponds to a z-score of 1.44 [1]. Finally, we want a margin of error to be within 0.0053 of the actual value. This corresponds to a sample size of 31 specimens. For this test, a sample size of 31 will be used, but this value can be changed to reflect any changes to the standard deviation, desired margin of error, and confidence interval. Additionally, once the data is received for this sample size, we will compare the assumed and actual standard deviations.

The results of this test for the sample size of 31 is anticipated to have a normal distribution. To characterize this distribution and determine if the results are valid, accurate, and precise, we will consider the following statistical parameters based on the calculated nut factors per trial:

- i. P-Value: In the Anderson-Darling Normality Test, a P-value is calculated from the results, which indicates the likelihood that the results follow a normal distribution. In this experiment, a p-value less than 0.1 (commonly used) will allow the conclusion that the nut factor values do not follow a normal distribution with 90% confidence. If the p-value is higher than 0.1, we cannot conclude that the nut factors do indeed follow a normal distribution [2].
- ii. Mean: the average of the test data. Do not use this value for design without interpretation of the rest of the statistical data.
- iii. Standard deviation: compare this value with the assumed standard deviation to calculate the sample size; if the actual standard deviation is less than the assumed, a smaller sample size would be required for the same desired confidence level and margin of error. However, if larger, calculate what the new sample size would be and determine if more fasteners would be needed to retrieve better results.
- iv. 85% confidence interval for mean: these two values indicating the minimum and maximum values of the nut factor 'K' will describe that the average nut factor 'K' is between these values with 85% confidence. It is recommended that the upper value of this interval be used for design as it provides the most conservative estimate. A larger confidence interval maybe specified but the sample size should be revisited.

The intent of this experiment is to provide designers with a more confident nut factor, while understanding that the nut factor has statistical variance related to it. Therefore, the nut factor 'K' determined in this experiment should be used while considering the variance in materials, statistical uncertainty, and other sources of error.

## Procedure

The test is conducted through a pre-test setup and main test procedure. This test is facilitated by the following components to setup, secure, and measure the bolt properties:

- i. Main test plate: a simple formed plate with four bolt-down locations to secure the apparatus to a surface. The test plate is used to hold the specimens in a simulated bolted joint.
- ii. Washer plates: used to provide additional thickness for the bolted connection, while also ensuring the main test plate does not locally deform at the testing locations. Two washer plates are required per test bolt.
- iii. Wrenches: one torque wrench with torque limiting capabilities is required to fasten the bolted joint to a specified torque. The torque wrench should not exceed more than 120 ft-lb than the set torque. Another simple wrench is used to hold the nut stationary so that it does not rotate while applying torque.
- iv. Digital micrometer: used to measure the initial and final lengths of the bolt length. Should be capable of measuring to a tenth of a thou.
- v. Fasteners: both studs and corresponding nuts in sufficient quantities to fasten the stud on both sides of the main test plate. Ensure that they are compatible with the diameter and depth of the holes on the test plate.

### Pre-test Setup

Prior to beginning the test, securing the test apparatus needs to be considered.

1. Verify the flatness of the top and bottom surfaces: watch for any local deformations around the testing holes.
2. Verify the surface finish of the top and bottom surfaces of the washer plates: ensure that they are consistent and to specification. These surfaces may need to be wiped down.
3. Verify the flatness of the top and bottom surfaces of the washer plates: watch for any warping or twisting in each.
4. Verify the thickness of the washer plates: ensure that it is to specification.
5. Clean the threads of the bolts and nuts with NFD Safety or similar solvent prior to testing to ensure all tapping fluid and other contaminants are removed.
6. Start with the main test plate, and bolt down to a sturdy surface that has minimal vibration interference, using the four bolt down locations on the two flanges on either side. Ensure that the main test plate is secured properly to ensure there is no movement in the test plate while applying torque to the test specimens. The test environment shall:
  - i. Be at room temperature: all components and ambient temperature shall be 18-25°C.
  - ii. Have vibrations and shock kept to a minimum.

### Test Procedure

7. Measure and record the initial dimensions of the test bolt, specifically the:
  - i. Nominal diameter
  - ii. Initial length
8. Apply Loctite 242 to the threads of the bolt in three equally spaced beads. Ensure that there is a uniform and controlled volume of Loctite on the threads.

9. Set the torque wrench to 120 ft-lb.
10. Slide a single washer plate onto the test bolt. Then fasten a nut on one side of the bolt, ensuring that all the threads of the nut are engaged. You may need to bring the nut to about a quarter of the way up, as the top nut is limited by the socket depth of the torque wrench. Hold the test bolt upright such that the washer plate is resting on the secured nut on the bottom. This is shown in Figure 1.

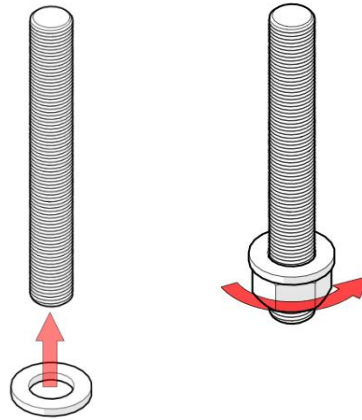


**Figure 1: Adding washer and nut to stud**

11. Place the test bolt into the one of the main test holes from the bottom. Hold the test bolt from the top, ensuring that the bottom washer plate is butted up with the bottom surface of the main test plate. This is shown in Figure 2.

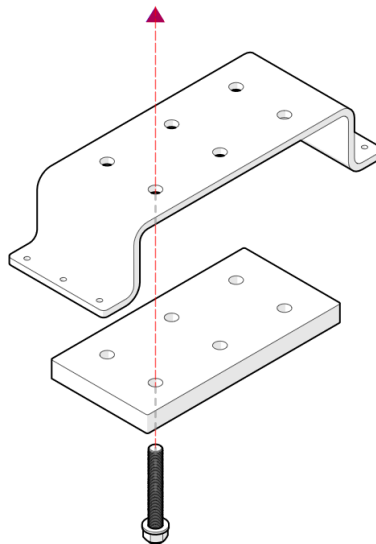


**Figure 2: Fastening bottom washer plate to main test plate**

12. While holding the bottom washer plate and stud in place, set the two top washer plates on top of the main test plate, ensuring that the holes align properly to the protruding stud. Figure 3 demonstrates this step.

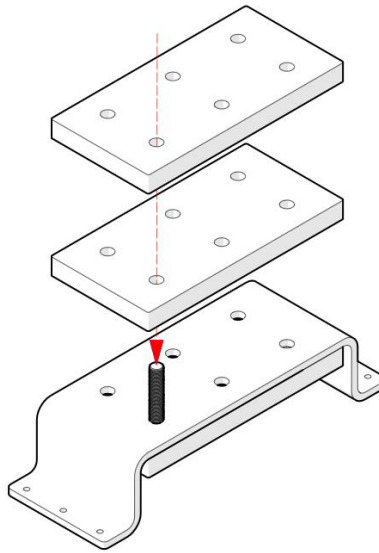


**Figure 3: Setting the two top washer plates into place**

13. Begin fastening the top nut onto the free threads above the top surface of the top plate.
14. A second fastener will be needed to be installed in any of the remaining five holes to ensure that the washer plates do not rotate during testing. Follow steps 7-13 to secure a second fastener. This one need not to be torqued to any specific value.
15. Using the torque wrench, begin tightening the top nut. Ensure that the bottom wrench is still kept in place and stationary.
16. Carefully bring the fastener to begin applying a clamping force on the washer plates and main test plate. Observe any deformations that may occur as well as any movements in the washer plates.
17. Continue to fasten until the torque wrench indicates that the specified torque has been achieved. Figure 4 shows applying torque to the bolted joint.

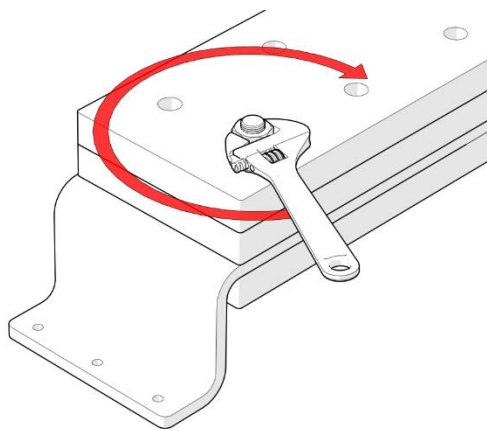


**Figure 4: Applying torque to the top nut using a torque wrench (simple wrench shown)**

18. Measure the elongated length of the stud using a micrometer or caliper as shown in Figure 5. Use the attached data sheet to record these values per trial.

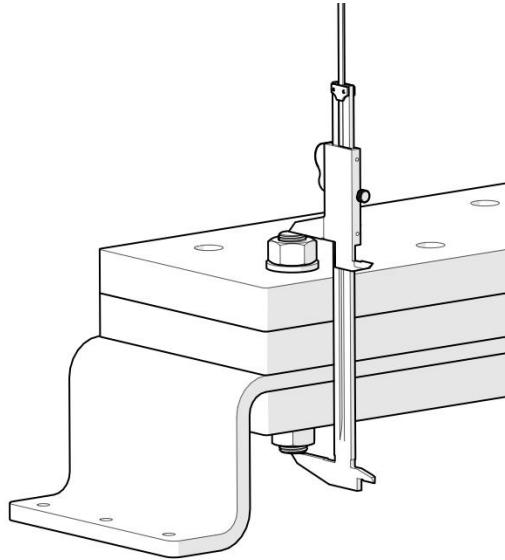


**Figure 5: Measuring the elongated stud length**

19. Unscrew the bolted connection. Observe any deformations in the threads of the bolt.
20. Repeat experiment the necessary number of times to retrieve a confident sample size for the determination of the nut factor.

## Data Sheet

Thickness of nut 1	Thickness of nut 2	Plate thickness	Modulus of Elasticity	Fastener Diameter	Pitch

[illegible]



## Analysis

Using the results from the data sheet, import this data into the appropriate locations indicated in the *Microsoft Excel* spreadsheet ‘Nut Factor Analysis’ where the following properties are automatically calculated as per the Background section:

- i. Change in length of stud.
- ii. Preload in stud.
- iii. Nut factor ‘K’
- iv. Probability of obtaining that specific ‘K’ value relative to the overall average and standard deviation.
- v. Average and standard deviation.

Using *Minitab* or any other statistical software, import the calculated nut factor ‘K’ values. Then use the ‘Graphical Summary’ function to retrieve the following information regarding the distribution:

- i. P-value.
- ii. 85% confidence interval of the mean.

Figure 6 shows a graphical summary for some sample data; the distribution is visualized with a normalized histogram and the values of interest are displayed, with a box-whisker plot also visualizing the 85% confidence interval of the mean.

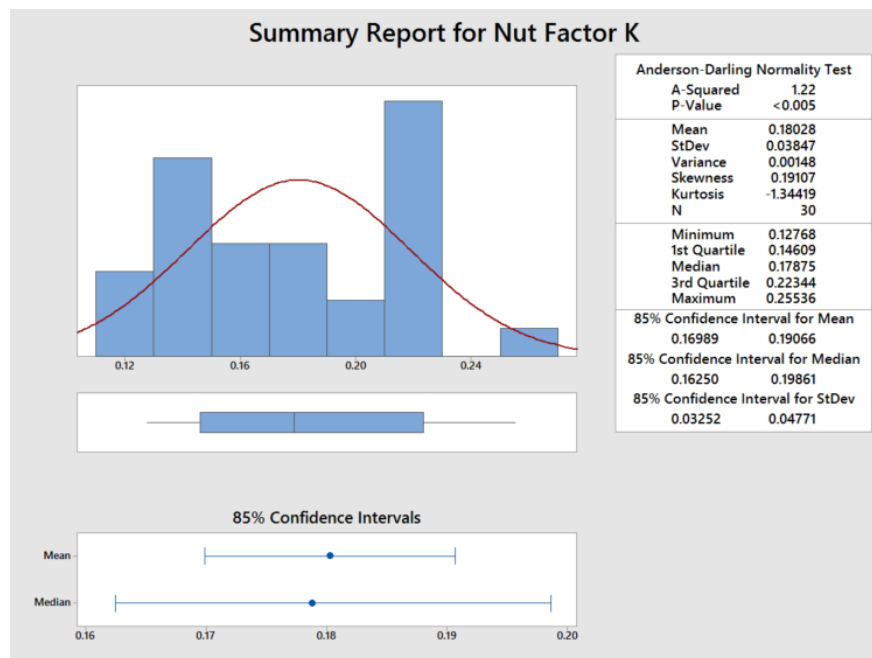


**Figure 6: Statistical summary of sample data from *Minitab***

### **Discussion**

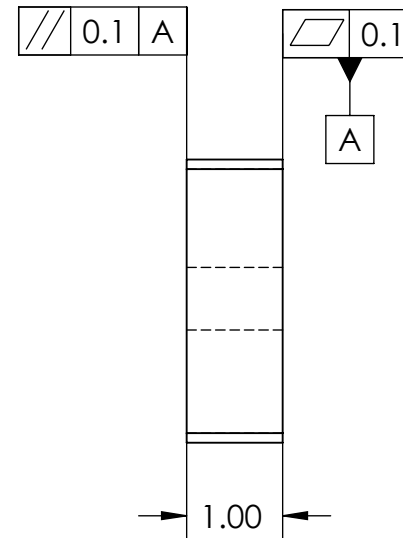
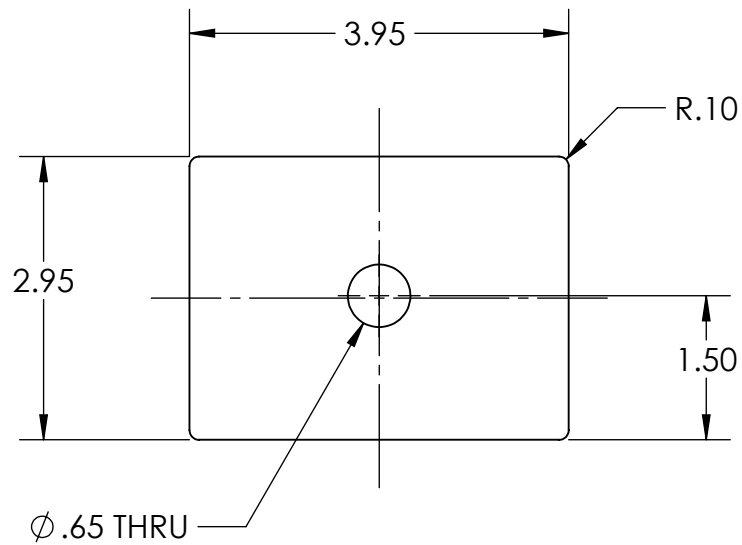
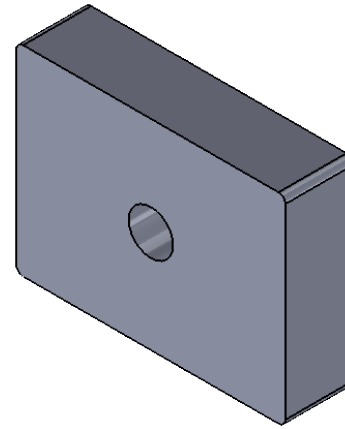
Once the results are retrieved, comment on the following to document any observations, recommendations, and possible sources of error.

- i. Comment on the sample size. Now that the standard deviation is known, should the sample size be revisited?
- ii. Discuss the distribution of the results, noting the p-value, minimum, maximum, and standard deviation. Is it a normal distribution? Describe the shape and spread.
- iii. Taking everything into consideration, what would be the nut factor 'K' you would recommend to a designer to use? Discuss why and justify why it is a safe value to use.
- iv. Given the distribution of the results, discuss possible sources of error. Try to focus on sources exclusive to this test, including apparatus, measurement equipment, and procedure.

### **References**

- [1] L. Online, "Small Table of z-values for Confidence Intervals," [Online]. Available: <https://www.ltconline.net/greenl/courses/201/estimation/smallConfLevelTable.htm>. [Accessed 24 November 2016].
- [2] "Anderson-Darling Normality Test," Variation.com, [Online]. Available: <http://www.variation.com/da/help/hs140.htm>. [Accessed 24 November 2016].

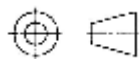
## **Appendix D: Test Apparatus Final Drawings**



**QTY:14**



**MECH 4860**



UNLESS OTHERWISE SPECIFIED:  
 DIMENSIONS ARE IN INCHES  
 TOLERANCES:  
 ANGULAR: MACH  $\pm 0^\circ 30'$   
 TWO PLACE DECIMAL  $\pm .01$   
 THREE PLACE DECIMAL  $\pm .002$

**UofM MECHANICAL ENGINEERING**

INTERPRET GEOMETRIC TOLERANCING PER: ANSI Y14. 5M-1994		NAME	DATE
DO NOT SCALE DRAWING	DRAWN	ASKORPAD	2016-11-13
MATERIAL <b>STEEL A36</b>	CHECKED	YGIN	2016-12-04
FINISH <b>N/A</b>	NUMBER		

TITLE:

**1 INCH WASHER PLATE**

SIZE  
**A**

DISCRIPTION:

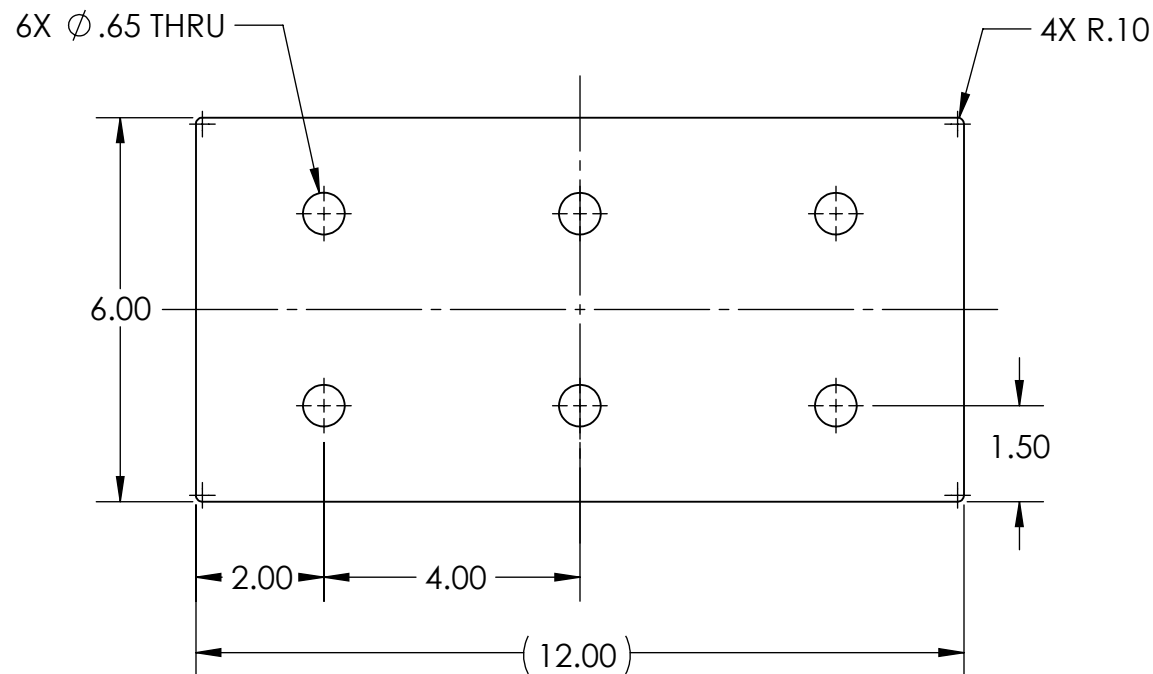
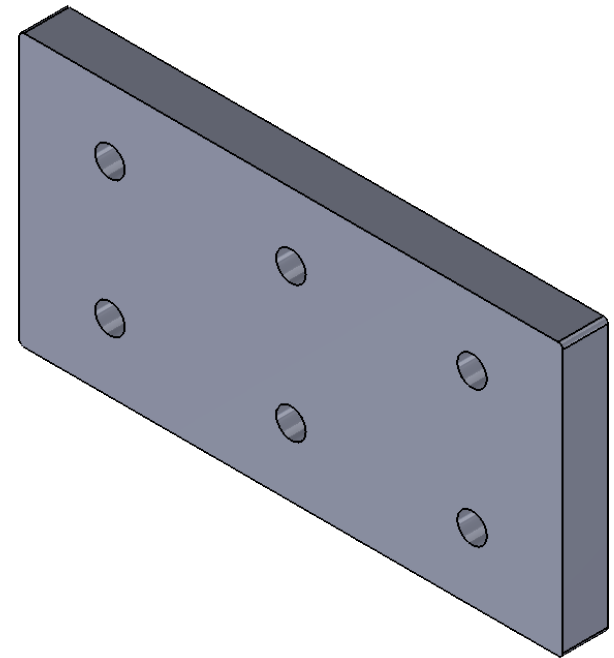
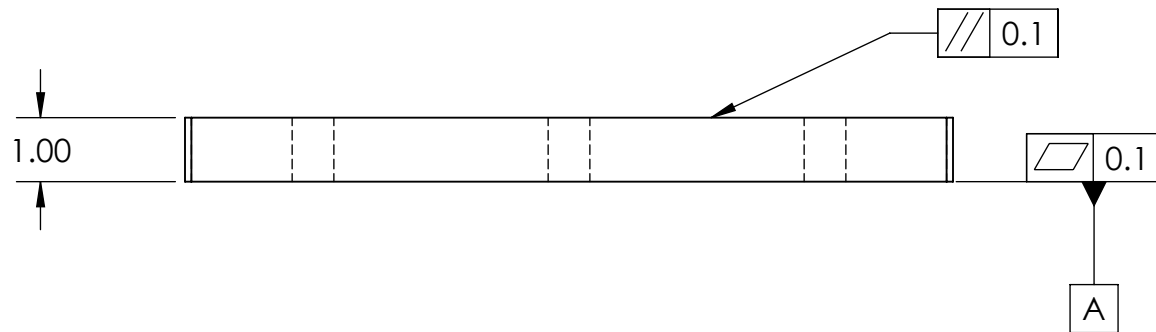
**OHWP-01**

REV  
**0**

SCALE: 1:2

WEIGHT:

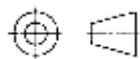
SHEET 1 OF 1



**1" STEEL PLATE  
QTY: 9**



**MECH 4860**



UNLESS OTHERWISE SPECIFIED:  
DIMENSIONS ARE IN INCHES  
TOLERANCES:  
ANGULAR: MACH  $\pm 0^\circ 30'$   
TWO PLACE DECIMAL  $\pm .01$   
THREE PLACE DECIMAL  $\pm .002$

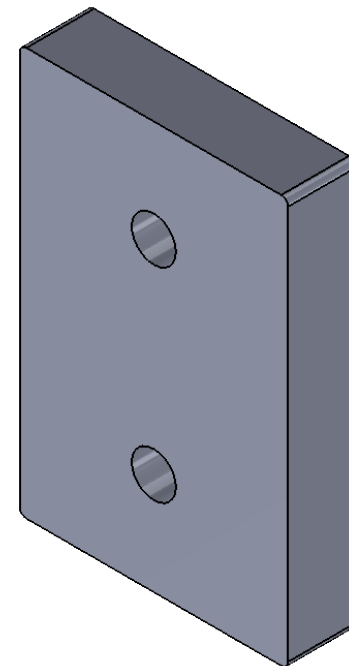
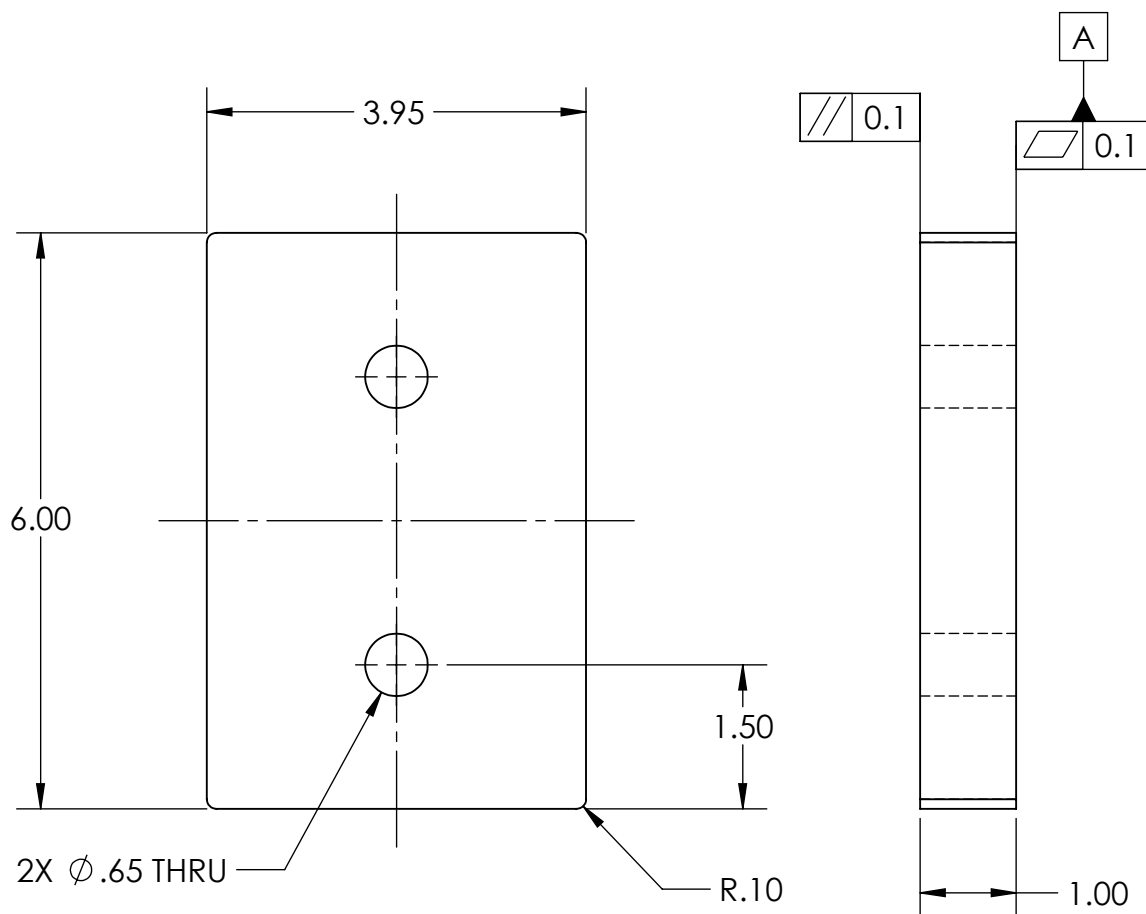
# **UofM MECHANICAL ENGINEERING**

INTERPRET GEOMETRIC TOLERANCING PER:	ANSI Y14.5M-1994	NAME	DATE
DO NOT SCALE DRAWING	DRAWN	YQIN	2016-11-16
MATERIAL	STEEL A36	CHECKED	YQIN
FINISH	N/A	NUMBER	2016-12-04

TITLE: **1 INCH SIX HOLE PLATE**

SIZE	DISCRIPTION:	REV
<b>A</b>	SHWP-01	0

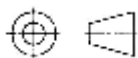
SCALE: 1:3 WEIGHT: SHEET 1 OF 1



**QTY: 9**



**MECH 4860**



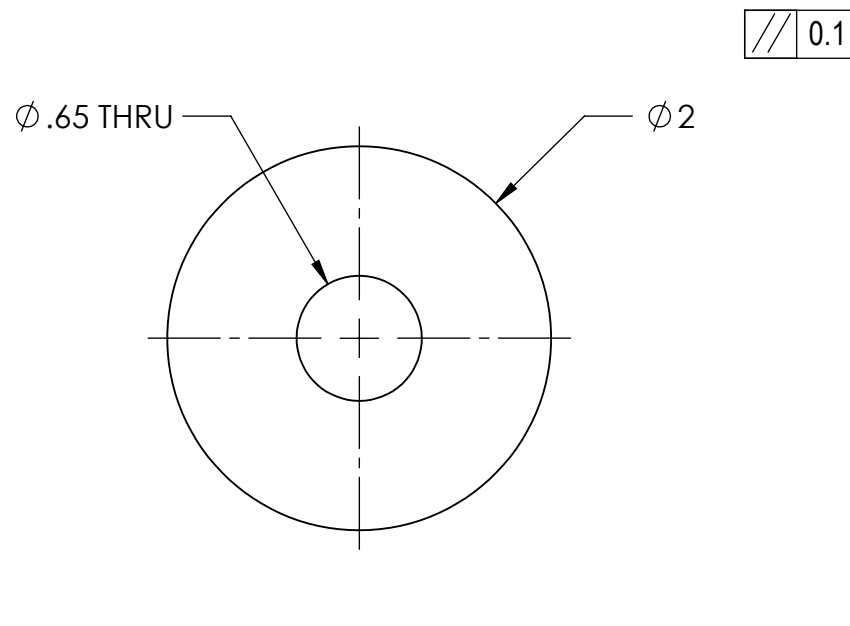
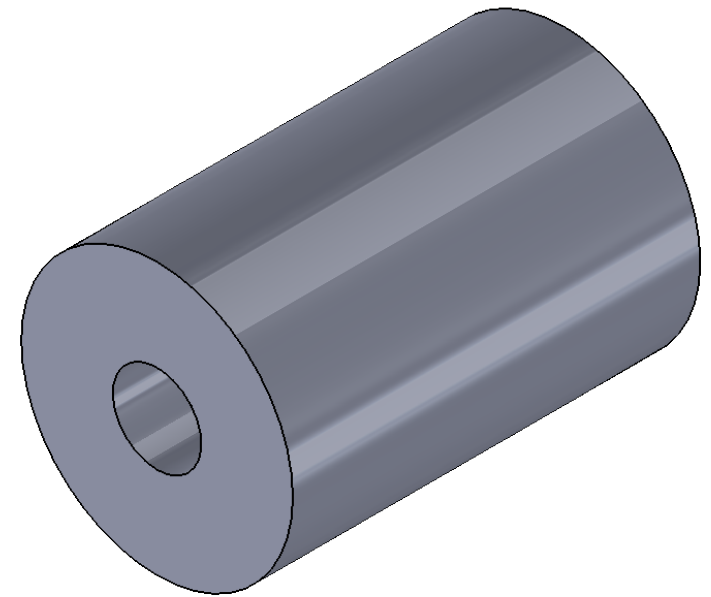
UNLESS OTHERWISE SPECIFIED:  
 DIMENSIONS ARE IN INCHES  
 TOLERANCES:  
 ANGULAR: MACH  $\pm 0^\circ 30'$   
 TWO PLACE DECIMAL  $\pm .01$   
 THREE PLACE DECIMAL  $\pm .002$

# **UofM MECHANICAL ENGINEERING**

INTERPRET GEOMETRIC TOLERANCING PER:	ANSI Y14.5M-1994	NAME	DATE
DO NOT SCALE DRAWING	DRAWN	YQIN	2016-11-16
MATERIAL	STEEL A36	CHECKED	YQIN
FINISH	N/A	NUMBER	2016-12-04

TITLE:  
**1 INCH TWO HOLE WASHER PLATE**

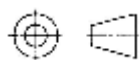
SIZE	DISCRIPTION:	REV
<b>A</b>	THWP-01	0
SCALE: 1:2	WEIGHT:	SHEET 1 OF 1



**QTY: 6**



**MECH 4860**



UNLESS OTHERWISE SPECIFIED:  
 DIMENSIONS ARE IN INCHES  
 TOLERANCES:  
 ANGULAR: MACH  $\pm 0^\circ 30'$   
 TWO PLACE DECIMAL  $\pm .01$   
 THREE PLACE DECIMAL  $\pm .002$

**UofM MECHANICAL ENGINEERING**

INTERPRET GEOMETRIC TOLERANCING PER: ANSI Y14.5M-1994		NAME	DATE
DO NOT SCALE DRAWING	DRAWN	ASKORPAD	2016-11-13
MATERIAL	STEEL A36	CHECKED	YQIN 2016-12-04
FINISH	N/A	NUMBER	

**TITLE:**  
**3 INCH ROUND WASHER PLATE**

SIZE	DISCRIPTION:	REV
<b>A</b>	RW-01	0
SCALE: 1:1	WEIGHT:	SHEET 1 OF 1

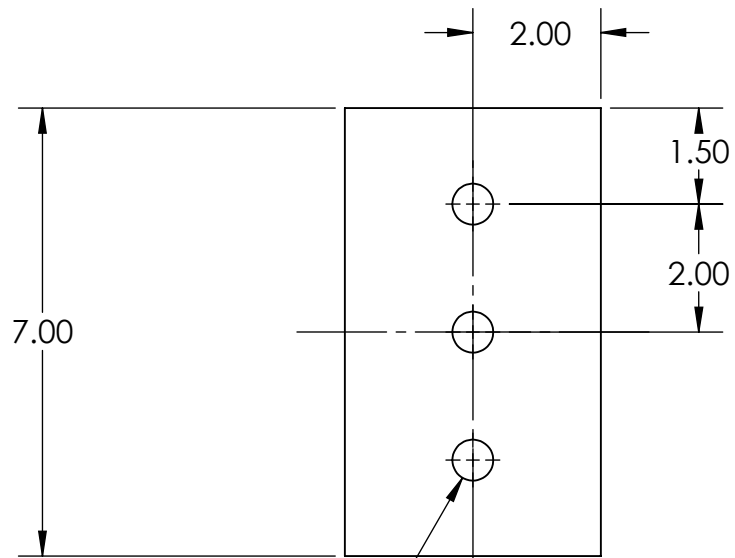
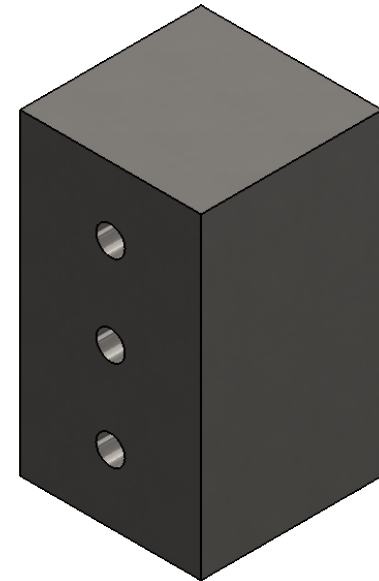
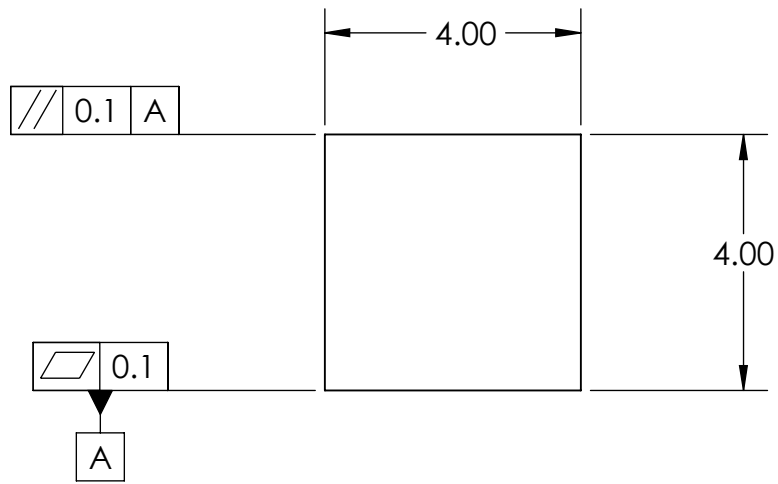
5

4

3

2

1

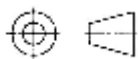


3X  $\varnothing .64$  THRU

**QTY: 1**



**MECH 4860**



UNLESS OTHERWISE SPECIFIED:  
DIMENSIONS ARE IN INCHES  
TOLERANCES:  
ANGULAR: MACH  $\pm 0^\circ 30'$   
TWO PLACE DECIMAL  $\pm .01$   
THREE PLACE DECIMAL  $\pm .002$

# UofM MECHANICAL ENGINEERING

INTERPRET GEOMETRIC TOLERANCING PER: ANSI Y14. 5M-1994		NAME	DATE
DO NOT SCALE DRAWING	DRAWN	YQIN	2016-11-22
MATERIAL	A36 STEEL	CHECKED	YQIN
FINISH	N/A	NUMBER	

TITLE:

4 X 4 BLOCK

SIZE

**A**

DISCRIPTION:

BLOCK-01

REV

0

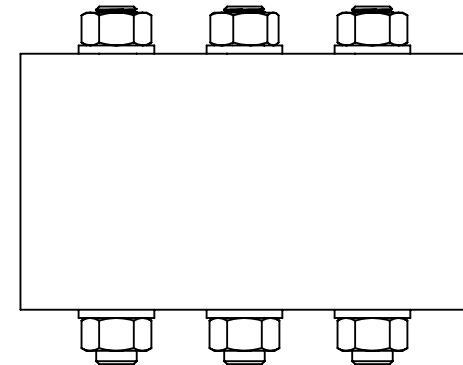
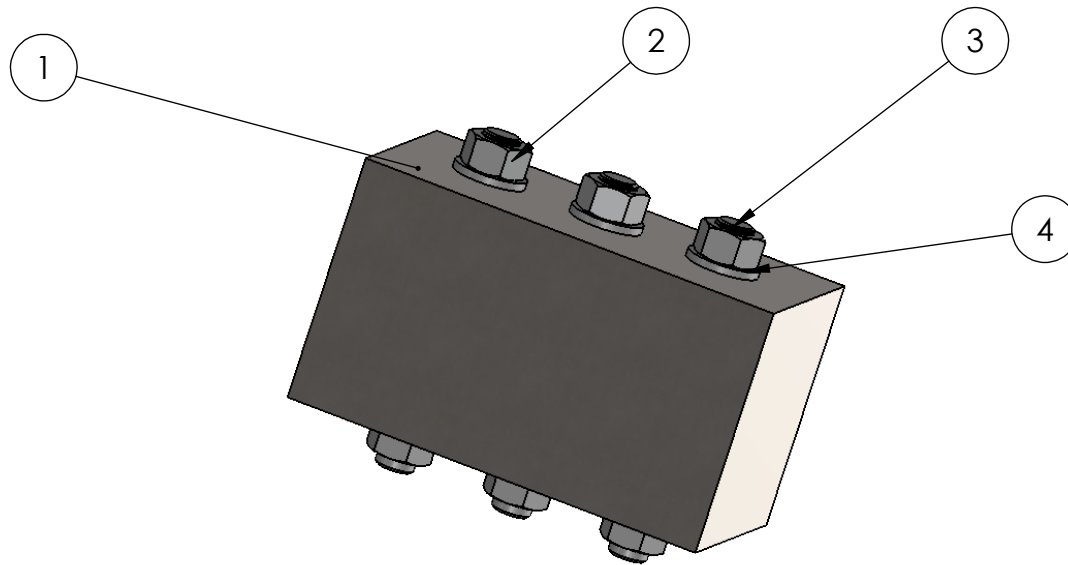
SCALE: 1:3

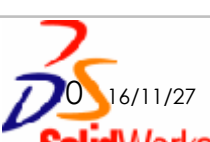
WEIGHT:

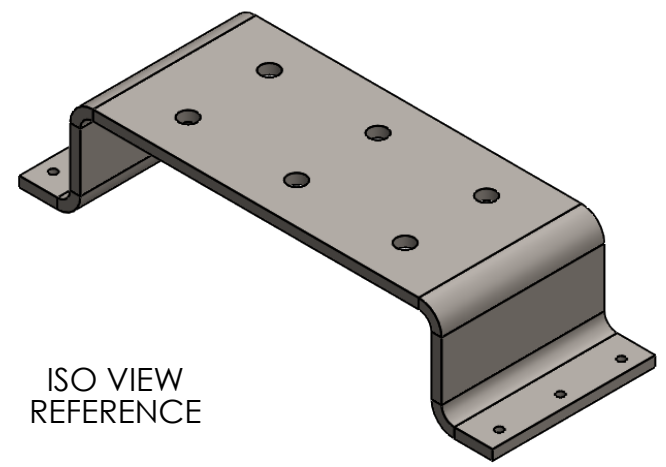
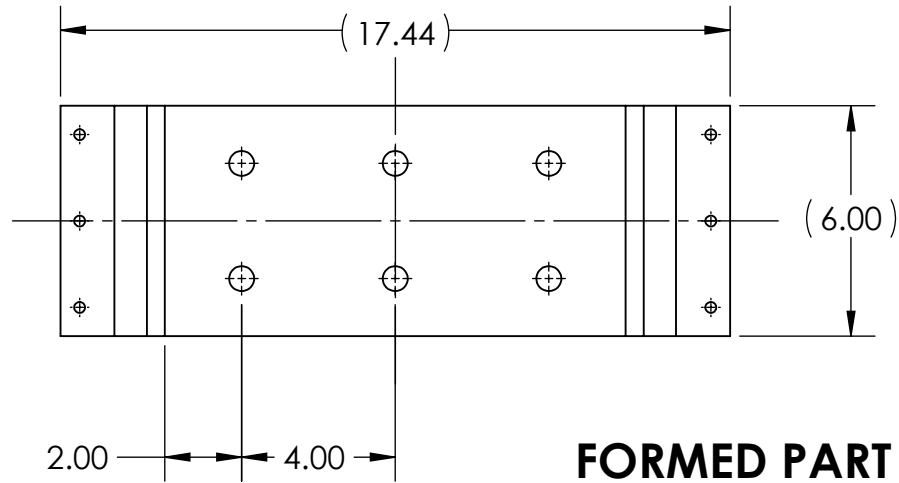
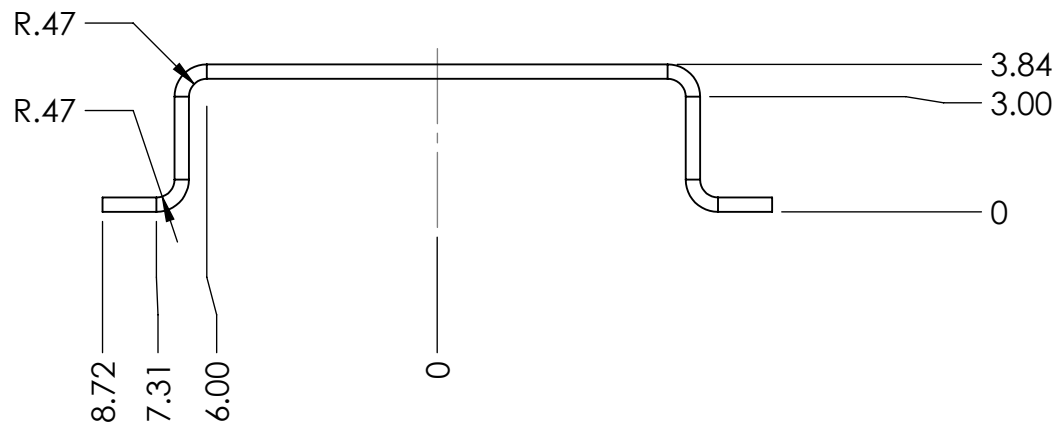
SHEET 1 OF 1



ITEM NO.	PART NUMBER	MATERIAL	DESCRIPTION	QTY.
1	4x4 block	A36 STEEL	TEST RIG	1
2	94223A105	ASTM A193-B7	5/8-11" HEX NUT	8
3	93000A622	ASTM A193-B7	5/8-11X6" THREAD ROD	3
4	90965A230	ASTM A193-B7	5/8" FLAT WSHR	6



		<b>MECH 4860</b>		UNLESS OTHERWISE SPECIFIED: DIMENSIONS ARE IN INCHES TOLERANCES: ANGULAR: MACH $\pm 0^{\circ} 30'$ TWO PLACE DECIMAL $\pm .01$ THREE PLACE DECIMAL $\pm .002$		UofM MECHANICAL ENGINEERING				TITLE: <b>TESTING BLOCK ASSEMBLY</b>			
						INTERPRET GEOMETRIC TOLERANCING PER: ANSI Y14. 5M-1994		NAME	DATE	SIZE	DISCRIPTION:		REV
						DO NOT SCALE DRAWING		DRAWN	YQIN	2016-11-27	TBA-01		0
						MATERIAL N/A		CHECKED	YQIN	2016-12-04			
						FINISH N/A		NUMBER		SCALE: 1:3			

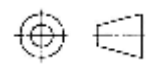


**FORMED PART**

**3/8 INCH SHEET METAL  
QTY: 1**



**MECH 4860**



UNLESS OTHERWISE SPECIFIED:  
DIMENSIONS ARE IN INCHES  
TOLERANCES:  
ANGULAR: MACH  $\pm 0^\circ 30'$   
TWO PLACE DECIMAL  $\pm .01$   
THREE PLACE DECIMAL  $\pm .002$

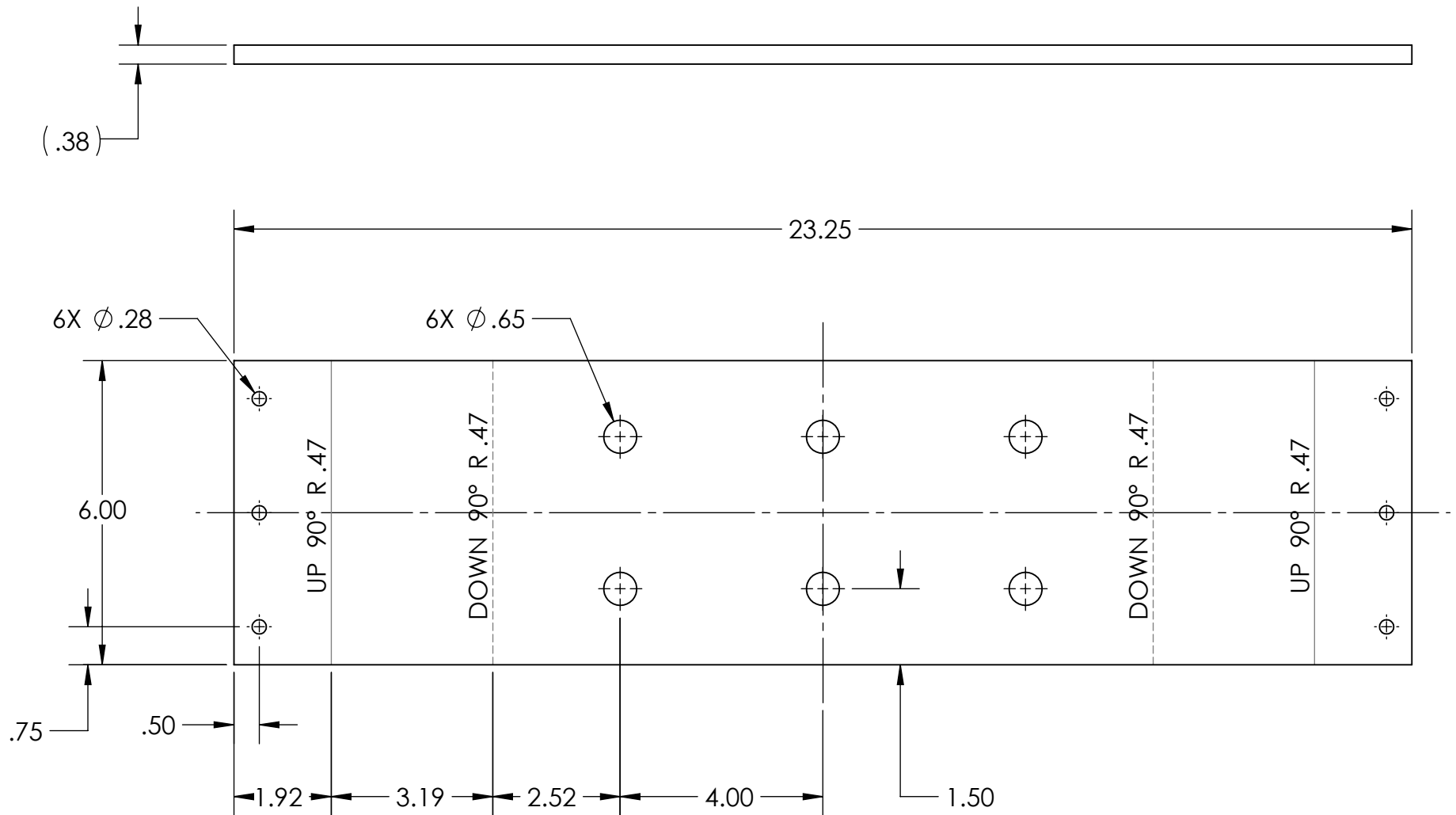
**UofM MECHANICAL ENGINEERING**

INTERPRET GEOMETRIC TOLERANCING PER: ANSI Y14. 5M-1994		NAME	DATE
DO NOT SCALE DRAWING	DRAWN	ASKORPAD	2016-11-06
MATERIAL <b>STEEL A36</b>	CHECKED	YQIN	2016-12-04
FINISH <b>N/A</b>	NUMBER		

TITLE: **TEST RIG**

SIZE <b>A</b>	DISCRIPTION: <b>TR-01</b>	REV <b>0</b>
---------------	---------------------------	--------------

SCALE: 1:5 WEIGHT: SHEET 1 OF 2

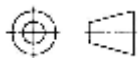


## FLAT PATTERN

**3/8 INCH SHEET METAL  
QTY: 1**



**MECH 4860**



UNLESS OTHERWISE SPECIFIED:  
DIMENSIONS ARE IN INCHES  
TOLERANCES:  
ANGULAR: MACH  $\pm 0^\circ 30'$   
TWO PLACE DECIMAL  $\pm .01$   
THREE PLACE DECIMAL  $\pm .002$

### UofM MECHANICAL ENGINEERING

INTERPRET GEOMETRIC TOLERANCING PER: ANSI Y14. 5M-1994		NAME	DATE
DO NOT SCALE DRAWING	DRAWN	ASKORPAD	2016-11-06
MATERIAL STEEL A36	CHECKED	YQIN	2016-12-04
FINISH N/A	NUMBER		

TITLE:

TEST RIG

SIZE

**A**

DISCRIPTION:

TR-01

REV

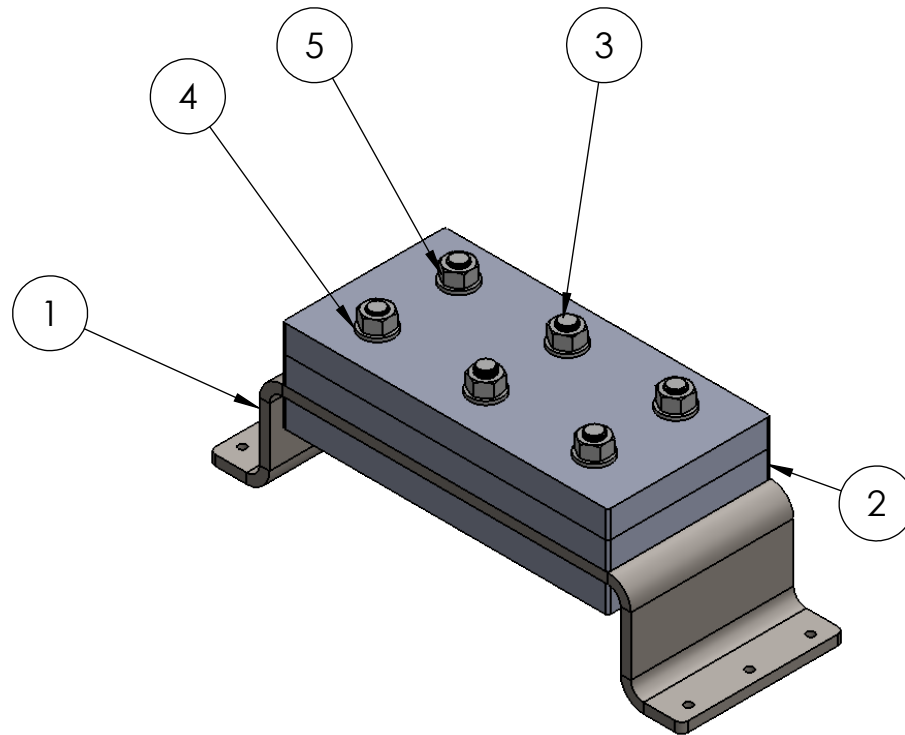
0

SCALE: 1:3

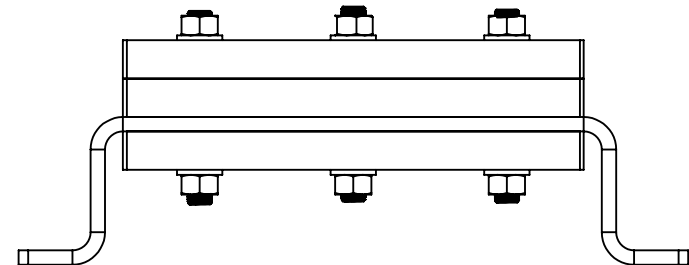
WEIGHT:

SHEET 2 OF 2

ITEM NO.	PART NUMBER	MATERIAL	DESCRIPTION	QTY.
1	nut factor k designs .375 inch	A36 STEEL	TEST RIG	1
2	1 inch washer plate with six holes	A36 STEEL	6 HOLE WASHER PLATE	3
3	93000A622	ASTM 193 B7	STEEL FULLY THREADED ROD	6
4	90965A230	ASTM 193 B7	STAINLESS STEEL FLAT WASHER	12
5	94223A105	ASTM 193 B7	STEEL HEX NUT	12



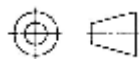
ISOMETRIC VIEW



FRONT VIEW



MECH 4860



UNLESS OTHERWISE SPECIFIED:  
DIMENSIONS ARE IN INCHES  
TOLERANCES:  
ANGULAR: MACH  $\pm 0^\circ 30'$   
TWO PLACE DECIMAL  $\pm .01$   
THREE PLACE DECIMAL  $\pm .002$

## UofM MECHANICAL ENGINEERING

INTERPRET GEOMETRIC TOLERANCING PER: ANSI Y14. 5M-1994	NAME	DATE
DO NOT SCALE DRAWING	DRAWN	YQIN 2016-11-17
MATERIAL	CHECKED	YQIN 2016-12-04
FINISH	NUMBER	

TITLE:  
TESTING APPARAUS ASSEMBLY

SIZE <b>A</b>	DISCRIPTION: TAA-01	REV 0
------------------	------------------------	----------

SCALE: 1:5 WEIGHT: SHEET 1 OF 1

## **Appendix E: Bolt Test Results**

### Nut Factor Analysis

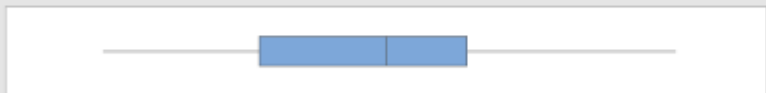
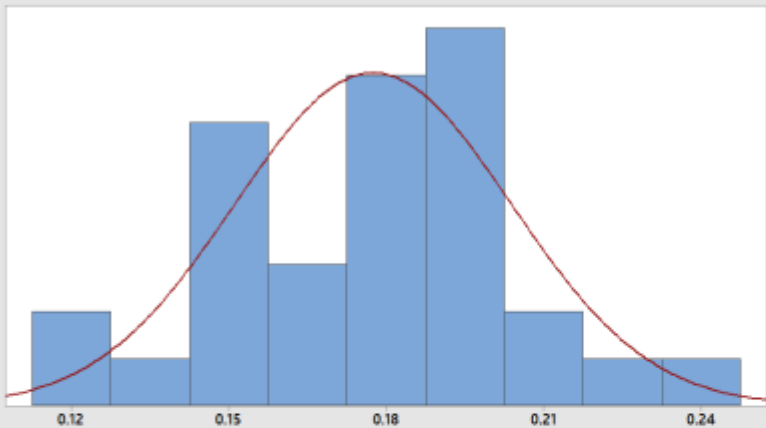
Thickness of Nut 1 (mm)	Thickness of Nut 2 (mm)	Plate Thickness (in)	Modulus of Elasticity (psi)	Fastener Diameter (mm)	Pitch (mm)
13	13	4	29700000	15.875	2.309090909
Thickness of Nut 1 (in)	Thickness of Nut 2 (in)		Length in Tension (in)	Fastener Diameter (in)	Cross-section Area (in^2)
0.511811024	0.511811024		4.511811024	0.625	0.228790827

Trial	New Length of Stud (in)	Torque Applied (ft-lbs)	Length of Stud (in)	Length in Tension (in)	Change in Stud Length (in)	Preload (lbs)	K	Coated?	Observations
1	5.3195	120	5.31	5.194	0.0095	12428.4428	0.19	Not coated	Dry run
2	5.3186	120	5.31	5.194	0.0086	11251.0114	0.20	Not coated	
3	5.3212	120	5.3097	5.2495	0.0115	14885.8952	0.15	Not coated	
4	5.255	120	5.2457	5.1913	0.0093	12173.1193	0.19	Coated	
5	5.3131	120	5.3046	5.1993	0.0085	11108.8501	0.21	Not coated	
6	5.2649	120	5.2508	5.1941	0.0141	18446.0705	0.12	coated	
7	5.3243	120	5.3046	5.1986	0.0197	25749.8606	0.09	coated	apparatus shift during torque
8	5.3236	120	5.3125	5.185	0.0111	14546.8606	0.16	uncoated	
9	5.324	120	5.313	5.192	0.011	14396.372	0.16	uncoated	
10	5.3237	120	5.311	5.196	0.0127	16608.4704	0.14	uncoated	
11	5.315	120	5.302	5.193	0.013	17010.6178	0.14	uncoated	
12	5.2515	120	5.24	5.189	0.0115	15059.4541	0.15	coated	filed versions begin
13	5.2527	120	5.2434	5.191	0.0093	12173.8229	0.19	coated	
14	5.2584	120	5.247	5.184	0.0114	14942.9009	0.15	coated	
15	5.247	120	5.238	5.187	0.009	11790.204	0.20	coated	
16	5.253	120	5.239	5.198	0.014	18301.5056	0.13	coated	
17	5.255	120	5.245	5.192	0.01	13087.6109	0.18	coated	
18	5.3201	120	5.3088	5.1967	0.0113	14775.6248	0.16	uncoated	
19	5.3071	120	5.298	5.2025	0.0091	11885.689	0.19	uncoated	
20	5.314	120	5.3048	5.1975	0.0092	12027.8606	0.19	uncoated	
21	5.2551	120	5.2441	5.206	0.011	14357.6572	0.16	coated	
22	5.25	120	5.2412	5.2076	0.0088	11482.5967	0.20	coated	
23	5.2503	120	5.2405	5.1984	0.0098	12810.0681	0.18	coated	
24	5.3205	120	5.3092	5.193	0.0113	14786.1524	0.16	uncoated	
25	5.3088	120	5.299	5.2018	0.0098	12801.6952	0.18	uncoated	
26	5.3222	120	5.3084	5.1863	0.0138	18080.7529	0.13	uncoated	
27	5.3215	120	5.3132	5.1801	0.0083	10887.6714	0.21	uncoated	
28	5.3111	120	5.3026	5.1997	0.0085	11107.9955	0.21	uncoated	
29	5.3133	120	5.3027	5.203	0.0106	13843.538	0.17	uncoated	
30	5.2553	120	5.2427	5.2044	0.0126	16451.0997	0.14	coated	
31	5.3168	120	5.3072	5.1888	0.0096	12571.8549	0.18	coated	
32	5.3132	120	5.3012	5.1917	0.012	15706.0406	0.15	coated	
33	5.3202	120	5.311	5.1993	0.0092	12023.6966	0.19	uncoated	
34	5.3121	120	5.3032	5.1903	0.0089	11651.7888	0.20	uncoated	
35	5.3132	120	5.3043	5.2083	0.0089	11611.52	0.20	uncoated	
36	5.3161	120	5.3066	5.1935	0.0095	12429.6393	0.19	uncoated	
37	5.3211	120	5.3092	5.1964	0.0119	15561.0696	0.15	uncoated	
38	5.3103	120	5.3007	5.1885	0.0096	12572.5818	0.18	uncoated	
39	5.3105	120	5.3049	5.186	0.0056	7337.54154	0.31	uncoated	
40	5.318	120	5.308	5.187	0.01	13100.2267	0.18	uncoated	
41	5.3055	120	5.295	5.3055	0.0105	13448.0105	0.17	uncoated	
42	5.311	120	5.3035	5.204	0.0075	9793.07394	0.24	uncoated	
43	5.316	120	5.308	5.197	0.008	10460.0155	0.22	uncoated	

AVG	0.18
STD DEV	0.04

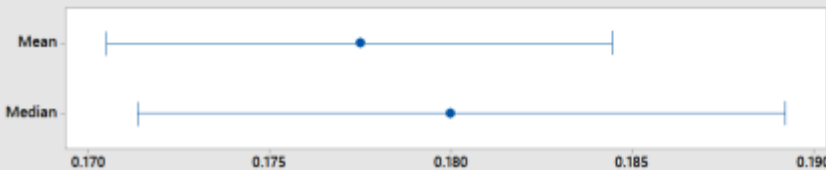
## **Appendix F: Test Results MiniTab Analysis**

# Summary Report for Nut Factor K



Anderson-Darling Normality Test	
A-Squared	0.22
P-Value	0.827
Mean	0.17748
StDev	0.02633
Variance	0.00069
Skewness	-0.073874
Kurtosis	-0.294946
N	31
Minimum	0.12589
1st Quartile	0.15582
Median	0.17998
3rd Quartile	0.19542
Maximum	0.23527
85% Confidence Interval for Mean	
	0.17050 0.18447
85% Confidence Interval for Median	
	0.17135 0.18924
85% Confidence Interval for StDev	
	0.02231 0.03252

## 85% Confidence Intervals



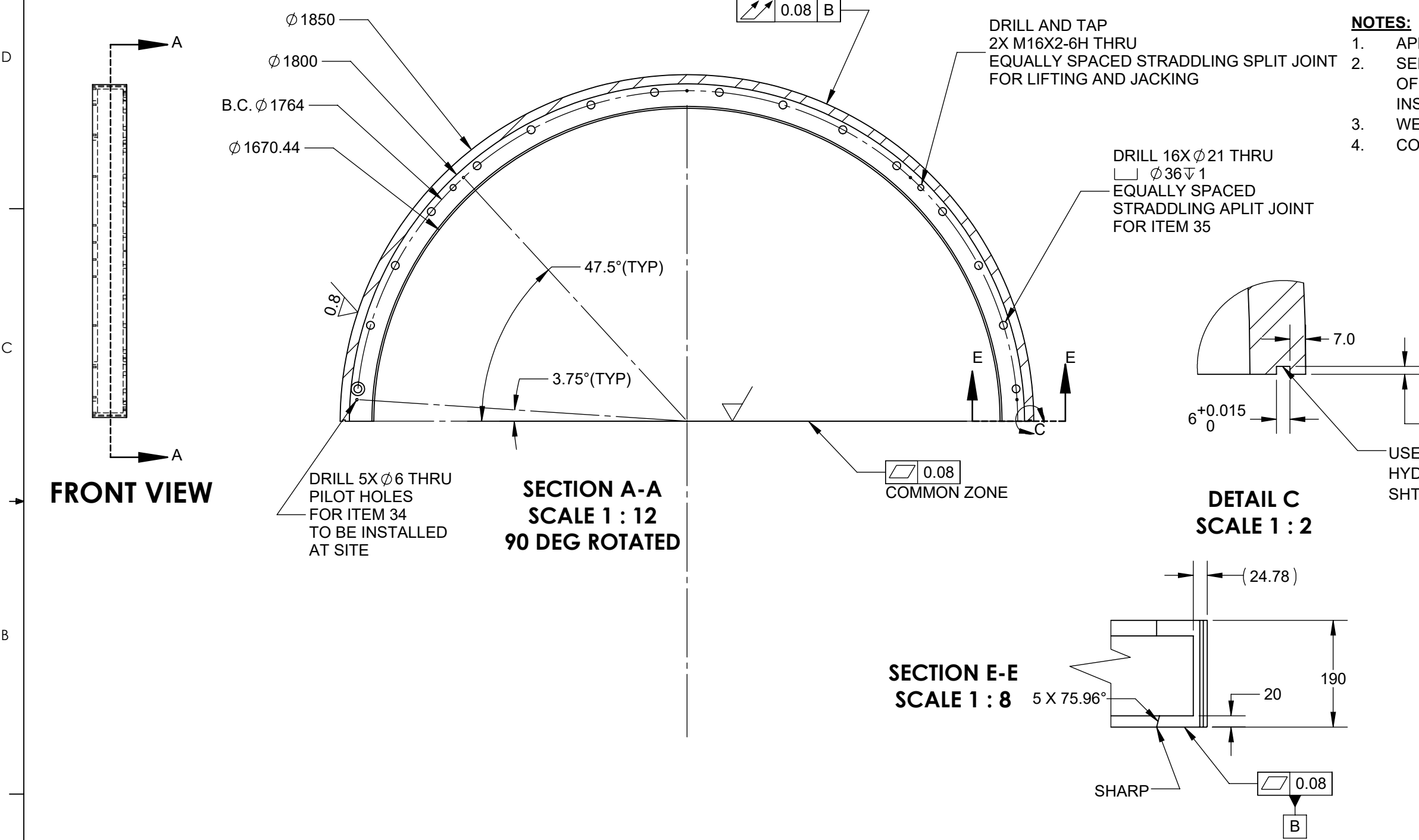


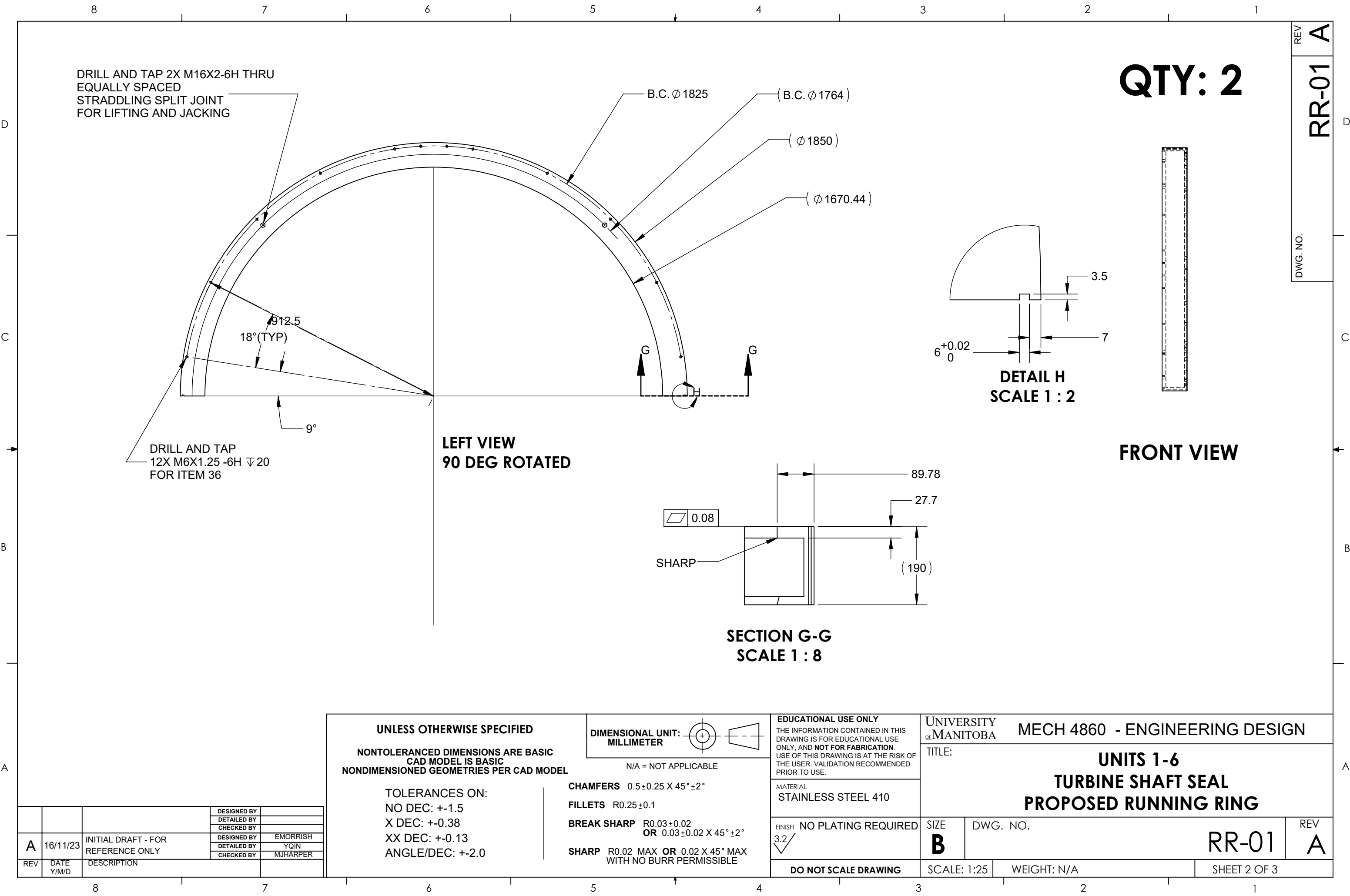
## **Appendix G: Updated Running Ring Final Drawings**

QTY: 2

REV  
RR-01  
A  
DWG. NO.

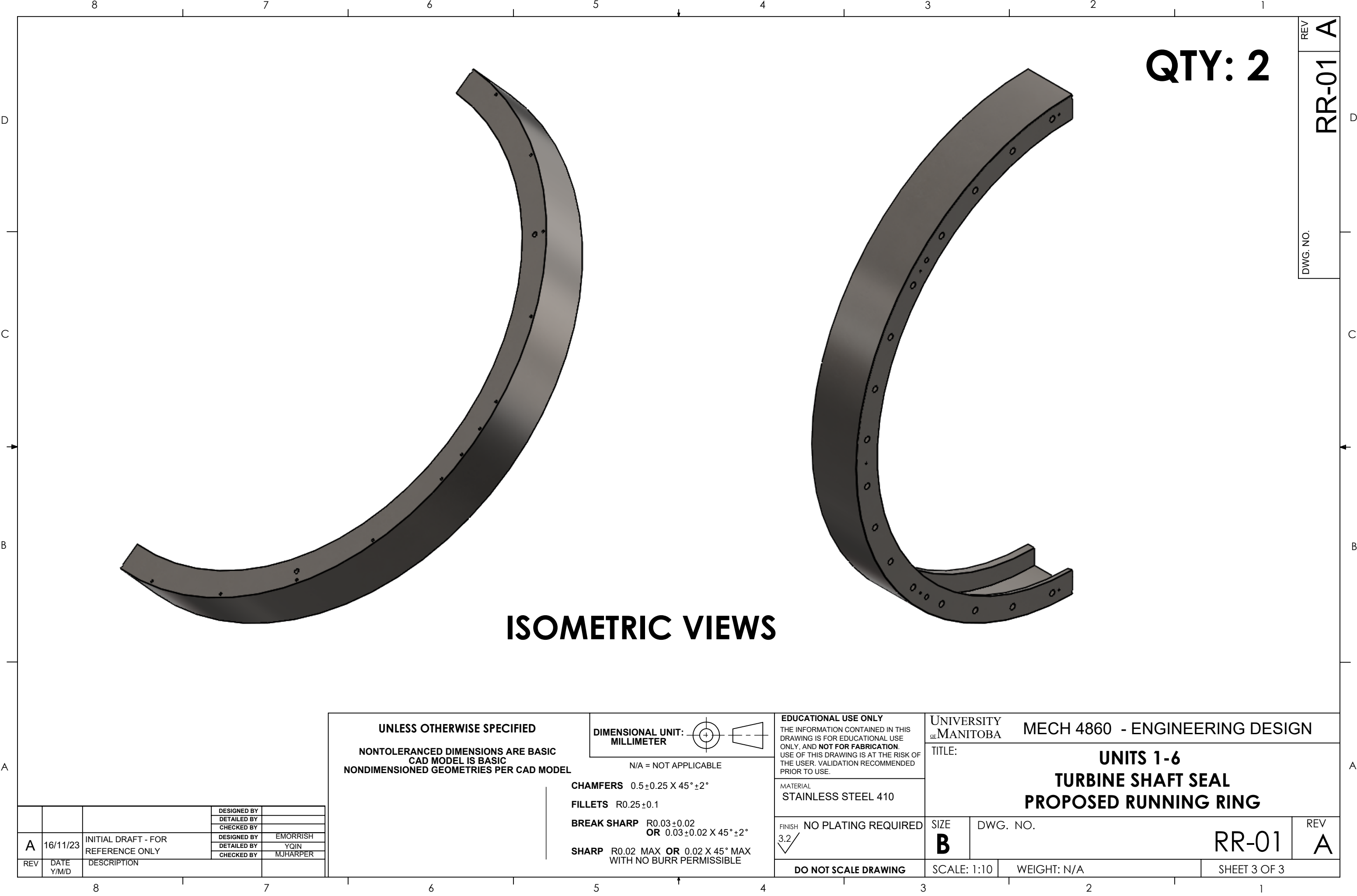
- NOTES:**
1. APPROXIMATE MASS PER HALF = 170 KG
  2. SEE MANITOBA HYDRO DRAWINGS FOR BILL OF MATERIALS, OTHER COMPONENTS, AND INSTALLATION PROCEDURE.
  3. WELDS NOT SPECIFIED.
  4. COATINGS NOT SPECIFIED.



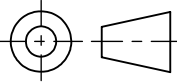


			DESIGNED BY	
			DETAILED BY	
			CHECKED BY	
A	16/11/23	INITIAL DRAFT - FOR REFERENCE ONLY	DESIGNED BY	EMORRISH
REV	DATE	DESCRIPTION	DETAILED BY	YQIN
	Y/M/D		CHECKED BY	MJHARPER

UNLESS OTHERWISE SPECIFIED		DIMENSIONAL UNIT: MILLIMETER		EDUCATIONAL USE ONLY		UNIVERSITY OF MANITOBA		MECH 4860 - ENGINEERING DESIGN	
NONTOLERANCED DIMENSIONS ARE BASIC CAD MODEL IS BASIC NONDIMENSIONED GEOMETRIES PER CAD MODEL		N/A = NOT APPLICABLE		THE INFORMATION CONTAINED IN THIS DRAWING IS FOR EDUCATIONAL USE ONLY, AND NOT FOR FABRICATION. USE OF THIS DRAWING IS AT THE RISK OF THE USER. VALIDATION RECOMMENDED PRIOR TO USE.		TITLE: UNITS 1-6 TURBINE SHAFT SEAL PROPOSED RUNNING RING			
				MATERIAL STAINLESS STEEL 410					
TOLERANCES ON: NO DEC: +-1.5 X DEC: +-0.38 XX DEC: +-0.13 ANGLE/DEC: +-2.0		CHAMFERS 0.5±0.25 X 45° ±2° FILLETS R0.25±0.1 BREAK SHARP R0.03±0.02 OR 0.03±0.02 X 45° ±2° SHARP R0.02 MAX OR 0.02 X 45° MAX WITH NO BURR PERMISSIBLE		FINISH NO PLATING REQUIRED 3.2 ✓		SIZE B	DWG. NO.		REV A
				DO NOT SCALE DRAWING		SCALE: 1:25	WEIGHT: N/A		SHEET 2 OF 3



			DESIGNED BY	
			DETAILED BY	
			CHECKED BY	
A	16/11/23	INITIAL DRAFT - FOR REFERENCE ONLY	DESIGNED BY	EMORRISH
REV	DATE Y/M/D	DESCRIPTION	DETAILED BY	YQIN
			CHECKED BY	MJHARPER

UNLESS OTHERWISE SPECIFIED  NONTOLERANCED DIMENSIONS ARE BASIC CAD MODEL IS BASIC NONDIMENSIONED GEOMETRIES PER CAD MODEL		DIMENSIONAL UNIT: MILLIMETER <div></div> N/A = NOT APPLICABLE		EDUCATIONAL USE ONLY THE INFORMATION CONTAINED IN THIS DRAWING IS FOR EDUCATIONAL USE ONLY, AND <b>NOT FOR FABRICATION</b> . USE OF THIS DRAWING IS AT THE RISK OF THE USER. VALIDATION RECOMMENDED PRIOR TO USE.		UNIVERSITY OF MANITOBA		MECH 4860 - ENGINEERING DESIGN	
				MATERIAL STAINLESS STEEL 410		TITLE:  UNITS 1-6  TURBINE SHAFT SEAL  PROPOSED RUNNING RING			
CHAMFERS 0.5±0.25 X 45° ±2°  FILLETS R0.25±0.1  BREAK SHARP R0.03±0.02 OR 0.03±0.02 X 45° ±2°  SHARP R0.02 MAX OR 0.02 X 45° MAX WITH NO BURR PERMISSIBLE		FINISH NO PLATING REQUIRED 3.2 ✓		SIZE B	DWG. NO.				
		DO NOT SCALE DRAWING		SCALE: 1:10		WEIGHT: N/A		SHEET 3 OF 3	

REV	A
DWG. NO.	RR-01